Assessment of saltwater origin in the Rub' al-Khali basin and its relation to the formation of sabkha Matti

by

Waleed Saeed

A thesis
presented to the University of Waterloo
in fulfillment of the
thesis requirement for the degree of
Doctor of Philosophy
In
Earth and Environmental Sciences

Waterloo, Ontario, Canada, 2020

Examining Committee Membership

The following served on the Examining Committee for this thesis. The decision of the Examining Committee is by majority vote.

External Examiner	Dr. Yousif K. Kharaka Research Hydrogeochemist Emeritus U.S. Geological Survey
Supervisor(s)	Dr. André Unger Associated Professor Earth and Environmental Sciences University of Waterloo
	Dr. Orfan Shouakar-Stash Adjunct Associated Professor Earth and Environmental Sciences University of Waterloo
	Dr. Beth Parker Professor School of Engineering University of Guelph
Internal Member	Dr. Shaun Frape Professor Earth and Environmental Sciences University of Waterloo
Internal-external Member	Dr. Vassili Karanassios Professor Chemistry University of Waterloo

Author's Declaration

This thesis consists of material all of which I authored or co-authored. Please see Statement of Contribution included in the thesis.

This is a true copy of the thesis, including any required final revisions, as accepted by my examiners.

I understand that my thesis may be made electronically available to the public.

Statement of Contributions

This research project was completely funded by the Saudi Aramco Oil Company and was conducted at the University of Waterloo by Waleed Saeed under the supervision of Dr. André Unger. and Dr. Orfan Shouakar-Stash. This thesis was written in paper format with the intention that each chapter (with the exception of chapters 1, 2, and 3) will be published separately. Due to this format, there is some repetition between chapters. As first author on each paper, Waleed Saeed was primarily responsible for development and implementation of the modelling approaches, data interpretation, and paper writing. The following summarizes the contributions of co-authors.

Waleed Saeed was the sole author for Chapters 1, 2, and 3 which were written under the supervision of Dr. André Unger. Dr. Orfan Shouakar-Stash and were not written for publication.

Chapter 4: This chapter is submitted for publication in Applied Geochemistry Journal and it is currently under review. The chapter investigates the origin and mechanism of saltwater intrusion in a regional multi-level sedimentary aquifer system. Waleed Saeed, Orfan Shouakar-Stash, and Warren Wood conducted a field trip to design the sampling campaign. Water and soil sample collection programs were designed by Waleed Saeed with assistance from Adnan Al-Zahrani, Bader Al-Ruhaili, and AbdulAziz Albishi. Waleed Saeed performed the isotope analyses at IT^2 laboratory with assistance from Adam Mihailov. Waleed Saeed wrote the draft manuscripts, which all co-authors contributed intellectual input on.

Chapter 5: This chapter is submitted for publication in Hydrogeology Journal and it is currently under review. This paper models the evolution of sabkha Matti and the underlying regional

aquifers. Waleed Saeed, Orfan Shouakar-Stash, and Warren Wood conducted two field trips to design the sampling campaign. Shallow piezometers installation and description of cutting samples were performed by Waleed Saeed. The water sample collection programs were carried out by Waleed Saeed with assistance from Adnan Al-Zahrani, Bader Al-Ruhaili, and AbdulAziz Albishi. Waleed Saeed performed the isotope analyses at IT^2 laboratory with assistance from Adam Mihailov. Waleed Saeed wrote the draft manuscripts, which all co-authors contributed intellectual input on.

Chapter 6: This chapter is to be submitted for publication in Hydrology Journal. The chapter quantifies the hydrologic budget for groundwater and solute fluxes in sabkha Matti. Waleed Saeed conducted all the field works and sampling collection with assistance from Adnan Al-Zahrani, Bader Al-Ruhaili, and AbdulAziz Albishi. Waleed Saeed wrote the draft manuscripts, which all co-authors contributed intellectual input on.

As lead author of these three chapters, I was responsible for contributing to conceptualizing study design, carrying out data collection and analysis, and drafting and submitting manuscripts. My coauthors provided guidance during each step of the research and provided feedback on draft manuscripts.

Abstract

The Rub' al Khali sand sea is the largest uninterrupted sand desert on Earth that occupies an area of approximately 650,000 km^2 of the Arabian Peninsula. Yet, the desert basin is underlying by one of the largest multi-level aquifer systems of the arid world that is the Rub' al Khali (RAK) structural basin. In this study, water resources in the Cenozoic aquifer systems within the RAK basin were assesses using a combination of geological, hydraulic, hydrochemical, and isotopic approaches. The main goal of this research is to initiate the building of a conceptual model of the regional hydrogeology of the RAK basin in order to assess the constraints and opportunities of the available water resources for future developments. The study shows that the RAK basin is a potential source of fresh to brackish water, with total dissolved solids concentrations (TDS) less than 10,000 mg/l. However, groundwater with up to 200,000 mg/L TDS has been found in the vicinity of a potential discharge zone, known as sabkha Matti. An isotope and solute evaluation was applied to identify the origin and mechanisms of this salinization in three major Tertiary aquifers in the RAK basin. The studied geological succession comprises sedimentary rocks of the Lower Paleocene to Lower Miocene age, and the aquifers primarily consist of the Umm Er Radhuma, Dammam, and Hadrukh. It is demonstrated that the groundwater chemistry evolved from a low- (< 2,000 ppm) to high- (>120,000 ppm) salinity Na-Cl water type, regardless of the aquifer. The similarity in water types between the groundwater from the different formations suggests that the same origin and geochemical processes may be controlling the salinity and major ion chemistry in these aquifers. The suite of hydrogeological, hydrochemical (Cl vs. Br), and isotopic (Cl vs $\delta^{18}O$ and Br vs $\delta^{81}Br$) data indicate that the source of solutes is associated with the entrapment of evaporated paleo-seawater (connate water) in nearshore and lagoonal environments during the time of deposition. Moreover, the results from the $^{87}Sr/^{86}Sr$ ratios show no evidence of

significant vertical connectivity between the three Tertiary aquifers. Instead, the data support that evaporated paleo-seawater was trapped in each aquifer individually during the time of deposition, and that each has evolved similarly through water-rock and redox reactions. The stable isotopic compositions of $\delta^{18}O$, $\delta^{2}H$, and ^{14}C show that the entrapped paleo-seawater was partially flushed out by fresh meteoric water during the wet Late Pleistocene and Early Holocene periods.

Sabkha Matti (SM) is a flat salt covered portion in the further northeastern part of the Rub al Kali sand sea and is underlain by the larger RAK structural basin. SM is the largest continues salt flat in the Arabian Peninsula and it extends about 150 km south from the western Abu Dhabi coastline and across the border between the United Arab Emirates and Saudi Arabia. The Matti sabkha is a potential discharge point for regional groundwater systems in the RAK topographic basin. The hydrogeochemical evolution of this sabkha and its role in the regional hydrogeological system of the RAK basin was assessed by using a combination of geological, hydraulic, hydrochemical, and isotopic approaches. A compilation of the geologic structure and lithology in combination with boron isotope data attributed the origin of salinity in the regional aquifers underlying SM to the entrapment of ancient seawater in a coastal lagoon environment during the depositional time of the late Oligocene-Miocene formations. Major ionic constituents and strontium isotope ratios from the trapped paleo-seawater were observed to resemble those obtained from the near-surface sabkha brine. These data, along with hydrostatic head measurements, suggest that the origin of the solutes in SM is associated with brines ascending from the underlying formations. The data also show that solute concentrations in SM are increasing over time through a combination of evaporation, mineral dissolution by recharge, and density-driven convection mechanism that circulates the solutes. On the other hand, stable isotopes of waters ($\delta^{18}O$, $\delta^{2}H$) and radio isotope data (^{14}C and ^{3}H) suggest that the existing waters in the sabkha and the underlying aquifers are relatively recent

and were recharged during the wet phase in the Late Pleistocene-Holocene between 3,200 and 14,000 BP. This study shows that the water and solutes in SM are a combination from different sources.

Furthermore, A hydrologic budget was constructed for SM, where water fluxes were calculated on the basis of hydraulic gradient and conductivities measured in both shallow and deep wells. Evaporation rates from the surface of the sabkha indicate that the annual rainfall is lost by surface evaporation. Steady-state estimates within a rectilinear control volume of the sabkha indicate that about 1 m^3/year of water enters by lateral groundwater flow; 2 m^3/year of water exits by lateral groundwater flow; 20 m^3/year enters by upward leakage; 780 m^3/year enters by recharge from rainfall; and 780 m^3/year are lost by evaporation. As per the source of solutes, the water flux multiplied by its solute concentration indicates that nearly all the solutes in the sabkha were derived by upward leakage from the underlying regional aquifers rather than weathering of the aquifer framework, from precipitation, or other sources.

Acknowledgments

First and foremost, I thank God for his guidance and support.

I would like to sincerely thank my advisor, Dr. André Unger and co-advisor Dr. Orfan Shouakar-Stash, for their generous guidance, support and constructive critical insights throughout this thesis. I would like also to express my genuine appreciation to Dr. Orfan for his help and guidance in the lab and for introducing me to highly respected scientists.

I wish to extend my thanks to my committee members, Dr. Beth Parker and Dr. Shaun Frape, for their feedback, advice, constructive comments, and guidance throughout this study.

I would like to acknowledge the Engage grant granted by the Saudi Aramco Oil Company for funding this work. To my management in Saudi Aramco, Misfir Azzahrani, Aus Al-Tawil, Saíd Al Hajri, Mohammed Abdo Hezam, and Abdulaziz Gaoud, thank you for this fortunate opportunity to pursue my study.

A special appreciation goes to Dr. Warren Wood from the University of Michigan for sharing his database on the coastal sabkha of Abu Dhabi. Warren, thank you very much for your valuable time and your critical and constructive comments that enriched my thesis.

I want to thank my colleagues in Saudi Arabia who helped me in collecting the samples from the filed. Thank you to Adnan Al-Zahrani, Bader Al-Ruhaili, AbdulAziz Albishi and Mohsin Hujailan for your patient and being by my side every time I was under pressure.

To my former mentor in Saudi Aramco, Dr. Mohammed Rasheeduddin, thank you for believing in me and for your friendship. You are really a great person and I said this to acknowledge one of

the most important people in my life that I have met. Thank you to my great friend Essam Sardar for the instructive discussions on the Rub al Khali structure.

I would also like to thank the Environmental Agency -Abu Dhabi (EAD) for granting access to the field sites in the United Arab Emirates and for the information derived from its website, which were used in the preparation of this work.

To Mirna Stas, Adam Mihailov, Nikki Nguyen, and Richard Drimmie from the IT^2 Isotope Tracer Technologies Inc., thank you for your endless support in analyzing countless samples and for the fast response to my phone calls and emails.

Thank you to my friends in and out-side Canada for their friendship. Special thanks to, Mohammad Araki, Mansour Al-Subhi, Abdulaziz Al-Bishi, Khaled Saad, Hamad Al-kusaibri, Lutfi Ameer, Turki Badhiduh, Mohammed Amoudi, Abdulkadir Al-Shiki, Tala Al-Ghamdi, Saad Al-Ghamdi, Alaaddin Fairah, Zayed Atwa, Fahad Al-Khashrami, Hamdan Al-Harbi, Fahad Suwaid, and Ayman Jewed.

I am indebted to my family for their support, endless patience and unconditional love. They inspired me to work hard and they taught me the value of education. Thank you to my father who teaches me what it means to be who I am and hold my head up high. Special thanks to my sisters and brothers who always encouraged me, trusted me and inspired me. My heartfelt appreciations are also extended to my in-laws for their continuous support and undying encouragement to pursue my dreams.

Above all else, my gratitude to my lovely wife Alaa and my four little angels Meshal, Aus, Aleen and Sadeen. The development and completion of this work would not have been possible without

their support, encouragement, belief in me and understanding. I am very grateful to God who blessed me with my wife and kids. I know that for the last five years I could not be there as much as I should have been. However, now that my formal education is complete, I can only hope that there will be many happy years ahead of us. Alaa, saying thank you hardly seems enough after all you have done for me. I ask Almighty God to keep us together forever.

Dedication

This thesis is dedicated to the memory of my mother.

She told me on her deathbed “it is challenging but you will do it”; as always, she was right.

Table of Contents

List of Figures

List of Tables

Chapter 1 Introduction

1.1 Background

The Rub' al Khali, Arabic term meaning the empty quarter, topographic basin is an outstanding geomorphic sand sea depression in the Arabian Peninsula (Figure 1-1). It is the largest dune field on Earth with some dunes reaching hundreds of meters high (Edgell, 2006). This topographic basin lies in a hyper-arid zone and experiences characteristically high temperature and low rainfall for most of the year with no perennial rivers or lakes. Due to this harsh climatic conditions and inaccessible terrain, the area is largely uninhabited and undeveloped. Few investigations have been made on groundwater resources in the Rub' al Khali area. Astonishingly, the outcome of these studies suggest that the desert basin is underlain by one of the largest exploitable aquifer systems of the arid world, within which groundwater reserves might be substantial (Quinn, 1986; UN, 2013). More interestingly, the general distribution of groundwater salinity within the aquifer systems underlain the desert indicates that sedimentary basin is a potential source of fresh to brackish water, with total dissolved solids concentrations (TDS) less than 10,000 mg/l (Figure 1-1). However, groundwater with up to 200,000 mg/L TDS has been found in the vicinity of a potential discharge zone, known as sabkha Matti (Figure 1-1). This variation in water salinity could be a limiting factor to the use of these resources for future development. Thus, one of the major objectives of the current study was to identify the origin and mechanisms of salinization of groundwater resources in the major exploitable aquifers in the Rub' al Khali area. In addition, the proposed research was aimed to investigate the role of sabkha Matti in the regional hydrogeological system as a surface discharge point.

Sabkha is an Arabic translation for a salt flat. Sabkhat (plural of sabkha) are ubiquitous features in arid and semi-arid areas of the earth, especially in the Middle Eastern and North African countries. The exceeding of evaporation over precipitation is the main requirement for the occurrence of these systems. Sabkhat are characterized by flat landscapes, shallow groundwater levels (usually less than one meter below the land surface), and high-water salinity. Geologically, sabkhat systems provide important information about sedimentary history, depositional environment, paleoclimate indicators, and economically valuable evaporite minerals and brines (Kinsman, 1969). Furthermore, these systems are important in water resource assessments because they represent the discharge point or base level of local and regional groundwater and surface-water flow systems.

Figure 1-1: Location and groundwater salinity map of the Paleocene aquifer system in the Rub' al Khali basin.

In general, there are two types of sabkha deposits: coastal and inland sabkha. A coastal sabkha is a marginal marine mudflat where displacive and replacive evaporite minerals form in the capillary zone above a saline water table (Wood et al., 2002; Robinson and Gunatilaka 1991). In contrast, inland sabkhat are found in basins, away from the coast, and typically surrounded by sand dunes (Yechieli and Wood 2002). The formation of both coastal and inland sabkhat are explained by evaporation of continental groundwaters through the surface, which produces brines and subsequently causes the precipitation of evaporite minerals (Wood et al., 2002). The length and shape of sabkhat vary greatly. The more localized sabkhat extend only few hundred meters, whereas the more developed ones can attain hundreds of kilometers of an uninterrupted length, with a width of 30 kilometers or more (Al-Guwaizani, 1994).

In the Arabian Gulf countries, sabkha deposits cover an extensive area along the coasts of the Red Sea and the Arabian Gulf in addition to many other inland sabkhat that are scattered throughout the Arabian Peninsula (Figure 2.1) (Schulz et al., 2015). From the point of view of 'the present is the key to the past', sabkha geology has been studied intensively as sabkhas in the geological past are believed to be one of the environments important for the formation of petroleum (Kendall et al., 1968, 1998; Alsharhan and Kendall, 2002). Several studies on the sabkhat systems were conducted in the Arabian Gulf area, mainly on the coastal sabkha of Abu Dhabi (e.g. Holm, 1960; Evans et al., 1964; Kinsman, 1966; Johnson et al., 1978; Patterson and Kinsman, 1981; Fryberger et al., 1983). One of the early works on the coastal sabkha of Abu Dhabi (Holm, 1960) recognized two types of sabkha deposits on the western coast of the Arabian Gulf; arenaceous (filled with sand) and argillaceous (carbonate dominant). It was also noted that the direction of wind plays an important role in the development and modification of the sabkha environment. However, only a limited number of studies have investigated the hydrogeology and geochemical part of the inland

sabkhat (e.g., Smith, 1981; Sultan et al., 2008; Sultan et al., 2019), which will be the subject of the current study.

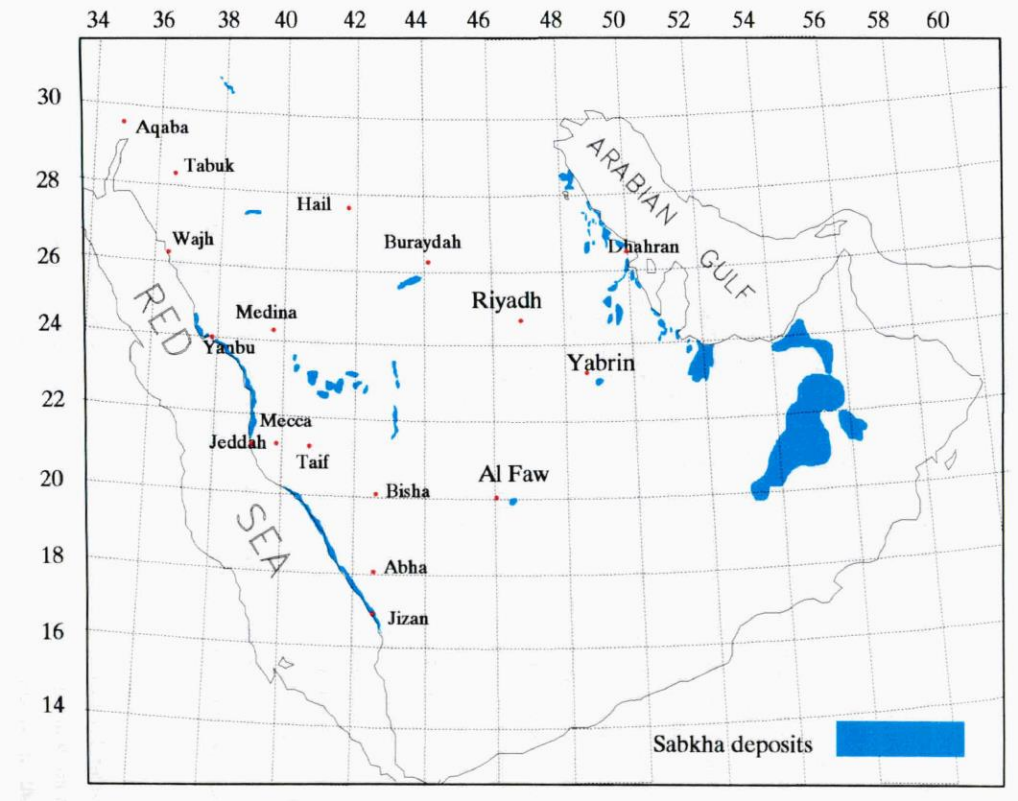

Figure 1-2: Map showing the spatial distribution of sabkha areas in the Arabian Peninsula (Adapted from Schulz et al., 2015)

1.2 Research Motivation

Water resources in arid areas such as the Arabian Gulf countries are very scarce due to the low rainfall and high evaporation. This complicates the supply of water for domestic and industrial uses. Currently, aside from this research work, there are no other published research projects that are dedicated to investigating the regional hydrogeology of the RAK. Most hydrogeological studies in the area have been restricted by the political borders between the countries. Thus, the main goal of this research is to initiate the building of a conceptual model of the regional hydrogeology of the Rub' al Khali basin in order to assess the constraints and opportunities of the

available water resources. In addition, understanding the mechanism and evolution of sabkha Matti system is important in the current study for assessing water resources because this sabkha represents a potential discharge point for the regional groundwater systems. Furthermore, the current research can provide valuable information about the sedimentary history, paleoclimate indicators, and depositional environment of the Rub' al Khali basin. Economically, sabkha Matti can be an important source of many economically valuable minerals for industrial and domestic purposes such as salts, magnesium, potassium and calcium. Understanding the characteristics of the sabkha system can lead to a better evaluation of its economic value.

1.3 Research Objectives and Scope

The main objective of this research is to initiate the building of a conceptual model of the regional hydrogeology in the Rub' al Khali basin. The research is aimed at assessing water resources in the Rub' al Khali basin and to investigate the role of sabkha Matti in the regional hydrogeological system as a surface discharge point. The objectives of the proposed research project are summarized as follows:

1. Examining the geology of the Rub' al Khali basin to develop structural and sedimentological concepts of the basin

2. Studying the hydrogeology of the Rub' al Khali basin to determine the regional water levels and water quality in the Tertiary aquifers

3. Characterizing and evaluating the geochemical and isotopic compositions of groundwater in the discharge zone of the Rub' al Khali basin at sabkha Matti area

4. Investigating the distribution of minerals (salt deposits) in the sabkha Matti, especially with regard to depth

5. Studying the sources of water and solutes to sabkha Matti and determining the contribution of underlying aquifers

6. Initiating the building of a conceptual model of the regional hydrogeology where the geology and groundwater flow as well as the water quality data are incorporated, with a special emphasis on the role of sabkha Matti

In order to achieve the objectives of this study, several approaches will be implemented. The research will consist of sedimentology, geochemical, isotopes, and analytical modeling components.

1.4 Research Methodology

Figure 1.4 illustrates the methodology that will be followed in this thesis to achieve the research objectives, and it is described below:

1. Acquiring and interpreting geophysical data from Saudi Aramco to investigate the tectonostratigraphic evolution of the Rub' al Khali basin
2. Study the impact of various geological features on the hydrology of the Rub' al Khali basin
3. An extensive literature review of:
    - The hydrogeology of the Rub' al Khali basin
    - The usefulness of stable and radioactive isotopes to study the hydrology in general
    - The utilization of hydrochemistry as a method of studying sources of salinity groundwater
3. Drilling boreholes and installing piezometers
4. Describing soil samples from the drilled wells in order to build a stratigraphic model
5. Collecting soil and water samples and analyze them for chemistry and isotopes

6. Conducting slug tests on selected wells to obtain the hydraulic parameters of the aquifers

7. Compiling all geological, stratigraphic, and hydraulic data to initiate the building of a regional hydrogeological model for the Rub' al Khali basin, with emphasis on the role of sabkha Matti.

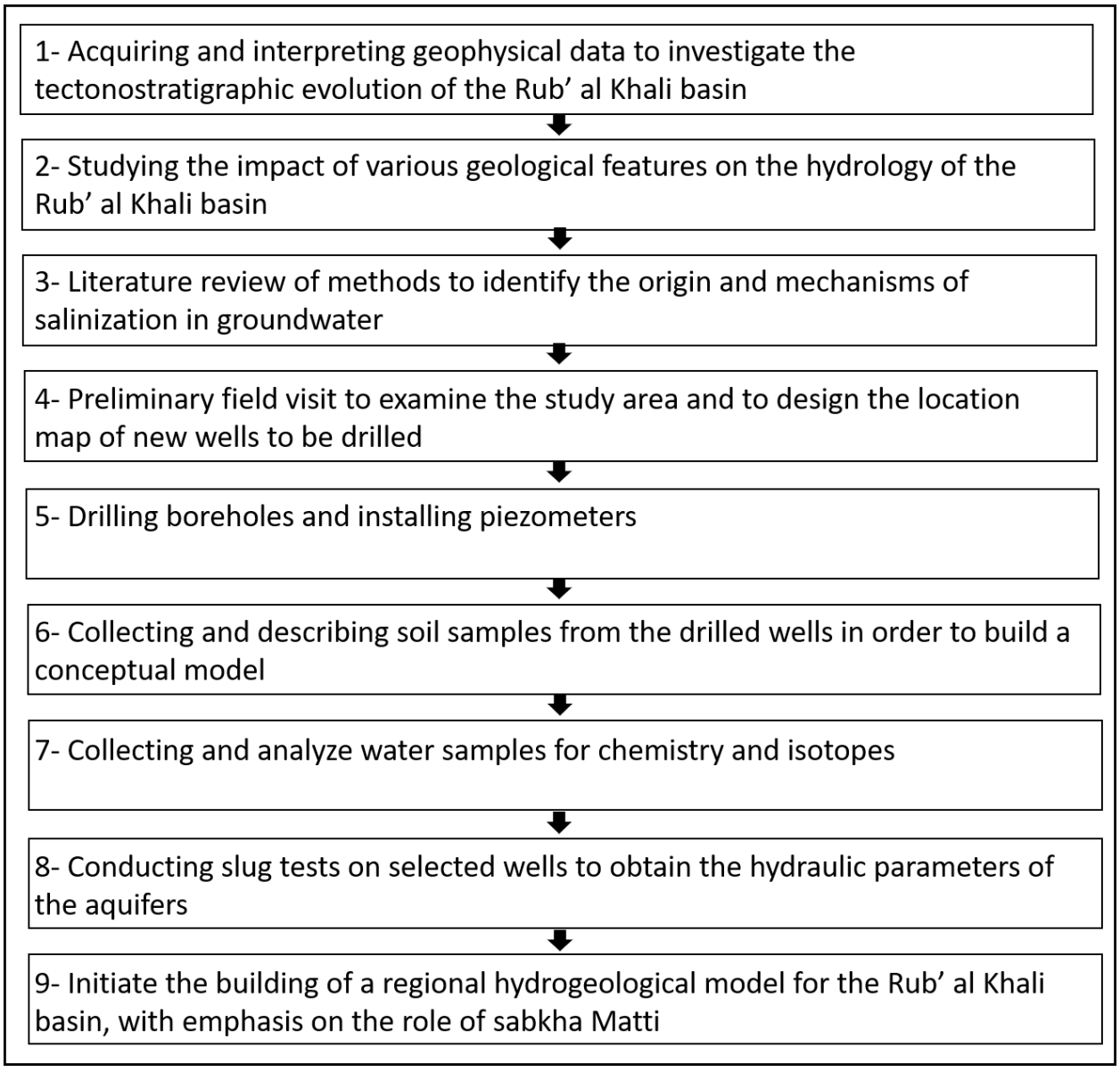

Figure 1-3: Research Methodology

1.5 Research Framework

In order to achieve the objectives of this study, several approaches were implemented. The research consisted of structure, sedimentology, geochemical, isotope, and modeling components. In general, it is important to review and understand the general geology of an area in order to build a good and comprehensive understanding of its water regime. This objective will include exploring the stratigraphy of the The Sabkha Matti and determining the distribution of minerals, especially with regard to depth. Understanding the water resources in any hydrogeological system is typically conducted by examining the geochemical parameters of the system along with its isotopic characteristics. Once all geological, hydrogeological, geochemical, and isotopic data are obtained and evaluated, it is possible to combine this information to initiate the building of a conceptual model of the geology and groundwater system of the Rub' al Khali basin. The framework and its working flow are shown in Figure 3.1 and will be explained in detail. The framework is divided into five modules, including: (1) Structural Conceptual Model; (2) Sedimentological Conceptual Model; (3) Groundwater Hydraulic Conceptual Model; (4) Geochemical and Isotopic Conceptual Model; and (5) Hydrogeological Conceptual Model.

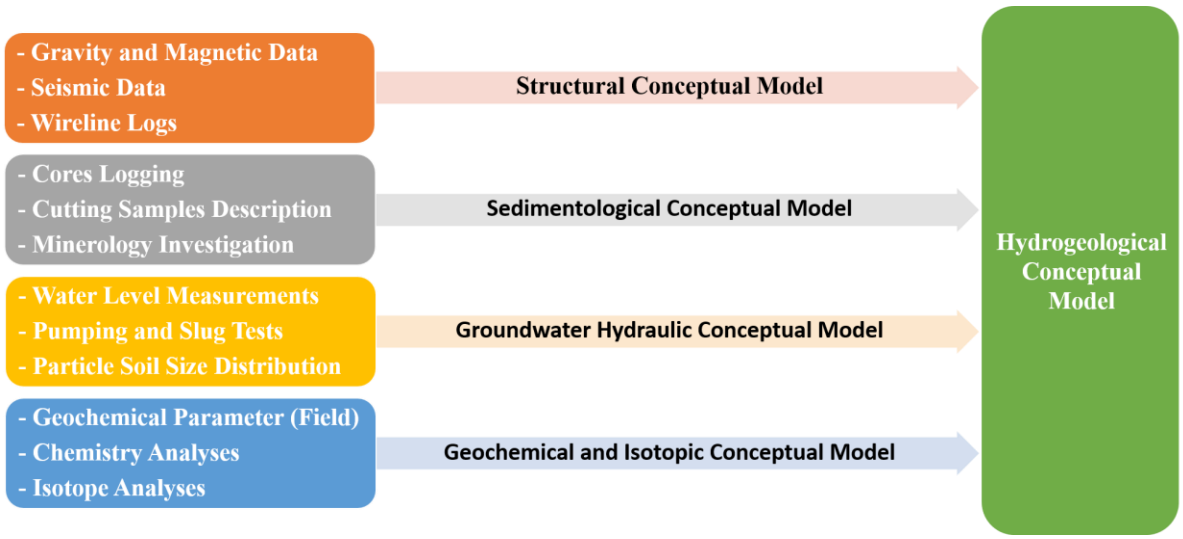

Figure 1-4: Research Framework

Chapter 2 Site Description

2.1 Location and Features

The Rub' al Khali basin (RAK) is a northeast-southwest trending, elongated depression in the southern Arabian Peninsula. It is the largest sand desert in the world, covering an area of about 250,000 square miles (650,000 square km) and extending from the center of the RAK sand sea towards the coast of Iran. A major part of the basin lies in southeastern Saudi Arabia, with lesser portions in Yemen, Oman, and the United Arab Emirates (Figure 2.1).

The sabkha Matti represents the northeastern edge of the RAK basin before the basin is open to the Arabian Gulf (Figure 2.1). The Sabkha Matti is one of the largest areas of continuous inland salt flats in Arabia. It is a wide, north-south trending, salt-covered depression that extends 150 km south from the western Abu Dhabi coastline and across the border between the United Arab Emirates and Saudi Arabia. Near the coast of Abu Dhabi, the sabkha Matti is characterized by a narrow strip of supratidal carbonate sands and evaporites that form a coastal sabkha. Southward it grades into an area of inland siliciclastic sabkha.

2.2 Climate

The Rub' al Khali basin falls within a hyper-arid zone of the world. The area has only two recognisable seasons: (1) a prolonged dry summer from April to November, and (2) a short winter from December to March. The average temperature for the day in the summer is 47° C, reaching as high as 56°, while it may fall to below 13° C in the winter.

Almost 90% of rain occurs during the winter, with very rare local showers occurring during July and August. The typical annual rainfall throughout the RAK interior is less than 25 millimetres. Around the fringe of the basin, the annual rainfall may range as high as 100 millimetres. Annual rainfall in the Oman highlands ranges from 150 millimetres to more than

300 millimetres. The Hadhramaut highlands in the southwest receive an average of between 100 and 500 millimeters of rain annually.

Figure 2-1: Map showing the location of the Rub al Khali basin and the sabkha Matti (Modified after Bishop, 2013)

2.3 Topography of the Rub' al Khali Basin

The Rub' al Khali basin is a large aeolian sand desert that occupies most of what is essentially a larger topographic basin. The basin is bounded by the topographic divides of: (1) the Tuwaiq Mountains to the west; (2) the Hajar Mountains in Oman to the east; (3) the Hadhramaut and Dhofar highlands to the south; and (4) the Zagros Mountains in Iran to the north, as shown in Figure 2.2.

The interior part of the basin is very restricted and includes only the area encompassed by the aeolian sands. Aeolian materials move into the area and pile up, as there is no topographic outlet

that coincides with the prevailing winds. This in turn causes the accumulation of sand dunes, which occur in a wide variety of shapes and sizes. The sand dunes range from small, simple, crescentic or rounded types to large complex massifs.

In the surrounding highlands of Oman, Saudi Arabia, and Yemen there are well-developed drainage systems. Toward the basin, however, these drainage patterns are buried by the sands and can rarely be traced. Other topographic forms that occur in the RAK include gravel plains and sabkhas. Gravel plains are more extensive in the northwest, and they are a typical plain of arid denudation. Sabkhas are more common in the lower topographic areas in the eastern part of the basin. They are usually underlain by sands with minor silt and clay size sediments, and are floored with salt and gypsum.

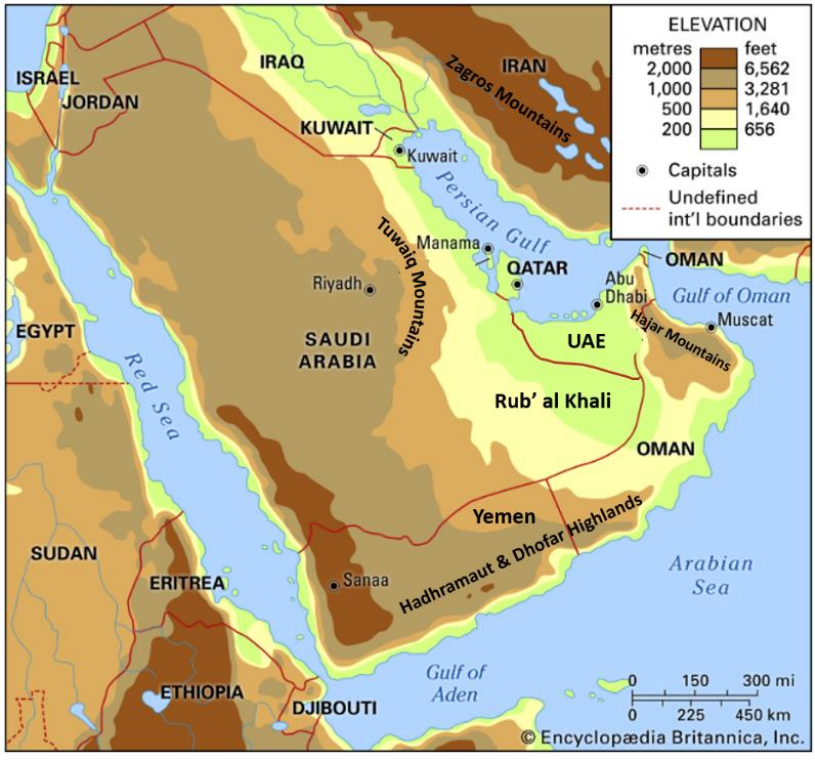

Figure 2-2: Topographic map of the Arabian Peninsula and surrounding plates (Source: britannica.com)

2.4 Geology of the Rub' al Khali Basin

The Arabian Peninsula consists of a large crustal plate which can be divided into two main structural provinces: (1) the Arabian shield; and (2) the Arabian shelf (Figure 2.3). The Arabian shield is located to the west of the Peninsula where Precambrian crustal rocks are exposed and locally covered by Tertiary volcanic. To the east, the Arabian shelf comprises a thick sequence of Paleozoic to Mesozoic sedimentary rocks. The Arabian shelf is bordered to the north and east by the mobile belts of the Zagros and Hajar Mountains, respectively. These mountains were formed during the Alpine orogeny, and are composed largely of Tertiary and Mesozoic carbonate rocks, which overlie a sequence of Paleozoic silicilastics.

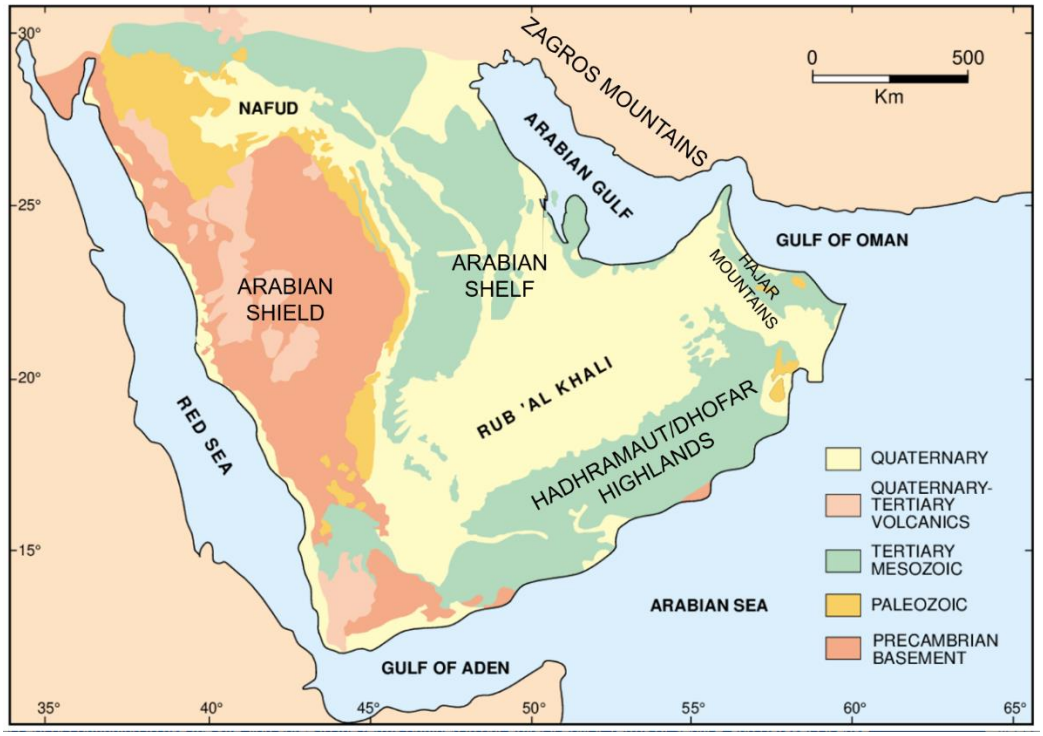

Figure 2-3: Geologic sketch map of the Arabia Peninsula (Modified after (Wender et al., 1998))

The RAK is part of a large depositional basin of the Arabian shelf (Figure 2.3). To the west of the RAK, a broad curved outcrop belt is exposed. These outcrops dip eastward at a low rate in ascending sequence off the Arabian shield and into the basin. In terms of the geological units which

occur within the RAK basin, all geological formations generally thicken basinward and most lateral lithologic changes are gradual over great distances. Marine carbonates are the dominant lithology within the basin. Evaporites are common, especially in the upper Jurassic and Lower Eocene while coarser clastic are more common in the Cretaceous.

2.5 Groundwater in the Rub' al Khali Basin

The majority of groundwater in the RAK basin occurs in the more porous and permeable rocks such as the coarser sands and more granular dolomite and dolomitic limestones. Groundwater also occurs in channel solution cavities in local areas. The groundwater in these rocks may be classed generally as connate, meteoritic, or a mixture of both. Groundwater occurs under either water table conditions or under artesian conditions. Water table conditions occur where the upper surface of the saturated zone in not bounded by impermeable formations such as in Quaternary sediments and outcrop areas. Artesian conditions occur where groundwater is confined under hydrostatic pressure by overlying impermeable formations. These conditions occur in most water-bearing zones below the Neogene aquifer system.

2.5.1 Recharge

Groundwater recharge is a hydrologic process by which water moves downward from surface water to groundwater. Recharge of the water-bearing zones in the RAK is derived mainly from precipitation. Rate of recharge from rainfall is dependent upon several factors: (1) amount of rainfall; (2) areal extent of the outcrops of the water-bearing formations; and (3) permeability of the intake beds. Despite the extreme aridity, studies using remote sensing techniques have demonstrated that recharge does currently occur across the entire RAK basin. While it is not clear how much of this recharge goes to the replenishment of the aquifers, isotope studies have indicated the presence of a local recharge component from present-day rainfall. The bulk of the groundwater

in the basin is, however, believed to have been recharged during the pluvial periods between 10,000 and 30,000 years ago. The areal extent of the outcrops is an important factor because more water may enter a water-bearing zone if its intake area is larger rather than smaller. The intake beds of some formations extend beyond the drainage divide of the surrounding highlands in the RAK. The magnitude of recharge to these formations is thus very challenging. Permeability of the intake beds is a limiting factor for recharge to water-bearing zones. Conditions are more favorable for recharge in unconsolidated sediments where permeability is high. Low permeability in outcrops of the denser rocks in the highlands promotes sheet wash, thereby restricting local recharge during periods of rainfall.

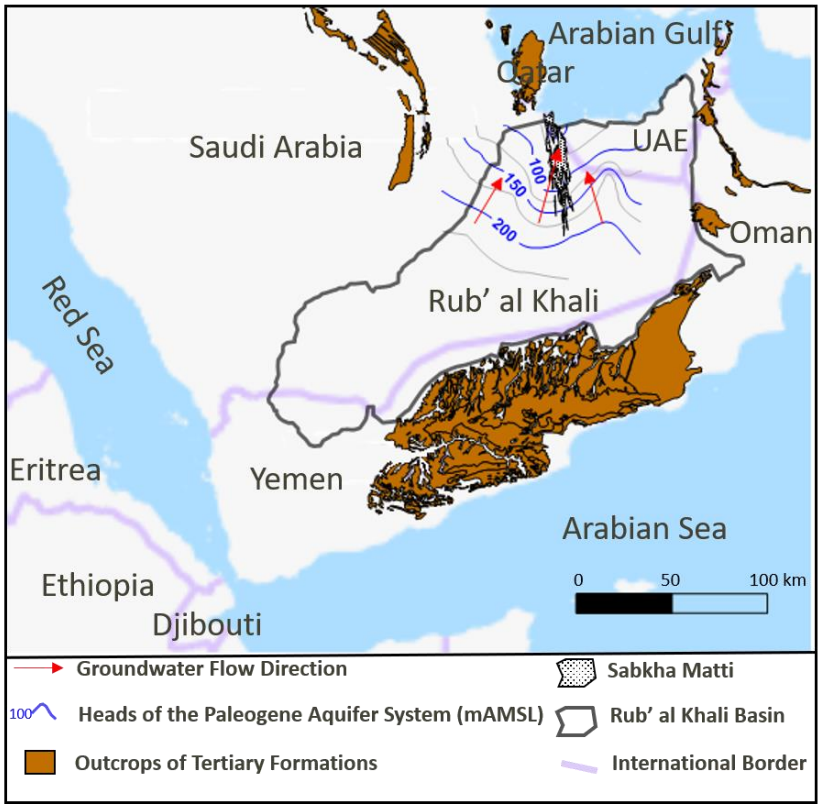

Figure 2-4: Regional movement of groundwater in the Paleogene aquifer system in the Rub' al Khali

2.5.2 *Movement of Groundwater*

Groundwater moves from points where the water table is high to points where the water table is low, and the resultant slope is known as the hydraulic gradient. Regional movement of groundwater in the RAK is simple. The water moves outward from the outcrops in the west and south where the water table has a higher altitude, and dips down in an easterly and north-easterly direction, where the hydrostatic head is progressively lower (Figure 2.4). Along the western edge, movement is to the east and east-southeast. However, the detail movement of water is extremely complex. There are several factors that affect the flow in the RAK basin, including heterogenicity of the water-bearing zones and variations in the thickness, porosity, and transmissibility. These factors will be ignored in order to simplify the behaviour of the water movement in the RAK area.

2.5.3 *Discharge*

Groundwater discharge is the term used to describe the movement of groundwater from the subsurface to the surface. In the RAK, groundwater is naturally discharged through springs and by evaporation. Depression springs occur where the topographic surface dips beneath the regional water table, mostly in the eastern and northern of the RAK. Many of the sabkhas in the eastern RAK act as depression springs as well. As this type of depression spring is large and shallow, there is a large amount of evaporation. Natural discharge from artesian water-bearing zones probably occurs by seepage through the confining beds into other water-bearing zones, but direct discharge to the surface is not known.

Capillary fringe is the subsurface layer above the water table and below the boundary of saturation in which groundwater seeps up from a water table by capillary action to fill pores. Evaporation of capillary fringe water is a common natural discharge in the southeastern area of the RAK, where the water table is only three to six feet below the surface. The evidence for this type of discharge

is the presence of soil moisture at or near the surface, even during dry seasons. The height to which capillary fringe water will rise depends upon local conditions. In fine materials such as silts, it may be as much as eight feet or more. In coarser materials, it is much less.

Chapter 3 A scoping review of research on methods to explain the origin of salinity in groundwater and the mechanism of sabkha formations

3.1 Introduction

This chapter reviews the existing literature to provide background on the mechanism of sabkhat formations and to review previous methods to explain the origin of water and solutes. Previous efforts are highlighted with respect to using hydrochemistry and isotopes to identify sources of water and solutes to sabkhas, and applying a geological approach to determine the regional extent of aquifers and explore the hydraulic connections between different geological formations. The chapter concludes with the recommendation of further steps to be developed in order to initiate the building of a conceptual hydrogeological model of the RAK basin with a special emphasis on the role of the sabkha Matti.

3.2 Mechanism of Sabkha Formations

The formation of sabkha deposits, their geological/geomorphological features and their geotechnical properties have been described by many investigators (e.g., Kinsman and Park, 1969; Butler, 1969; Ellis, 1973; Hsü and Siegenthaler, 1969, Kinsman, 1969; Hsü and Schneider 1973; Gavish 1974; McKenzie et al., 1980; Akili and Torrance, 1981; Patterson and Kinsman, 1981; Abu-Taleb and Egeli, 1981). Based on these studies, three main models have been proposed to explain the formation of sabkhat: (1) the seawater-flooding model; (2) the evaporative-pumping model; and (3) the ascending-brine model (Figure 3.1). Kinsman (1969) recognized the presence of seawater in the supratidal zone of the aquifer underlying the coastal sabkha of Abu Dhabi and proposed the "seawater-flooding model" (Kinsman, 1969; Butler, 1969; Butler et al., 1973; Patterson and Kinsman, 1977, 1981, 1982). This model suggests that storm surges force seawater inland which then recharges the aquifer to be refluxed to the Arabian Gulf (Figure 3.1A). Although this model is widely referred to, there are several physical and hydrologic problems with this

model. For example, the seawater is less dense than the interior sabkha water and therefore would lie on top of the waters, and not mix.

A combination of field observations and laboratory studies by Hsü and Siegenthaler (1969), Hsü and Schneider (1973), McKenzie et al. (1980), and Müller et al. (1990) led them to propose a conceptual model of the hydrology of a sabkha based on "evaporative-pumping model". This model suggests that annual evaporation from the sabkha induces lateral flow of both seawater and groundwater into the aquifer underlying the sabkha to replace the water lost to evaporation (Figure 3.1B). This model has the advantage of introducing observed continental solutes into the system. Moreover, it has been suggested that the process of evaporative-pumping has an important role to play in the dolomitization process (McKenzie et al., 1980) but the exact cause of dolomitization in the northern Gulf is controversial (Gunatilaka, 1991). This association is based on the premise that the presence of a vertical hydrologic gradient facilitates a greater supply of Mg ions to the carbonate factory in the wet sediments. This is in contrast to a normal horizontal hydrologic gradient. More recently, Wood et al. (2002) examined the water and solute fluxes and isotope geochemistry of the Abu Dhabi sabkha in order to evaluate the previous models; the seawater-flooding and evaporative-pumping models. The results showed that the previous models are inappropriate for this system, and a new "ascending-brine model" was proposed (Figure 3.1C). Based on this model, it was concluded that that 95% of the solutes are derived from ascending continental brines; minor amounts are derived from rainfall and from groundwater entering from up-gradient areas. It was also found that nearly 100% of the annual water loss is from evaporation and not lateral discharge. Furthermore, the investigation revealed that direct rainfall on the sabkha and subsequent recharge to the underlying aquifer account for 90% of the annual water input to the system, while the remaining 10% comes from both lateral and ascending groundwater flow.

Therefore, this study showed that water and solutes in this sabkha system are from different sources.

Among the three models, the ascending-brine model is the only hydrologically balanced model, which makes it the most acceptable model. This model has been verified on the coastal sabkha in the Emirate of Abu Dhabi, which is exposed as a strip of sediments 300 km long and 15 km wide (Figure 1.2). In the current study, the applicability of this model on an inland sabkha Matti that is 150 km long and 80 km wide within the RAK desert will be evaluated. In addition, in the study done by Wood and Sanford (2002), it was assumed that one of the Tertiary deep formations was the main source of solute to the sabkha. This assumption was made based on the direction of the groundwater gradient and the water flux calculations. This assumption has not been validated by chemistry or isotope analyses, which will be the subject of the current study. Knowing that there are several major aquifers in the relevant area which can be dated from the Tertiary era, determination of the particular Tertiary formation that contributes to the sabkha was not achieved in the previous study. This is mainly because the maximum depths of the wells were ~100 m, covering only the shallow sections of the Tertiary aquifers. In the current study, access to hydrogeological data that covers the entire Tertiary section to ~1000 m will be obtained. knowing the exact source of salinity is crucial to exploring the hydraulic connections between different formations in the area.

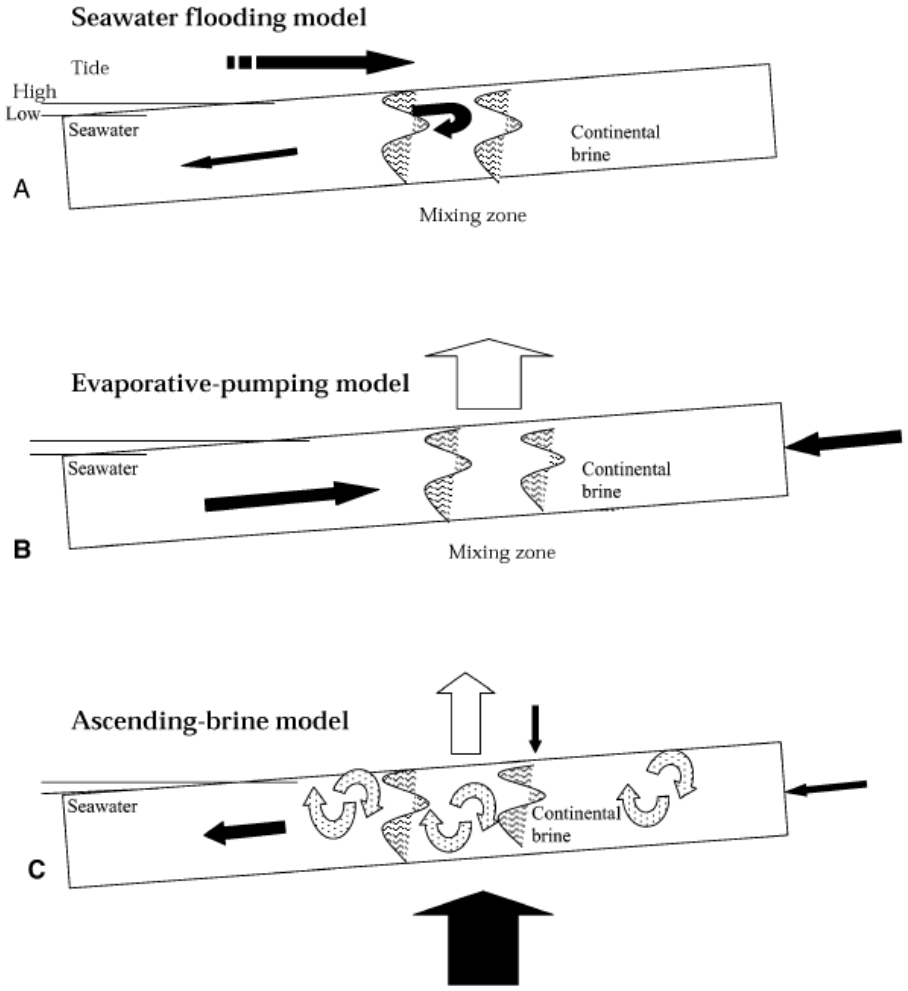

Figure 3-1: Diagram illustrating sources of solutes in the (A) seawater-flooding model, (B) evaporative-pumping model, and (C) ascending-brine model. (From Wood et al., 2002).

3.3 Isotopes in Hydrology

Isotopes are variant atoms of an element containing the same number of protons, but a different number of neutrons, in their nuclei. They are notated by their atomic mass numbers, which represent the total number of protons and neutrons in the nucleus (Clark, 2015). For example, the most abundant isotope of oxygen is Oxygene-16 (^{16}O), which has eight protons and eight neutrons. Most elements have known isotopes, and for the most part, the different isotopes of an element remain nearly identical in terms of chemical behavior, as they still have the same number of protons (Yurtsever and Araguas, 1993). However, there are some small variances that occur due to the differences in mass between isotopes. These differences in mass are the main cause of isotopic fractionation during physical, chemical, or biological processes (Kendall & Caldwell, 1998). Some isotopes are stable, while others are radioactive (Clark, 2015). Stable isotopes will not break down, while radioactive isotopes will undergo radioactive decay and the decaying nuclei will form other isotopes (Genereux et al., 2009). Both types of isotope have a number of scientific applications.

In the sabkha setting, the use of stable isotopes has been successfully applied to determine the presence of different water sources/types and to investigate the hydraulic connections between different formations. Some of the main applications of stable isotopes in the sabkha setting are summarized in Table 1.1. To identify a source of water, the stable isotopes oxygen (^{18}O) and hydrogen (^{2}H) are the most relevant isotopes. Robinson and Gunatilaka (1991) used ^{18}O and ^{2}H to show that deep, ancient groundwater in southern Kuwait is a major source of water in the sabkhas of the northern Arabian Gulf. To investigate the origins of the formations' waters or to explore the geochemical evolution processes that influence formation water chemistry in sedimentary basins, the use of chlorine (^{37}Cl) and bromine (^{81}Br) isotopes can be a valuable tool (Eastoe et al., 2001;

Bagheri et al., 2014; Shouakar-Stash et al., 2006 and 2007; Shouakar-Stash, 2008. Duane et al. (2004) and Wood et al. (2005) used chlorine stable isotopes (^{37}Cl) to identify water mixing zones and determine the role of physical mechanisms such as diffusion.

Table 3-1: Potential application of stable isotopes in a sabkha environment

Isotope	Potential Application
Oxygen (^{18}O) and Hydrogen (^{2}H)	• Origins of water • Source of replenishment of groundwater • Hydraulic interconnections • Palaeohydrological indicators
Chlorine (^{37}Cl) and Bromine (^{81}Br)	• Origins of original formation water • Geochemical evolution processes
Sulfur (^{34}S)	• Natural tracer for sulfate in water
Strontium ($^{87}Sr/^{86}Sr$)	• Water-mineral interactions
Carbon (^{13}C)	• Origin of carbon compounds
Boron (^{11}B)	• Zone of continental and marine water mixing

Analyses of bromine stable isotopes were used to examine the geochemical evolution of the Abu Dhabi sabkha in the UAE (Shouakar-Stash et al., 2006). To determine sulfur sources, the stable sulfur isotopes (^{34}S) are mainly used. Moreover, additional information about the sources of sulfate and about the geochemical environment in which the sulfate is found can be obtained from analysis of the stable oxygen isotope (^{18}O) of dissolved sulfate. Berner et al. (2002) used (^{34}S) and (^{18}O) of SO_4^{2-} to identify zones of variable groundwater mixing and significant amounts of bacterial sulfate reduction. To assess water-mineral interactions, especially where marked hydrogeological variations occur, the strontium isotopes ($^{87}Sr/^{86}Sr$) are commonly applied.

Müller et al. (1990) used Sr isotopes to separate groundwater and marine water in sabkhas in Abu Dhabi. Insights on water-mixing zonation can be obtained from analyses of the stable isotopes of Boron (^{11}B). Duane and Zamel (1999) used preliminary B isotopic trends in the Al-Khiran sabkha (Kuwait) to signature fluid flux and noted that east–west gradients in B isotopic values along which indicate a narrow zone of mixing of continental and marine waters. To determine the origin of carbon compounds in groundwater, the stable isotopes of carbon (^{13}C) will be used.

Radioactive isotopes are generally used for age dating of waters. Information about the age of groundwater can be used to differentiate between different water sources at various times. There are several radioactive isotopes which are generally used for the age dating of waters. In groundwater studies, tritium (^{3}H) and carbon (^{14}C) are the most used. Analyses of $E^{3}H$ allow dating groundwater in the 1- to 50-year range, and it can be used to identify hydraulic connections between an aquifer and water input from different sources. Furthermore, the analyses of ^{14}C will allow the estimation of residence times and provide patterns in ages, which will be useful for comparison among different aquifers. In order to use isotopes as an approach when investigating the origin or fate of formation waters, it is crucial to understand the isotopic behaviors associated with various natural processes (Singleton and Moran, 2010).

3.4 Hydrochemistry as a Method of Studying Salinity in Groundwater

In this section, the sources of groundwater salinization will be investigated using geochemical techniques. These techniques are utilized to identify and characterize different potential saltwater sources that mix and deteriorate the groundwater in the Tertiary aquifer in the vicinity of the Sabkha Matti. Identification of salinization sources is indicated simply by increasing in total dissolve solid (TDS) and all or most individual chemical constituents. Based on Richter and

Kreitler (1986), Kloppmann et al. (2002), and Mace et al. (2006), a variety of chemical constituent ratios can be used to distinguish between different salinity sources, including:

$$\left(\frac{K}{\mathrm{Na}}\right);\left(\frac{\mathrm{Ca}+\mathrm{Mg}}{\mathrm{Na}+\mathrm{K}}\right);\left(\frac{Na}{\mathrm{Cl}}\right);\left(\frac{\mathrm{Ca}}{\mathrm{Cl}}\right);\left(\frac{\mathrm{Mg}}{\mathrm{Cl}}\right);\left(\frac{\mathrm{SO4}}{\mathrm{Cl}}\right);\left(\frac{\mathrm{K}}{\mathrm{Cl}}\right);\left(\frac{\mathrm{Ca}+\mathrm{Mg}}{\mathrm{SO4}}\right);\left(\frac{\mathrm{SO4}}{\mathrm{Na}+\mathrm{K}}\right);\text{ and }\left(\frac{\mathrm{SO4}}{\mathrm{TDS}}\right)$$

In addition, minor trace elements such as bromide, strontium, and boron have been suggested by researchers when other chemical reactions occur after mixing of the saltwater source and fresh water (Whittemore & Pollock, 1979; Richter & Kreitler, 1986). The usefulness of these constituent as a salinization tracer may be, however, restricted to certain geographic areas (Richter & Kreitler 1986).

The four potential salinity origins related to similar fields are: (1) halite solution; (2) seawater intrusion; (3) upward leakage of natural deep saline groundwater; and (4) saline seep. Each potential salinity source is discussed in detail regarding the physiochemical characteristics and the significant geochemical parameters that can be utilized to distinguish it from other sources. In addition, the mechanism by which each source of salinity can contribute to the water salinity in this study area is also discussed.

(1) Halite solution

Johnson (1997) summarized the requirements for dissolution of halite as: (1) a supply of water unsaturated with respect to halite; (2) a deposit of salt located within the water flow regime; (3) a discharge point that will accept the resultant brine; and (4) hydrostatic pressure gradient to cause a flow of water through the system. If those requirements are met and the discharge point of the resultant brine is at the surface, mixing of brine and fresh water will occur. In order to

distinguish the brine forms by halite solution, the weight ratio between sodium and chloride is known to be a major indicator (Atapour, 2012).

In halite, the ratio between sodium and chloride is constant ($Na/Cl_{\text{weight ratio}} = 0.648$) (Richter & Kreitler, 1986). Brines that originate from halite solutions within groundwater systems exhibit a similar ratio as long as the concentration of TDS is high enough that the ratio is not affected by ion-exchange reactions (Diaw et al., 2012). Bromide is relatively conservative and is not easily removed by processes such as ion-exchange reaction or precipitation (Diaw et al., 2012). Therefore, it can also be used as a useful tracer of halite solutions in combination with chloride. The Br/Cl ratio in halite dissolution brines is expected to be less than 5×10^{-4} (Kharroubi et al., 2012).

According to Husseini and Husseini (1990), Allen (2007), and Smith (2012), late Ediacaran to early Cambrian salt is well known in the Zagros foreland (Hormuz Series) and Oman (Ara Group). Although reflection seismic line across the Sabkha Matti do not show any evidence of salt pillows or diapirs, other salt occurrences are located within local or regional groundwater flow systems and could be dissolved. Stewart et al. (2016) showed the extent of Hormuz salt continuing south from the UAE into the eastern RAK. Moreover, more than 500 exposed and buried salt daipiric structures in Iran along the northern coastal areas of the Arabian Gulf have been reported by Amini et al. (2010).

(2) Seawater intrusion

The principal mechanism governing the dynamic equilibrium between the seawater and groundwater in shallow coastal aquifers includes the frequency and intensity of tidal actions and their impact on introducing seawater inland, as well as changes in aquifer potentiometric

surface due to variation in recharge and discharge (Zarei et al. 2013). The Arabian Gulf contains roughly 45,000 mg/L of dissolved solids; of which 23,000 mg/L is chloride (Bashitialshaaer et al., 2011). Thus, it is possible that high chloride concentrations in shallow coastal aquifers can be attributed to seawater intrusion. Below are several indicators that can be used to distinguish seawater intrusion from other sources of salinity (Bear et al., 1999):

1. An elevated chloride concentration
2. The ratio of Cl/Br. In the Arabian Gulf, the Cl/Br of around 287 can be used as a tracer, because both chloride and bromide act conservatively.
3. Na/Cl ratios less than 0.86
4. Ca/Mg > 1
5. Ca/ (HCO_3 and SO_4) > 1

The positioning of the Arabian Gulf makes it a potential source of salinization for the shallow aquifers within the Sabkha Matti. Under natural conditions, groundwater flow in unconfined and shallow confined coastal aquifers is toward the ocean because of flow potential driven by topography. The flow in these shallow aquifers, however, responds to slow changes in sea level relatively quickly. During high tide periods, the seawater head can become higher than the water head in the nearby shallow aquifers. This will change the dynamic equilibrium and cause a reversal flow from the sea to the aquifers (Kelly, 2005). Conditions in deep confined aquifers may be somewhat different where regional groundwater flow reacts more slowly to changes in sea level elevations (Moujabber et al., 2006).

(3) Upward leakage of natural deep saline groundwater

The origin of natural saline groundwater in deep aquifers can be attributed to various sources, including connate water from the time of deposition in a saline environment, solution of mineral matter in the unsaturated and saturated zones, concentration by evapotranspiration, intrusion of sea water, or any mixture of the above (Pinti et al., 2011).

Numerous geochemical tracers have been used to investigate the sources of salinity in deep aquifers, including Cl/Br and Na/Br ratios (Davis et al., 1998). Cl and Br ions are commonly considered to be conservative tracers; hence they can be applied as indicators of water sources and rock interactions (Fontes and Matray, 1993; Davis et al., 1998). Calcium concentrations are sometimes very high in deep-basin brines, as TDS concentrations can approach several hundred mg/L (Ahmed et al. 2013). These brines will be composed almost entirely of NaCl and $CaCl_2$ (Lee, 2010). In addition, natural brines associated with mineral deposits often contain unusually high concentrations of ions not normally concentrated in most other brines, such as Cu, Zn, Ni, Co, Mb, Pb, and Ag (Mirnejad et al., 2011). Several fault systems have been determined in the eastern Rub Al Khali (Stewart et al., 2016), and if there has been little displacement along a fault, then the fault is more likely to develop fracture permeability and can act as a pathway for upward leakage from the underlying aquifers.

(4) Saline seep

A potential mechanism by which the salinity in the Sabkha Matti aquifer has evolved could be attributed to the saline seep phenomenon. Saline seep is defined as recently developed saline soils that are wet some or all of the time, often with salt crusts (Bahis and Miller, 1975). Several conditions have to be met for saline seep to develop, such as excess percolation of recharge water, soluble soil or aquifer minerals, a low-permeable unit at a relatively shallow depth, an internally drained flow system, and evaporation (Bahis and Miller, 1975).

Although the current aridity condition in the area does not seem to favour the saline seep mechanism, it could be hypothesized that this phenomenon contributed to the Sabkha Matti evolving during periods of enhanced precipitation during wetter paleoclimatic conditions in the past. Several periods of enhanced precipitation during the mid-Holocene and earlier episodes have been documented (Wood et al., 2010). In contrast to all other saline sources, dissolved sulfate concentrations in seep water may far exceed concentrations of dissolved chloride, which can be used as a distinguishable tracer (Thompson and Custer, 1976).

As a summary, significant geochemical parameters that are used to differentiate between various salinity sources are presented in Table 2.3.

Table 3-2: Significant geochemical parameters used to differentiate between various salinity sources

Source of Salinity	Significant Parameter
Halite solution	$Na/Cl_{\text{weight ratio}} \sim 0.648$ Br/Cl ratio $< 5 \times 10^{-4}$
Seawater intrusion	Cl/Br ratio around 287 Na/Cl ratios < 0.86 High Ca/Mg > 1 Ca/(HCO3 + SO4) > 1
Upward leakage of natural deep saline groundwater	Subtle and regional increase in salinity Brine comprised almost entirely of NaCl and $CaCl_2$ High concentrations of Cu, Zn, Ni, Co, Mb, Pb, or Ag
Saline seep	Major anion is dissolved sulfate

3.5 Geological Approach for Determining Reginal Aquifer Extents

The aim of this approach is to develop structural and sedimentological concepts of the Cenozoic formations in the RAK basin, particularly in the vicinity of the sabkha Matti. The nature and distribution of aquifers and aquitards in a geological system are controlled by two geological parameters: (1) lithology and stratigraphy; and (2) structure of geological formations. Each parameter is discussed in detail as follows:

3.5.1 Lithology and Stratigraphy

Lithology is the physical makeup of the sediments or rocks that make up a geological system, including mineral composition, grain size, and grain packing, while stratigraphy describes the geometrical and age relationships between various formations in any geological system. Generally, the lithology of the Cenozoic formations in the study area mainly comprises Neogene clastic sediments and Paleogene (Paleocene-Eocene) carbonate and evaporite rocks. A generalized stratigraphy and hydrogeological units of the studied aquifers are shown in Fig. 3. The principal aquifers of the studied aquifer system are from bottom to top: the Umm Er Radhuma, Dammam, and Hadrukh aquifers.

Throughout the Paleogene, the eustatic sea level was generally high, with high-frequency transgressive events, and sediments were deposited within a foredeep-setting during rapid erosion and subsidence of the sedimentary structures along the eastern margin of the Arabian plate (Powers et al., 1966). In the Paleocene, deeper-water environments were close to the eastern margin of the basin (e.g., Pabdeh Formations, Iran), while shallow-marine carbonates of Umm er Radhuma Formation extended far into the RAK as a lagoonal depositional environment. The depositional environment of Umm er Radhuma eventually shoaled to become a restricted lagoonal to supratidal sabkha setting in which the Rus and Sachun evaporite formations were deposited (Guiraud et al.,

2001). During the Eocene, maximum flooding was reached which favoured the deposition of shallow to deep marine sediments (Dammam Formation).

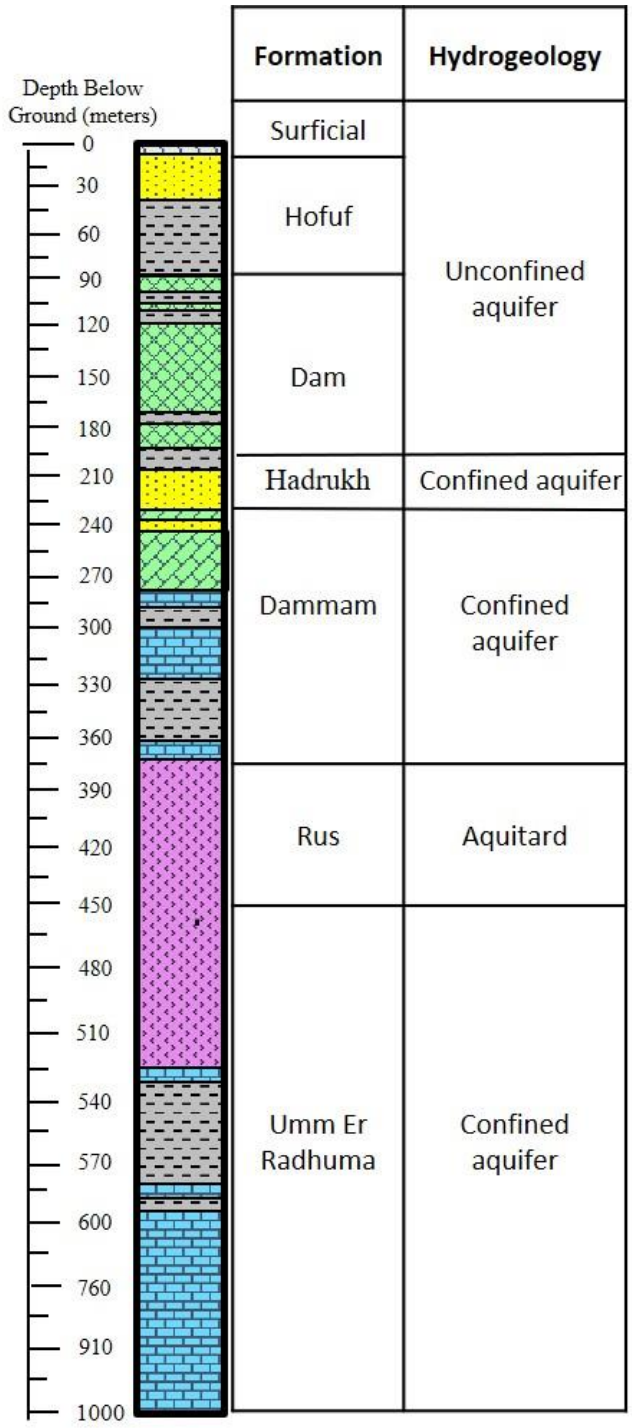

Figure 3-2: Generalized stratigraphy and hydrogeological units of the study area.

During the Neogene, a strong compression occurred as Arabia separated from Africa by the Red Sea rift in the west and was driven into Eurasia to the east. As a result of this continental compression and collision, a massive supply of continental (Hadrukh Formation) to transitional-marine sediments (Dam Formation) were deposited on the eastern flank of the RAK basin (Al Jallal, 1995). In the interior of the basin, lacustrine sediments belonging to the Hofuf Formation were deposited. In the subsiding Zagros foredeep, continental to deltaic clastics occurred and shallow-marine clastics accumulated (Agha Jari Formation).

3.5.2 Structure

Structural features such as folds and faults are the geometrical properties of the geologic systems produced by deformation after deposition or crystallization. Folding and faulting of sedimentary rocks can create very complex hydrogeologic systems in which determination of the locations of recharge and discharge zones and flow systems is challenging. A fault is a planar feature or discontinuity across which the elevations of specific rock horizons are displaced. Several Precambrian fault-bound basins subcropping the RAK Phanerozoic succession (Dyer and Husseini, 1991). Faults can act either as pathways for water movement or as flow barriers, depending upon the nature of the material in the fault zone. If the fault zone consists of fine-sized materials, the fault zone will have a very low hydraulic conductivity. In contrast, if the fault zone has hydraulically conductive materials and high porosity, it can serve as a conduit for groundwater movement.

A geological fold occurs when one or a stack of originally flat or planar surfaces is bent or curved as a result of permanent deformation. Several folds with an ENE-WSW axis trend were identified in the RAK basin (Hessami et al., 2001). Folding can affect the hydrogeology of sedimentary rocks in several ways. The most obvious one is the creation of confined aquifers at the centers of

synclines. The confined portions of the aquifer in the fold may have low hydraulic conductivity because of poor groundwater circulation (Fetter, 2000). If the fold is broad and gentle, a shallow, confined aquifer that extends over a large area can be created. This might be a good source of water if sufficient recharge can occur through the confining layer.

Late Ediacaran to Early Cambrian salt is well known as the Hormuz Series in the Zagros foreland, UAE and Oman (Smith, 2012). In Late Pliocene, these salts have risen to surface piercing through overlying thick sedimentary rocks and profoundly influenced the forms of salt domes, plugs, and other diapiric structures (Li et al., 2012). Several factors have caused the rise of the Hormuz salts, including salt overburden, salt buoyancy, and basement faulting. These have caused the production of salt-flowage anticlines, and rows of such anticlines were formed by compressional-folding in the Late Pliocene (Thomas et al., 2015). The highly plastic Hormuz salt layer acted as a decoupling layer, disconnecting the sedimentary cover structures from the crystalline basement structures (Li et al., 2012; Mouthereau et al., 2012; Thomas et al., 2015; Perotti et al., 2016). The cross-section in Figure 2.13 highlights the Hormuz salt layers in black as well as the general structure of the eastern RAK basin. This cross-section has been generated based on both preliminary interpretations of collected data from field visits and published data in order to support the proposed research.

The process of implementing the geological approach for determining the regional aquifer extent starts with geological and geophysical data collection and compilation, such as on existing well data, logs, cores, seismic data, structures, and aquifer properties. Detailed geological investigation into the shallow geological formations is carried out by drilling shallow boreholes using methods such as Enviro-core or rotosonic. The cores are collected, transferred to the lab, and logged. Stratigraphic logs are produced, and the two cross-sections will be constructed. In addition, soil

samples are investigated via a polarized microscope for mineral compositions and examined by X-ray fluorescence and electron microprobe for their chemical compositions.

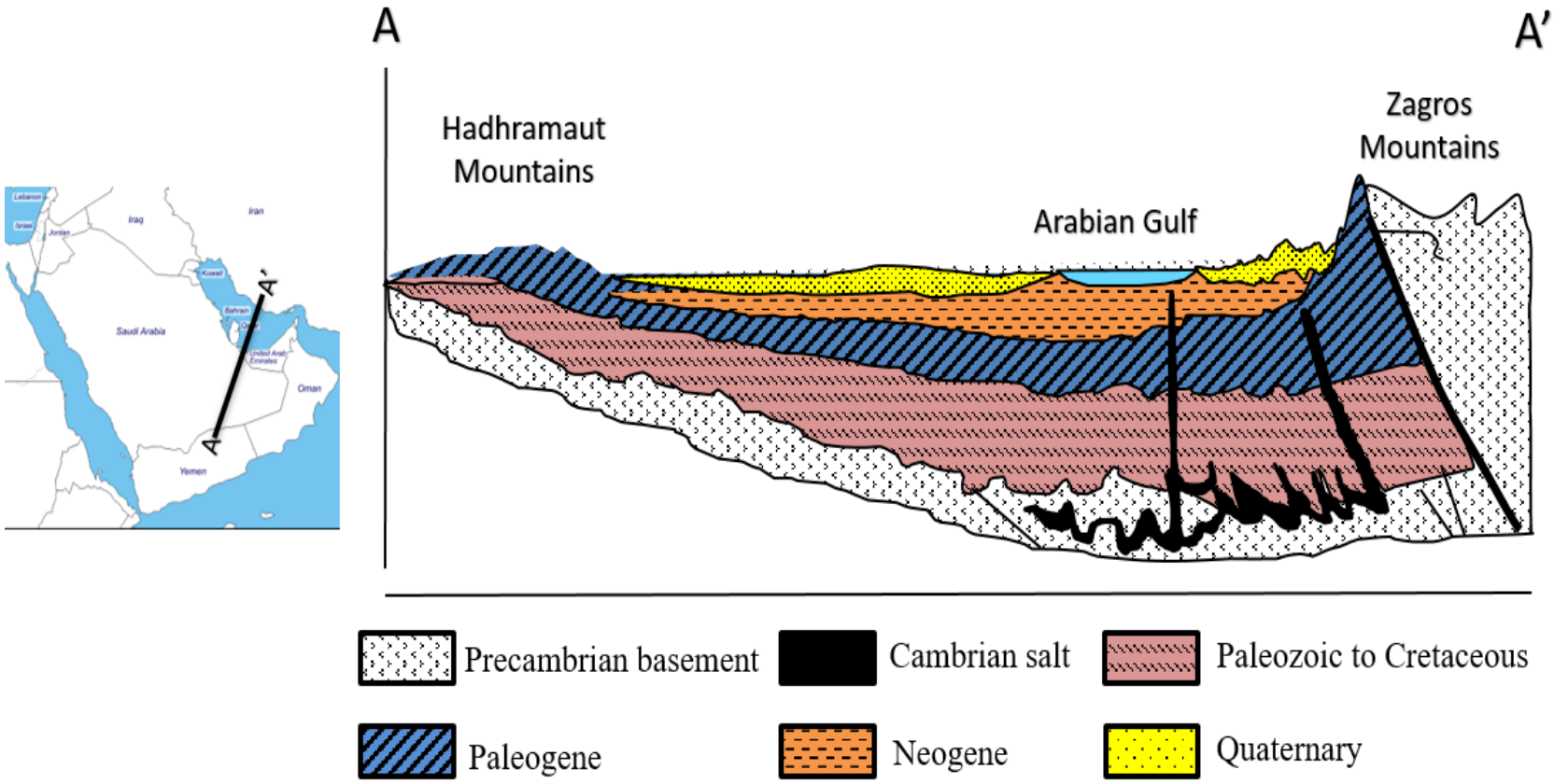

Figure 3-3: Cross-section showing the general structure and geology of the Rub' al Khali basi

Chapter 4 Origin of Solutes in a Regional Multi-Layered Sedimentary Aquifer System

This chapter is under review by the Applied Geochemistry Journal as follows:

Manuscript ID: APGEO-D-20-00581

4.1 Introduction

The Arabian Peninsula occupies an area of approximately 3,000,000 km^2 in southwestern Asia. It encompasses the political units of Saudi Arabia, Kuwait, the United Arab Emirates, Oman, Qatar, and Bahrain. A large portion of the peninsula is covered by sand desert, apart from narrow coastal and mountain areas. Natural water resources in the Peninsula are generally limited due to low surface rainfall and high evaporation rate, resulting in a scarcity of fresh surface water bodies such as rivers and lakes (Alsharhan et al., 2001). In fact, the region has some of the fewest absolute freshwater resources per capita (Elasha, 2010). Countries depend mainly on non-renewable, fossil groundwater that is stored in deep sedimentary aquifers. Most of these aquifers are being seriously depleted due to excessive pumping. Moreover, groundwater quality has deteriorated in many areas owing to salt-water intrusion, the management practices of waters produced by the oil industry, and intensive agricultural activities (Alsharhan et al., 2001). Rapid development and rises in populations have placed additional substantial strains on water resources in the region (Odhiambo, 2017), and currently, considerable effort is being spent to wisely manage and conserve groundwater aquifers, maintain water quality, and restore deteriorated aquifer systems in many areas of the Arabian Peninsula (UN, 2013). The Rub' al Khali (RAK) topographic basin is a northeast-southwest-trending, elongated depression in the southern Arabian Peninsula. It is the largest uninterrupted sand desert in the world, covering an area of about 650,000 km^2. A major part of the basin is in southeastern Saudi Arabia, with lesser portions in Yemen, Oman, and the United Arab Emirates (Fig. 4.1). The RAK basin lies in an arid region with no perennial rivers or lakes; however, groundwater reserves in mega Tertiary aquifers in the RAK basin have been estimated to be substantial (Quinn, 1986; UN, 2013).

The majority of the stored groundwater is brackish, with total dissolved solids (TDS) of less than 10,000 mg/l (UN, 2013), although groundwater with more than 100,000 mg/l TDS has been found near the border between Saudi Arabia and the United Arab Emirates. It is important that the origin and mechanisms influencing this elevated salinity be understood for better water resource management. The studied geological succession in this study comprises sedimentary rocks of the Lower Paleocene to Lower Miocene age, and the sediments primarily consist of the Umm Er Radhuma, Rus, Dammam, and Hadrukh Formations. In general, the thickness of each Formation increases from west to east, with average thicknesses of about 300, 180, 100, and 30m, respectively.

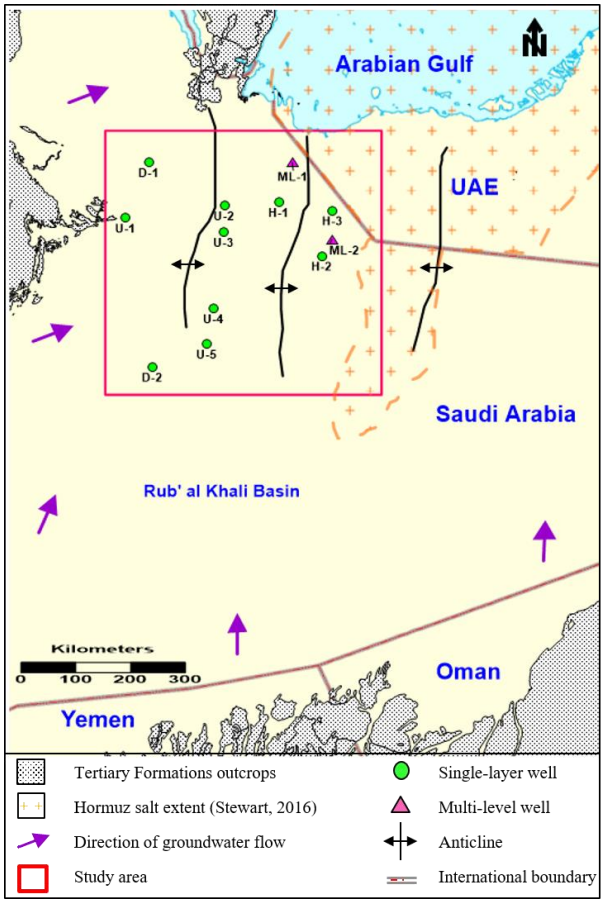

Figure 4-1: Location of the study area with principal hydrogeological features and sampling point locations

4.2 Hydrogeological Framework

The generalized stratigraphy and hydrogeological units of the study area are shown in Fig. 4.2. Outcrops of the Tertiary Formations occur along the western and southern borders of the RAK basin (Fig. 4.1). All the Formations dip gently away from the outcrops toward the east-northeast. The Umm Er Radhuma (UER) Formation of the late Paleocene to early Eocene age was deposited during a major transgression event that spread marine conditions over the Arabian Peninsula (Ziegler, 2001). Thus, the UER Formation ranges from a few to a maximum of 800 meters thick, and consists mainly of calcarenite and finely crystalline limestone which are deposited over initial calcareous shales at the base of the Formation. The top 60 meters of UER Formation is considerably dolomitized and karstified, which makes the Formation the most important aquifer in the RAK basin. In the part of the study area farther northeast, however, the upper part of the formation became marly, which may indicate a nearshore to lagoonal depositional setting. After the deposition of the UER Formation, the depositional environment shoaled to become a supratidal sabkha setting in which the Rus evaporite Formation was deposited (Guiraud et al. 2001). The Rus Formation is composed mainly of massive and dense anhydrite and gypsum, and can be mostly considered an aquitard. Throughout the Eocene, maximum flooding was reached (Ziegler, 2001), which favoured the deposition of shallow to deep marine sediments (Dammam Formation). The basal part of the Dammam Formation consists mostly of dense marl, and the best porosity has developed in the middle part of the Formation in association with the deposition of granular textured limestones. The uppermost portion of the Dammam Formation consists mainly of finely crystalline dolomitic limestone interbedded with compacted limestone and dense marl, which acts as a strong aquitard. In the Neogene, a strong compression occurred as Arabia separated from Africa as a result of the Red Sea Rift and was driven into Eurasia to the east (Ziegler, 2001). As a

result of this continental compression and collision, a massive amount of continental to transitional-marine sediments were deposited. The Neogene within the study area can be divided into three Formations, which are from oldest to youngest: the Hadrukh, Dam, and Hofuf Formations. In the Hadrukh Formation, about 30-50 meters of clean sandstone facies with excellent groundwater productivity were deposited only on the eastern flank of the RAK basin during the late Oligocene-Miocene. The confining unit for the Hadrukh aquifer belongs to 20-30 meters of marl and clay from the basal of the overlaid Dam Formation, while the Hofuf Formation is sandy marl with minor calcareous sandstone. Superficial Quaternary eolian sand dunes cover the surface of the study area.

All the targeted aquifers lie under confined conditions in the western and southern parts of the study area. Toward the east-northeast, artesian confined conditions are observed. Groundwater flow is generally directed toward the Arabian Gulf (Fig. 4.1). Moreover, the piezometric surfaces indicate the hydraulic potential for upward vertical groundwater flow in the study area. An important geological feature in the study area is a series of mainly north-south trending anticlines (Fig. 4.1), within which trapped hypersaline waters in deep oil reservoirs at about 900m are quite common (Birkle et al. 2013). Another geological feature in the study area is the distribution of 10km-deep salt pillows or diapirs of Ediacaran-Cambrian Hormuz salt (Fig. 4.1), which will be evaluated as a potential source of salinization. The extent of this mobile salt has been delineated in the vicinity of the study area only on the basis of seismic structuring using seismic data (Stewart, 2016), and has never been observed or cut into in any exploratory wells.

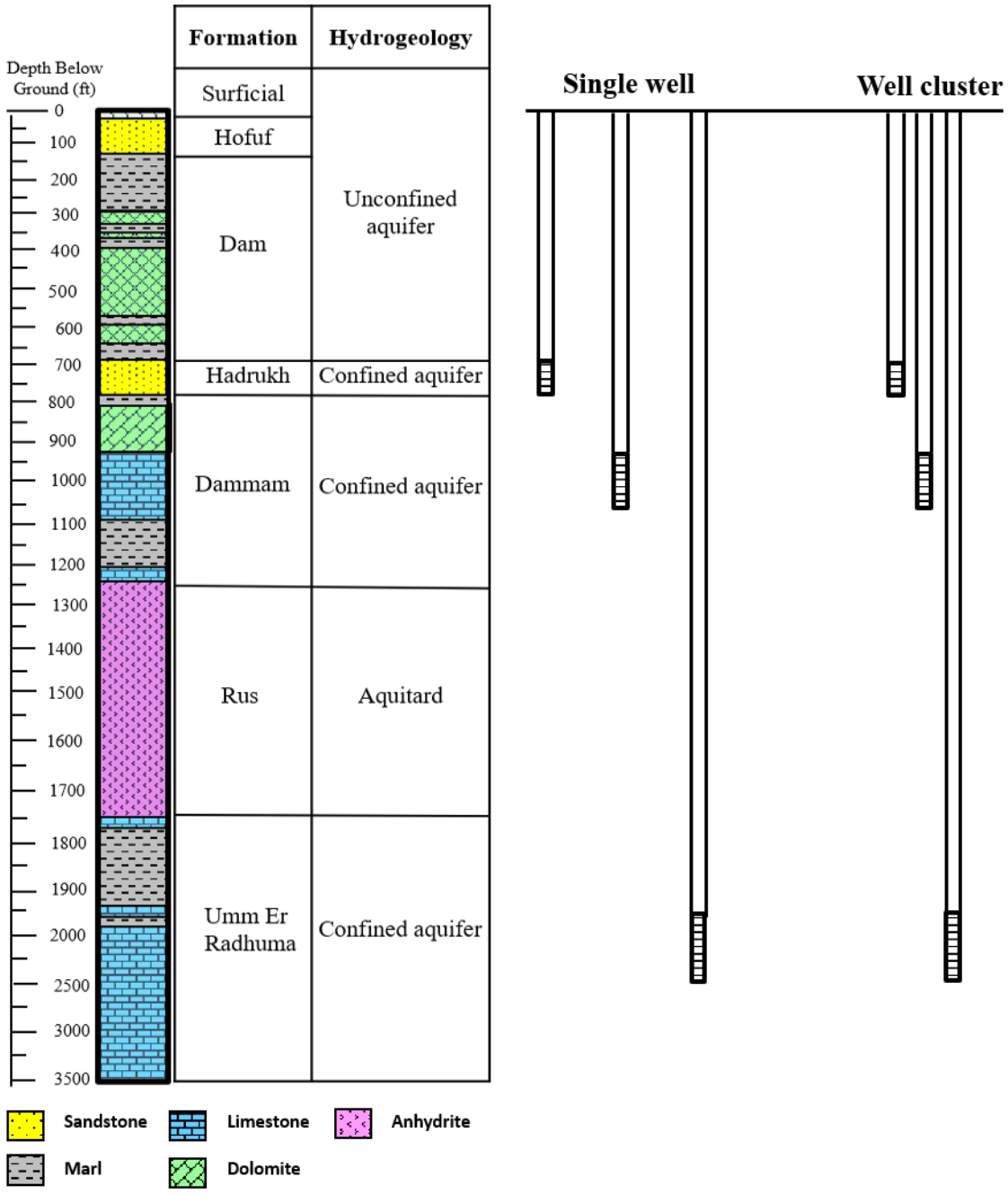

Figure 4-2: Generalized stratigraphy and hydrogeological units of the study area along with well types and designs

4.3 Sampling and methods

All the water wells were drilled with rotary drills into Tertiary aquifers in the Rub' al Khali basin. The wells were finished with 18 5/8" of surface casing up to the top of the targeted aquifer and were left without casing (i.e., open hole) for the remaining depth (Fig. 4.2). Each of the wells was provided with a cap, shut-off valve, and pressure gauge. Groundwater was sampled from ten single-aquifer drilling supply wells during three field campaigns between December 2015 to February 2017. Based on preliminarily field measurements from the three campaigns, two well cluster systems were drilled in an area where extremely high-water salinity had been detected. Each of the cluster wells was completed at different depths, and groundwater samples were collected from each aquifer individually to investigate any chemical or isotopic variations among the aquifers. In addition, one oil field water sample, from the Cretaceous oil reservoir within the study area, was taken after it was separated from the petroleum phase. Water samples from the Arabian Gulf were also collected during the course of this investigation. The locations of the sampling points are shown in Fig. 4.1. Analyses of the water samples for electrical conductivity (EC), pH, temperature, and dissolved oxygen content were carried out in the field using a portable HQ40d meter (Hach Ltd.). Field measurements of alkalinity were done using a Hach field titration kit and expressed as mg/L of equivalent HCO_3. The water samples were filtered through 0.45 μm filters and then acidified with double-distilled nitric acid for cation analysis and preserved unacidified for anion analysis. Analyses of major and minor ions were performed by the Isobrine Solutions laboratory in Edmonton, Canada, and the ALS laboratory group in Waterloo, Canada. Analyses of stable and radioisotopes were performed at the Isotope Tracer Technologies Inc. (IT^2) laboratory in Waterloo, Canada.

4.4 Results and Discussion

4.4.1 Hydrochemistry and distribution of salinity

The groundwater quality data for the collected samples are presented in Table 4.1. According to the classification scheme for formation fluids based on TDS load (Carpenter, 1987), the study area can be classified into brackish and saline zones (Fig. 4.3). The water samples in the brackish zone had TDS concentrations between 1,000 to 10,000 mg/L, while the saline zone contained water with a TDS concentration of >10,000 mg/L. For visual areal distribution and comparison of the relative ionic composition in the collected groundwater samples, Stiff diagrams were constructed (Fig. 4.4). The results from the Stiff diagrams show the changes in water type in all aquifers along the flow direction from the brackish to the saline zone. For instance, the relative proportions of major ions in the groundwater samples collected from the UER and DMM aquifers indicate a change in water type from Ca-SO_4 in the brackish zone to Na-Cl in the saline zone. Similarly, the ion compositions data from the groundwater samples obtained from the HDRK aquifer indicate a change in water type from Na-SO_4-Cl to Na-Cl. These geochemical evolutions in the three mega aquifers indicate that the studied aquifers were not under steady state condition and reveal that different geochemical processes for salinization between the brackish and saline zone may occur. Moreover, the vertical distributions of TDS concentrations and ionic composition were assessed based on the data collected from the two multi-level wells in the saline zone as well as the water sample from the oil field (Table 4.1). All these samples had remarkably similar ion compositions (Na-Cl), regardless of the aquifer (Fig. 4.4). The similarity in water type between the different Formation waters suggests that similar geochemical processes may be controlling the major ion chemistry in the saline zone of the aquifers (Appelo and Postma, 2005). The TDS concentration was observed to increase substantially with depth, as the median TDS concentration for

groundwater samples collected from the oil field, UER, DMM, and HDRK were 216,799, 116,382, 50,585, and 35,647 mg/L, respectively. This vertical variation in TDS concentration is probably due to flushing of fresh water to the residual saline water in the aquifer, as will be discussed in the stable isotope discussion section. The flushing-out processes seem to progressively decrease with increasing depth across all the geological Formations.

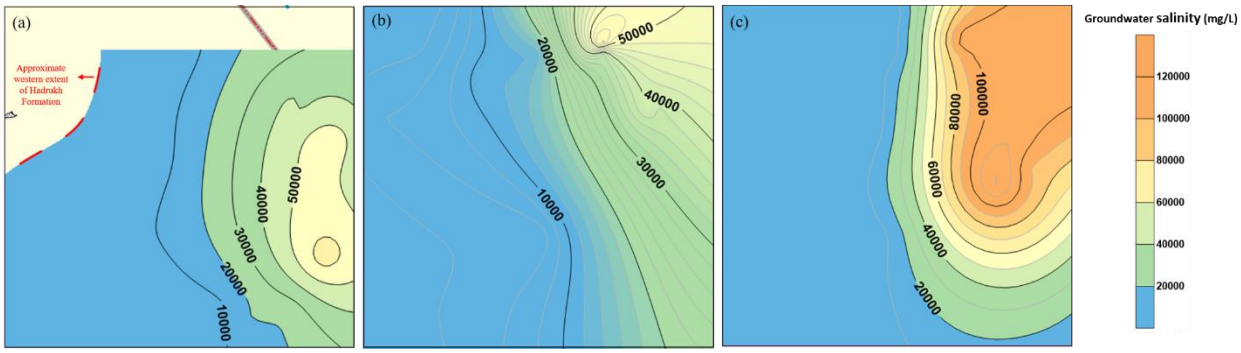

Figure 4-3: Groundwater salinity map for: (a) Hadrukh, (b) Dammam, and (c) Umm Er Radhuma Formations (Location of the mapped area is shown in Fig-4.1)

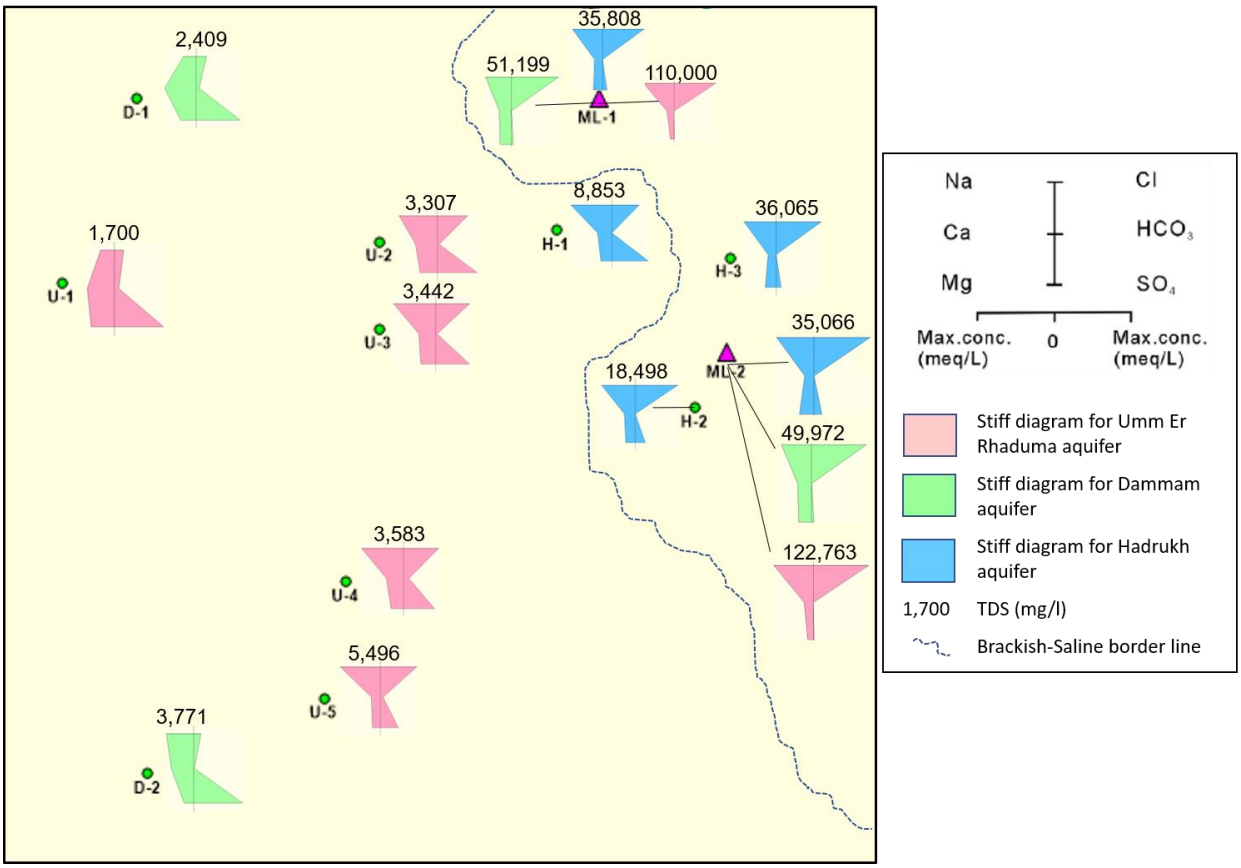

Figure 4-4: Stiff map plot for groundwater samples collected from Umm Er Radhuma, Dammam, and Hadrukh wells

4.4.2 Origin of salt

Major sources in the study area which may contribute to the production of an Na-Cl water type include: 1) present or paleo-seawater, or 2) dissolution of deeply seated Hormuz salt. To differentiate between these two sources, several geochemical indicators were used.

Cl/Br ratio

Chlorine (Cl) and bromine (Br) ions are highly soluble and are considerably conservative tracers during subsurface transport. Thus, both ions have been commonly used to investigate sources of salinity in Formation waters (Carpenter, 1978; Kharaka and Hanor, 2004; Frape et al., 2007; Shouakar-Stash et al., 2007; Shouakar-Stash, 2008; Bagheri et al., 2014). Moreover, the Cl/Br ratio has been historically applied to distinguish between different salinity sources such as halite

dissolution versus seawater intrusion (Carpenter, 1978). Carpenter (1978) evaporated seawater to generate the SET (seawater evaporation trend) of Cl versus Br (Fig.4.5). Evaporated seawaters plot directly on the SET, while halite dissolution waters plot above and to the left of the SET. The concentrations of Cl versus Br for all samples plotted on or below Carpenter's (1978) curve (Fig. 4.5).

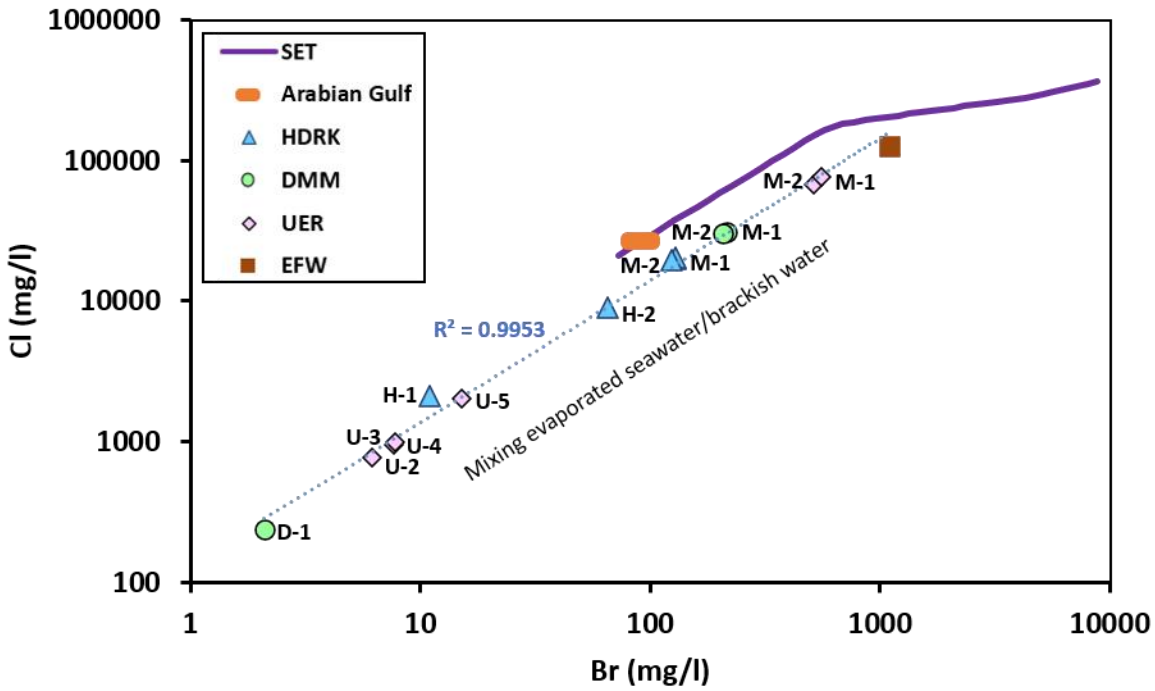

Figure 4-5: Br versus Cl concentrations of the oil field Formation water (EFW), Umm Er Radhuma (UER), Dammam (DMM), and Hadrukh (HDRK) aquifers. The solid line represents the seawater evaporation trend (SET) from (Carpenter 1978).

The Cl/Br ratio in the formation water from the oil reservoir which was produced as a co-product with hydrocarbons, almost coincides with the SET line. This result suggests that evaporated seawater is the main cause of the elevated salinity in the water from the oil reservoir. This explanation is common in the study area, as the presence of trapped paleo-seawater has been regularly proposed in water produced from hydrocarbon reservoirs (Birkle, 2013). Accordingly, the sample from the oil field will be considered as a probable paleo-seawater end member, and hereafter will be referred to as EFW (evaporated formation water). The elevated salinity in the

EFW sample is perhaps associated with a residual evaporated paleo-seawater that may have been trapped in the Formation during the time of deposition and/or during one of the seawater intrusion events throughout the geological history of the area. The ion concentrations of the saline samples from the three Tertiary aquifers plot on the right and below the SET. This suggests that evaporated seawater components may significantly contribute to the high groundwater salinity in these aquifers (Fig. 4.5). The downward displacement of the saline samples relative to the SET might be due to mixing between the brackish water and the evaporated seawater end members. This hypothesis is supported by a high linear correlation coefficient (R^2>99) of the mixing trend between samples from the brackish zone and the EFW sample. The high linear correlation coefficient of the mixing line implies a conservative behavior of Cl and Br during mixing.

Chloride versus $\delta^{18}O$

A comparison of the chloride concentrations and $\delta^{18}O$ values is illustrated in Fig. 4.6 in order to understand the salinization mechanism in the Tertiary aquifers. An increase in chloride concentrations due to dissolution of soluble salt should not theoretically correspond with $\delta^{18}O$ enrichment. In contrast, increasing chloride concentrations by evaporation would correspond with a gradual increase in $\delta^{18}O$ composition. This was the case for the EFW sample, where the highest chloride concentration (Cl =216,799 mg/L) corresponded to a significantly enriched oxygen isotope value ($\delta^{18}O$ =3.8‰). Similarly, high linear correlation coefficients appeared between the Cl concentrations and $\delta^{18}O$ values for the groundwater samples obtained from the three Tertiary aquifers (Fig. 4.6). Samples with high chloride concentrations correlate with higher $\delta^{18}O$ values, whereas samples with relatively lower chloride concentrations correspond to lower $\delta^{18}O$ values. A hypothetical halite dissolution trend does not explain any of the water compositions in the Tertiary aquifers, indicating that the solutes are being enriched mainly by evaporation.

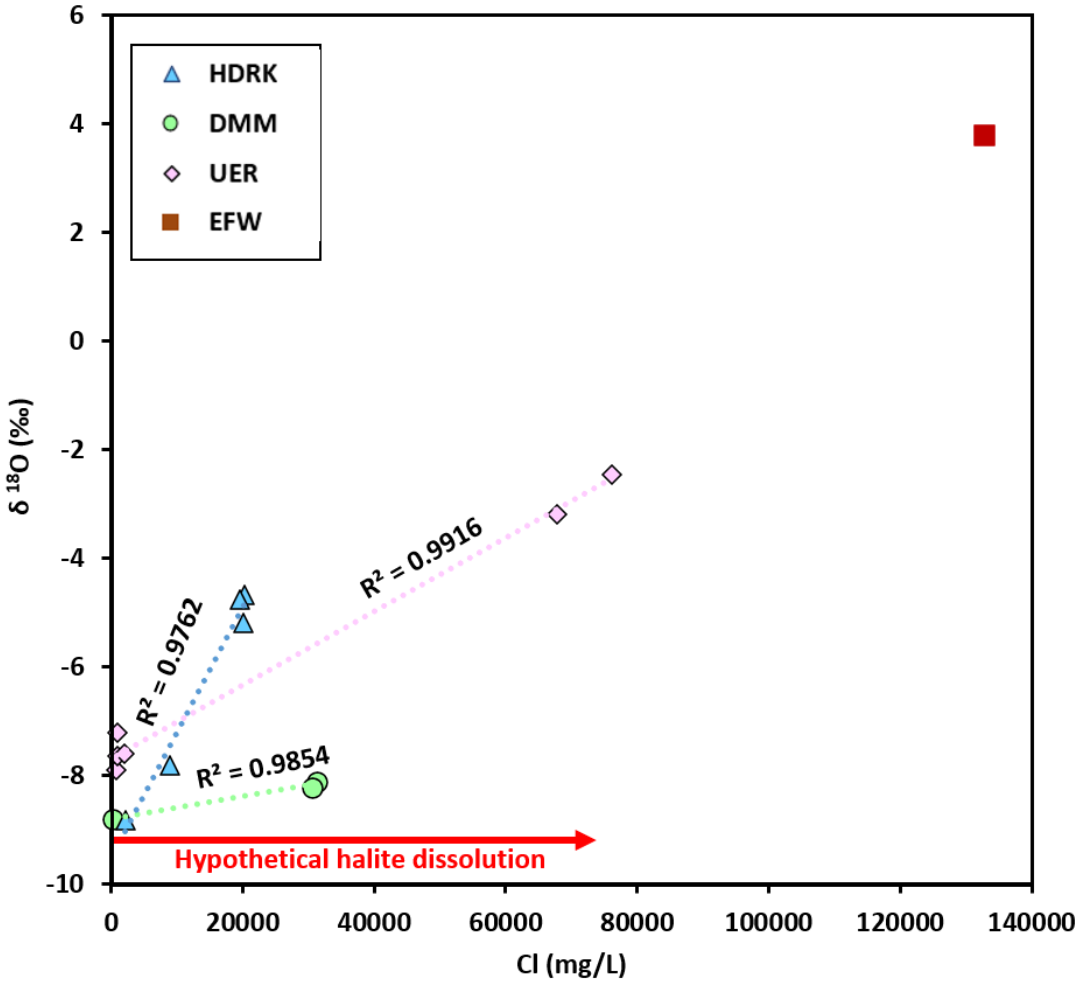

Figure 4-6: Plot showing the relationship between the isotopic composition of oxygen ($\delta^{18}O$) and chloride (Cl) concentrations for groundwater samples from the oil field Formation water (EFW), Umm Er Radhuma (UER), Dammam (DMM), and Hadrukh (HDRK) aquifer. The best- fit line for each aquifer (dashed line) is drawn through the brackish and saline waters. The solid red line represents the hypothetical halite dissolution trend for meteoric water.

δ^{81}Br compared to bromine concentration

The stable bromine (δ^{81}Br) isotope is considered conservative to changes in water-rock reactions, which makes it a valuable tool to investigate the origins of Formation waters (Shouakar-Stash, 2008). The δ^{81}Br isotopic compositions versus Br concentrations for the saline groundwaters from the three Tertiary aquifers are shown in Fig. 4.7. Moreover, data from the literature for the expected range of halite dissolution between +0.62‰ and +0.88‰ are also shown (Eastoe et al., 2001; Bagheri et al., 2014). The δ^{81}Br isotopic compositions for the Formation waters from the three

Tertiary aquifers are not within the range of halite dissolution (Fig. 4.7). This result rejects halite dissolution as the source of salinity. Remarkably, the range of $\delta^{81}Br$ for the two UER Formation waters (-0.12‰ to -1.11‰) was much lower compared to the $\delta^{81}Br$ range in Formation waters from the DMM (1.69‰ to 1.79‰) and HDRK (1.88‰ to 2.10‰) aquifers. In addition, the low $\delta^{81}Br$ signature of the UER samples was associated with the highest Br concentration among the three aquifers. In contrast, the relatively enriched isotopic signatures of $\delta^{81}Br$ from the DMM and HDRK Formation waters were accompanied by low Br concentrations. This may reveal that different dilution/mixing rates may occur for samples from various depths. The result also suggests the presence of two end members, low Br content/high $\delta^{81}Br$ fresh meteoric water with high Br concentration/low $\delta^{81}Br$ brackish and hypersaline water, the latter source as a product of evaporated seawater. This dilution/mixing hypothesis is supported by the general linear correlation ($R^2 = 0.96$) between the Br content and $\delta^{81}Br$ ratios which was drawn through all the samples obtained from the saline zone. Based on the Br concentration, the dilution/mixing rates for the evaporated seawater end member were higher in the shallower aquifers (DMM and HDRK) as compared to the dilution rate in the deeper aquifer (UER). This agrees with the observed vertical stratification in the chemical compositions between the three Tertiary aquifers where the TDS concentrations significantly increase with increased depths of the geological Formations.

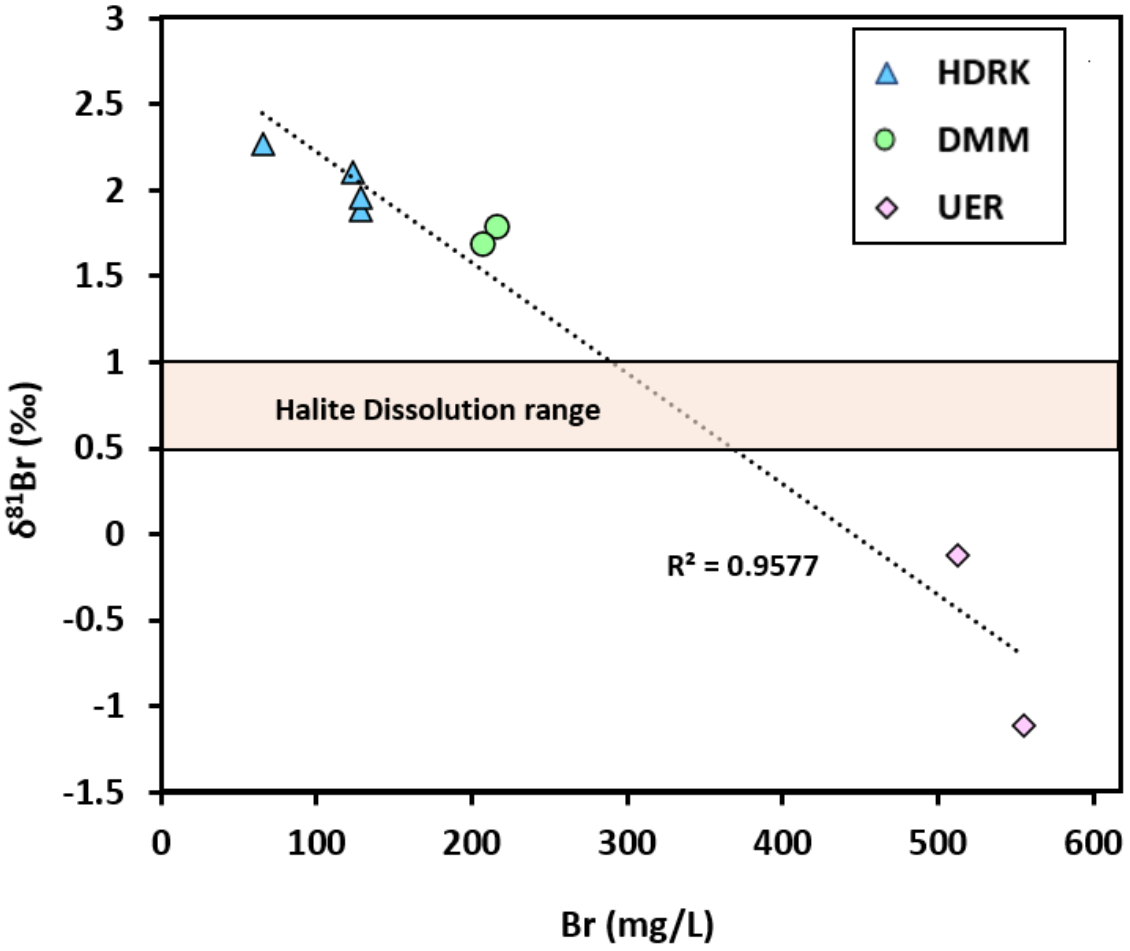

Figure 4-7: δ^{81}Br versus Br concentrations for the groundwater samples collected in the saline zone from the aquifer, Hadrukh (HDRK), Dammam (DMM), and Umm Er Radhuma (UER). The δ^{81}Br range of halite dissolution is taken from Eastoe et al. (2001) and Bagheri et al. (2014).

4.4.3 Salinization pathway and interconnection of aquifers

The risk assessment for groundwater salinization in the regional Tertiary aquifers requires a better understanding of the source of the evaporated paleo-seawater. Potential pathways for the observed seawater intrusion include: 1) ancient evaporated seawater trapped at the time of sediment deposition, or 2) cross-formational flow by which the seawater migrated upward through preferential pathways in the overlaid aquitard (e.g., faults, or thinner aquitard sections) (Cherry and Parker, 2004). Isotope tracers such as $^{87}Sr/^{86}Sr$ have been recently used as indicators for inter-aquifer leakage and mixing in regional groundwater investigations (Dogramaci and Herczeg, 2002;

Brenot et al., 2015; Priestly et al., 2017). Also, similarity in the isotope ratios between aquifers may indicate mixing or inter-aquifer leakage, whereas clear contrasts in the isotope ratios indicate that there is insignificant vertical flow.

$^{87}Sr/^{86}Sr$

The alkali earth metal strontium (Sr) was present in all the groundwater samples from the saline zone in the study area (Table-4.1). The $^{87}Sr/^{86}Sr$ fractionation ratio during most geochemical reactions is small (Priestly et al., 2017); thus, the observed $^{87}Sr/^{86}Sr$ ratio in groundwaters is expected to resemble the ratio in the sourced minerals. This makes $^{87}Sr/^{86}Sr$ a useful indicator of formation water origin and mixing of different water sources. In the saline zone, the highest Sr concentration (average=247 mg/L) in the water samples from the UER aquifer corresponded to the lowest $^{87}Sr/^{86}Sr$ ratios (0.70770-0.70785). In contrast, the lowest Sr concentrations (average=37.7 mg/L) corresponded to the highest $^{87}Sr/^{86}Sr$ ratios (0.70819-0.70822), which were found in the groundwater samples collected from the HDRK aquifer. The two groundwater samples from the DMM aquifer showed an identical $^{87}Sr/^{86}Sr$ ratio of 0.70789 and an average Sr concentration of 86.7 mg/L. These data show high variabilities in Sr concentrations and $^{87}Sr/^{86}Sr$ ratios between the aquifers, indicating the absence of connectivity between them. Moreover, the $^{87}Sr/^{86}Sr$ ratios for all aquifers were significantly less radiogenic compared to the current Arabian Gulf ($^{87}Sr/^{86}Sr$ = 0.7093), which rejects any mixing with modern seawater. Instead, the $^{87}Sr/^{86}Sr$ values for the UER, DMM, and HDRK aquifers match the $^{87}Sr/^{86}Sr$ values expected for Paleocene, Eocene, and Oligocene seawaters, respectively (Fig. 4.8). This suggests that the $^{87}Sr/^{86}Sr$ ratios of each aquifer may reflect the $^{87}Sr/^{86}Sr$ ratio of seawater at about the times of deposition of the respective Formations.

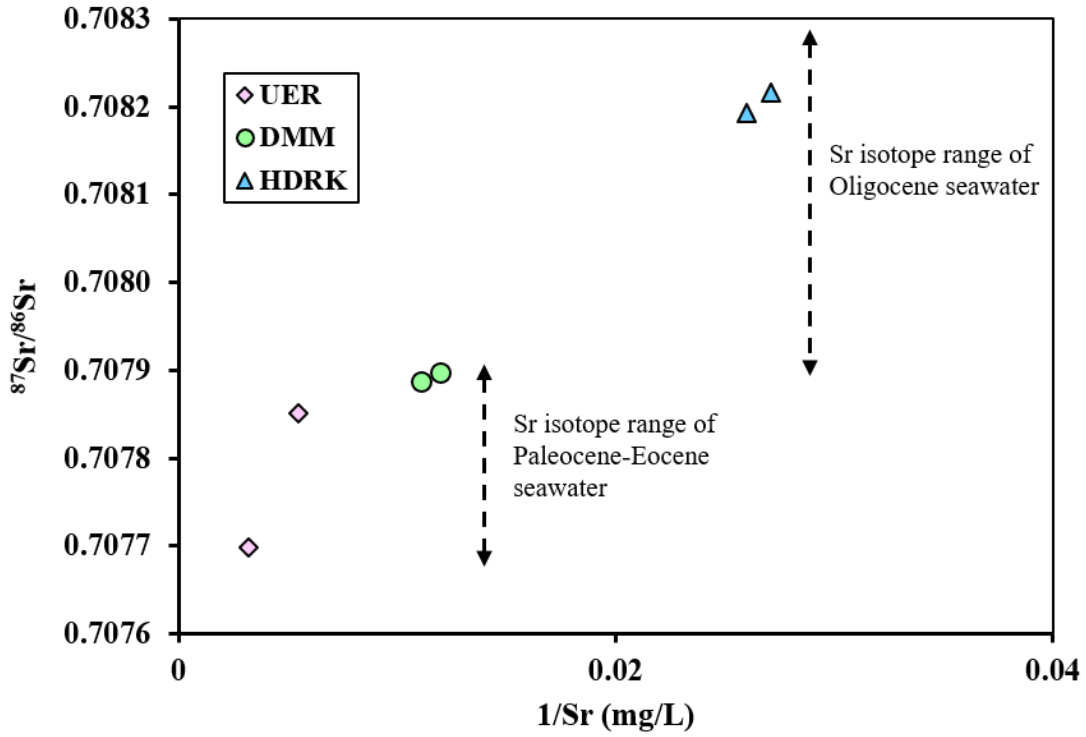

Figure 4-8: Relationship between $^{87}Sr/^{86}Sr$ and 1/Sr of groundwater samples from the two multi-level wells for Umm Er Radhuma (UER), Dammam (DMM), and Hadrukh (HDRK) aquifers. The Sr isotope ranges for the Oligocene (Sugarman et al. 1997) and Paleocene-Eocene Ages (Hodell et al., 2007) are also shown.

4.4.4 Origin and time of aquifer recharge

The chemical-isotopic compositions of the groundwater samples collected from the Tertiary aquifers were utilized to evaluate the recharge conditions of the aquifers. The main objectives were to: (1) provide insights on natural effects controlling water chemistry by dilution, and (2) to verify the origins and times of recharge of the aquifers.

$\delta^{18}O$ and $\delta^{2}H$ isotope compositions

Values for the stable isotopes deuterium ($\delta^{2}H$) and oxygen-18 ($\delta^{18}O$) have been widely used to distinguish between the meteoric and marine origins of formation waters (Clark and Fritz, 1997). The seawater evaporation trend (SET), global meteoric water line (GMWL), standard mean ocean water (SMOW), and $\delta^{2}H$ and $\delta^{18}O$ data of the samples collected from the Tertiary aquifers and the

EFW are plotted in Fig. 4.9. The EFW sample coincides with the SET line, which supports the suggestion that evaporative seawater is the major source of salinization in the oil reservoir. In contrast, the brackish and saline waters from the three Tertiary aquifers plot close to the GMWL (Fig. 4.9), which normally suggests meteoric waters as the primary components of groundwater (Clark and Fritz, 1997). Moreover, the $\delta^{18}O$ ratios for all the groundwater samples were relatively lower relative to present-day precipitation, which has mean $\delta^{18}O$ values of 0.05‰ (Wood, 2011). These lower $\delta^{18}O$ values may indicate the infiltration of paleo-meteoric water during cooler historical climatic conditions compared to the present. Relatively, the saline water samples had higher $\delta^{2}H$ and $\delta^{18}O$ values compared to the brackish samples. This may suggest the presence of two end members, fresh water with depleted $\delta^{2}H$ and $\delta^{18}O$ values and hypersaline evaporated seawater with enriched $\delta^{2}H$ and $\delta^{18}O$ values. This result reveals that fresh paleo-meteoric water may be flushing previously entrapped hypersaline autochthonous ancient seawater. The extent of the flushing process is controlled by the depth of the formation and the distance from the recharge zone. Less groundwater circulation and flushing are theoretically expected for aquifers that are deeper and more distant from the recharge zone. This was observed and supported by the vertical variations in groundwater salinity in the multi-level wells, where the TDS concentrations were observed to increase substantially with depth and distance from the recharge zone (Table-4.1 and Fig. 4.3).

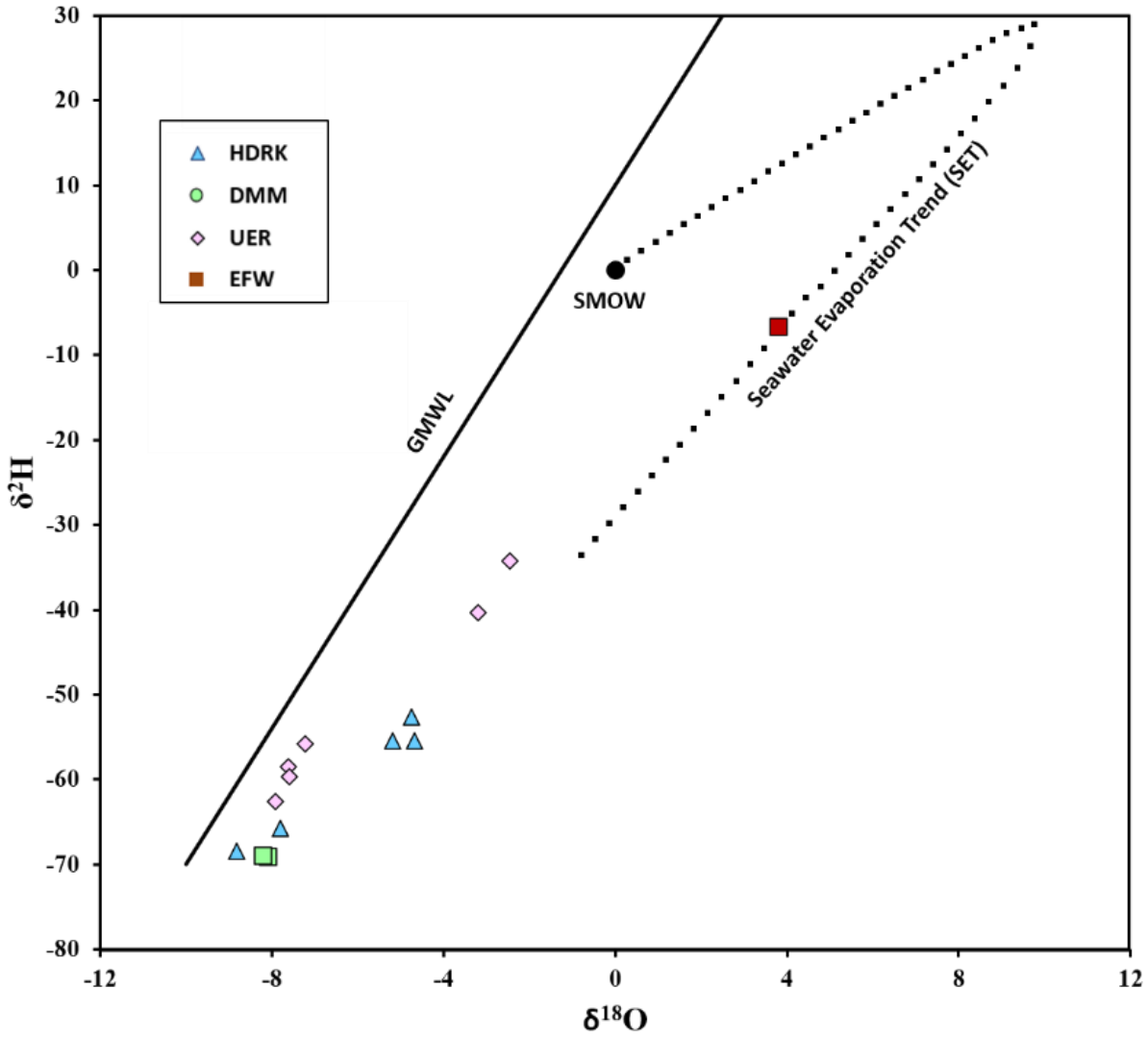

Figure 4-9: δ^2H versus $\delta^{18}O$ isotopes of the samples from the oil field Formation water (EFW), Umm Er Radhuma (UER), Dammam (DMM), and Hadrukh (HDRK) aquifers. The seawater evaporation trend (SET) is taken from Hosler (1979) and Kanuth and Beeunas (1986).

Groundwater age

Based on the age of the Formation, groundwater can be categorized as either connate or meteoric. Connate water is defined as water that was trapped at the time of sedimentation, while meteoric indicates groundwater that originated as precipitation (Singleton and Moran, 2010). The half-life of the radioactive ^{14}C is 5,730 years, which makes it a useful indicator of groundwater age on scales ranging from "recent" to a maximum of tens of thousands of years (Clark and Fritz, 1997).

By definition, the age of connate water coincides with the age of the host sediments of up to 2.5 to 65 million years ago, and should be free of ^{14}C. In contrast, all groundwater samples from the Tertiary aquifers in the saline zone had ^{14}C ranging between 8.1 and 38.7 pMC (Table 4.1). This result suggests a young water component in each of the three Tertiary aquifers. Furthermore, the observed ^{14}C measurements agree with the lower content of the current groundwaters in the aquifers and verify their paleoclimatic origins during the cooler Late Pleistocene and Early Holocene periods. The lowest ^{14}C values (8.1 - 10.1 pmc) were observed in groundwater samples from the deeper aquifers, i.e., UER and DMM. In contrast, the highest ^{14}C values (24.9-38.7 pmc) were associated with groundwater samples from the relatively shallower HDRK aquifer. This observation supports the proposed model, that meteoric water has partially replaced the connate water and that due to different flow paths, the flushing out processes increase with decreasing depths across all the Formations. A compilation of these results confirms that the paleo-seawater entrapped in the three Tertiary aquifers was partially flushed out by relatively younger and fresher meteoric recharges.

4.5 Conclusion

A multiple line of evidence approach was applied to determine the sources and mechanism of salinization in Tertiary formations of the northeastern part of the regional Rub' al Khali topographic basin, in the southern Arabian Peninsula. The major cycles of transgression and regression of paleo-seawater during the Tertiary period formed lagoonal and sabkha environments in the study area. Evaporated paleo-seawater existed as connate water in these geological settings during the time of deposition and has evolved through water-rock interaction. The connate water as evaporated seawater was later partially flushed and mixed with fresh paleo-meteoric water during the Late Pleistocene and Early Holocene periods. The data suggest that mixing between the

aquifers and modern seawater is unlikely. Furthermore, the chemical and isotopic data are consistent with the absence of significant vertical connectivity between the regional Tertiary aquifers, as determined from distinct strontium isotope ratios in the study area. This new appreciation for the evolution of groundwater chemistry in this multi-layered sedimentary rock sequence will inform future decisions regarding the sustainable use of groundwater resources by municipalities and the oil and gas industry for balancing extraction and the land disposal of waste.

Table 4-1: Major and trace element concentrations and radioisotope ^{14}C for groundwater samples from the Rub' al Khali basin aquifers Umm Er Radhuma (UER), Dammam (DMM), and Hadrukh (HDRK)

Sample ID	Aquifer	TDS (mg/L)	Na (mg/L)	Ca (mg/L)	Mg (mg/L)	SO_4 (mg/L)	HCO_3 (mg/L)	Cl (mg/L)	Br (mg/L)	Sr (mg/L)	^{14}C pmc
M-1	UER	110,000	32,000	6,460	2,120	820	215	67,872	513	318	10.1
	DMM	51,199	10,800	4,510	2,510	1,809	104	31,251	215	97.4	
	HDRK	35,856	9,060	2,160	1,490	2,893	64	20,012	128	48.7	24.9
M-2	UER	122,945	34,600	7,080	2,640	1601	210	76,076	555	183	
	DMM	50,068	10,400	4,430	2,440	1,827	183	30,484	207	97.5	8.1
	HDRK	35,102	8,090	1,820	1,720	3,652	76.4	19,583	124	36.9	38.9
U-1	UER	1,798	127	240	124	1,043	118	145	1	n.d	
U-2	UER	3,321	597	313	150	1,374	94	772	6	15.3	
U-3	UER	3,457	726	264	140	1,279	76	948	8	16.1	
U-4	UER	3,600	734	271	120	1,182	268.4	999	8	17.7	
U-5	UER	5,517	1,400	276	150	1,357	268.4	2,029	15	20.8	
D-1	DMM	2,409	165	402	119	1,361	122	238	2	n.d	
D-2	DMM	3,771	592	439	111	2,324	49	256	n.d	n.d	
H-1	HDRK	8,864	1,990	620	286	3,818	25	2,103	11	11.5	
H-2	HDRK	18,521	4,500	1,280	687	2,928	41	8,996	65	23.4	
H-3	HDRK	36,111	8,990	2,020	1,650	2,988	73.6	20,215	129	46.1	
EFW	Cretaceous	216,799	57,059	22,080	2,045	315	98	132,770	1,100	1332	
Arabian Gulf		47,573	14,900	555	1,730	3,587	190	26,711	90	12	

Chapter 5 Chemical Evolution of an Inland Sabkha

This chapter is under review by the Hydrogeology Journal as follows:

Manuscript ID: HYJO-D-20-00002

5.1 Introduction

Sabkha is an Arabic word for a salt flat. Sabkhas are widely distributed in the Arabian Peninsula and occupy an area of about 36,500 km^2 (Schulz et al., 2015). Sabkha Matti (SM) is the largest continuous salt flat in the Arabian Peninsula. It extends about 150 km south from the western Abu Dhabi coastline and across the border between the United Arab Emirates and Saudi Arabia (Fig. 5.1). Near the coast of Abu Dhabi, SM is characterized by a narrow strip of supratidal carbonate sediments with nodular anhydrite and gypsum crystals that form a coastal sabkha (Evan et al., 1969). Landward, SM shifts from a deflationary marine shelly lag surface into an area of inland siliciclastic sabkha with displacive sulfate and halite evaporite minerals (Goodall, 1995). Sabkha Matti represents a potential discharge point for regional groundwater systems in the Rub' al Khali desert basin. The aim of the current study is to assess the hydrogeochemical evolution of SM in order to evaluate its impact on the regional aquifer systems. To achieve this objective, a combination of geological, hydraulic, hydrochemical, and isotopic methods were used. First, the structural framework for the deep and shallow segments of SM were investigated using seismic and well data. This is to enhance the understanding of the evolution of the sedimentary basin and to investigate the influence of geological structures on fluid flow. Second, hydraulic data were examined to determine the hydraulic properties of the geological formations and to model the groundwater flow and solute transport. Finally, hydrochemical and isotopic tracers were utilized to evaluate potential sources of water and solutes in the area, and to propose a mechanism for salinization and interaction between different sources. For this purpose, a water mass balance, δ^2H vs $\delta^{18}0$, ^3H, and ^{14}C were utilized for the hydrologic flow system analysis, whereas $\delta^{11}B$ isotope and $^{87}Sr/^{86}Sr$ isotope ratios were used for the solutes approach.

Sabkhat systems are important in assessing water resources because they represent the discharge point or base level of local and regional groundwater and surface water flow systems. In addition, studying the evolution of sabkhat can provide valuable information about the sedimentary history, depositional environment, and paleoclimatic changes. An excess of evaporation over precipitation and shallow groundwater tables are critical components for the occurrence of these features. Several conceptual models have been proposed to explain the historical evolution of sabkhat. The main difference between the proposed models depends on the contribution of marine versus non-marine sources to the sabkha. For instance, the seawater-flooding model was proposed as a mechanism for cycling seawater in a coastal sabkha (Kinsman, 1969; Butler, 1969; Butler, 1973; Patterson and Kinsman, 1982). In contrast, the upward-leakage model suggests that natural upward leakage of deep saline groundwater is the main source for the water and solutes in an inland sabkha (AlSaaran, 2008). The evaporative-pumping model suggests that annual evaporation from the sabkha induces the lateral flow of both seawater and groundwater into the aquifer underlying the sabkha to replace the water lost to evaporation (Hsü and Siegenthaler, 1969, Hsü and Schneider, 1973, McKenzie et al., 1980, Müller et al., 1990). Wood et al. (2002) examined the solute and water fluxes of the Abu Dhabi sabkha, United Arab Emirates, and proposed the ascending-brine model. This model posits that 95% of the solutes are derived from ascending continental brines, while direct rainfall on the sabkha and subsequent recharge to the underlying aquifer account for 90% of the annual water input to the system. Van Dam et al. (2009, 2014) theorised that density-driven convection is responsible for the elevated concentration of solutes in the coastal sabkha of Abu Dhabi; herein, the viability of this hypothesis on a large inland sabkha was tested.

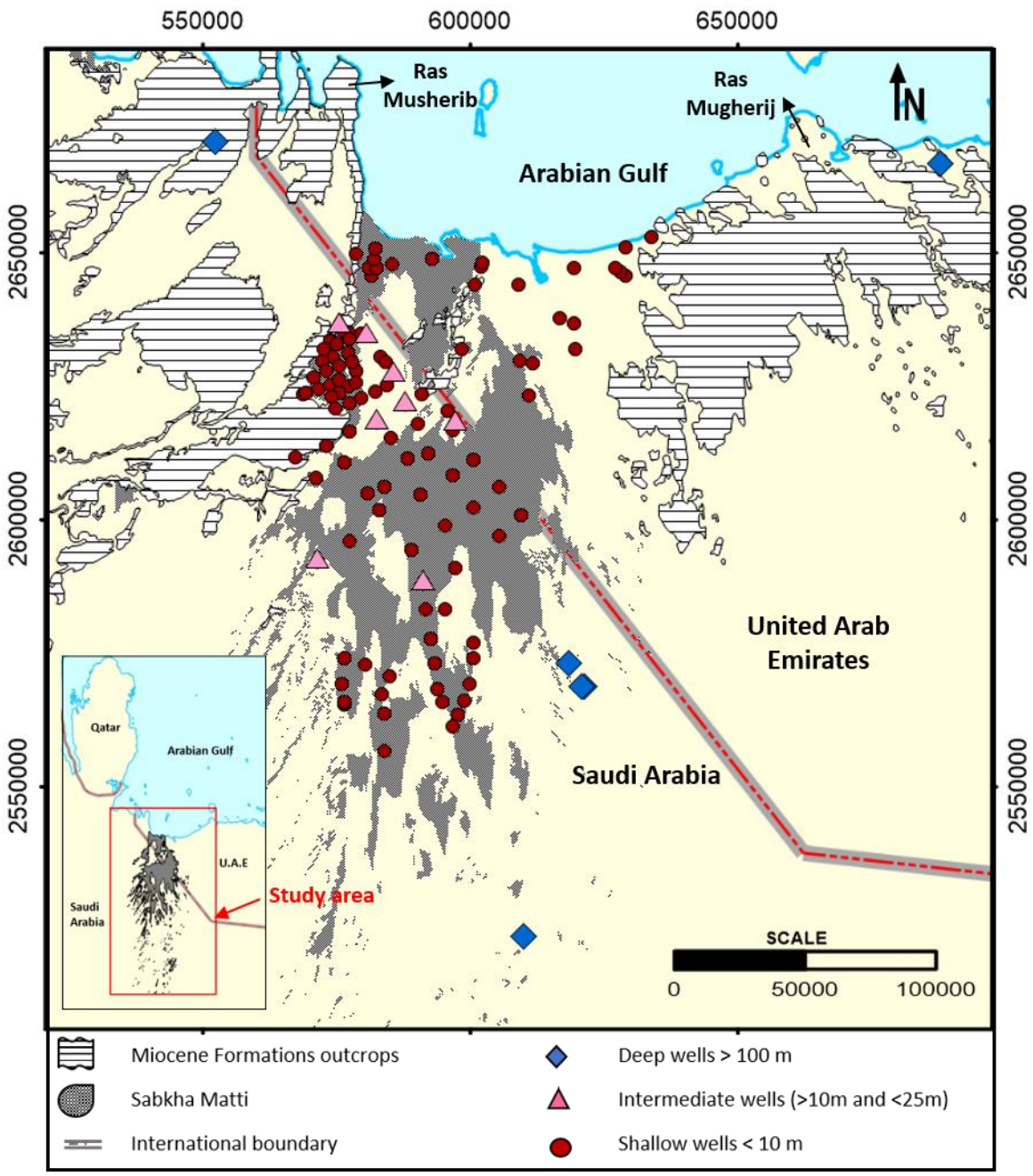

Figure 5-1: Map showing the location of Sabkha Matti, general geological features, and sampling wells.

5.2 Geological Framework

Sabkha Matti lies at the northeastern edge of the Rub' al Khali structural basin, the largest continuous sand desert in the world. It is a wide, north-south trending, salt-covered depression that

extends about 150 km south from the western Abu Dhabi coastline and across the border between the United Arab Emirates and Saudi Arabia. The sand dune system of the Rub' al Khali basin forms the southern margin of the SM embayment, while the western and eastern boundaries are formed by N-S linear margins of the Neogene-age outcrops (Fig. 5.1) known as Ras Musherib and Ras Mugherij, respectively (Goodall, 1995). A generalized geologic cross-section of SM is shown in Fig. 5.2. Beneath SM lies a 6,000-8,000m-thick) Paleozoic-Cenozoic sedimentary sequence of carbonates, clastics, and evaporites that accumulated on the stable Arabian platform (Nairn and Alsharhan, 1997). During the late Oligocene-Miocene, fluvial sandstone facies of the Hadrukh Formation were deposited above the Paleozoic-Cenozoic sedimentary sequence (Nairn and Alsharhan, 1997). Following the deposition of the Hadrukh sandstones, the Arabian Gulf area was subjected to a lagoonal-evaporitic deposition (Ziegler, 2001). In this setting, marl, clay, dolomite, dolomitic limestone, anhydrite, and nodular gypsum of the Dam Formation were deposited (Powers et al., 1966). During the Mid-Miocene, the area was subjected to tilting and rapid erosion of the Arabian shield basement as a result of the Miocene-Pliocene uplift (Zagros Orogeny) (Al-Hajari, 1991). This setting favoured the deposition of continental clastic sediments of the Shuweihat Formation in fluvial, aeolian, and sabkha environments (Bristow, 1999).

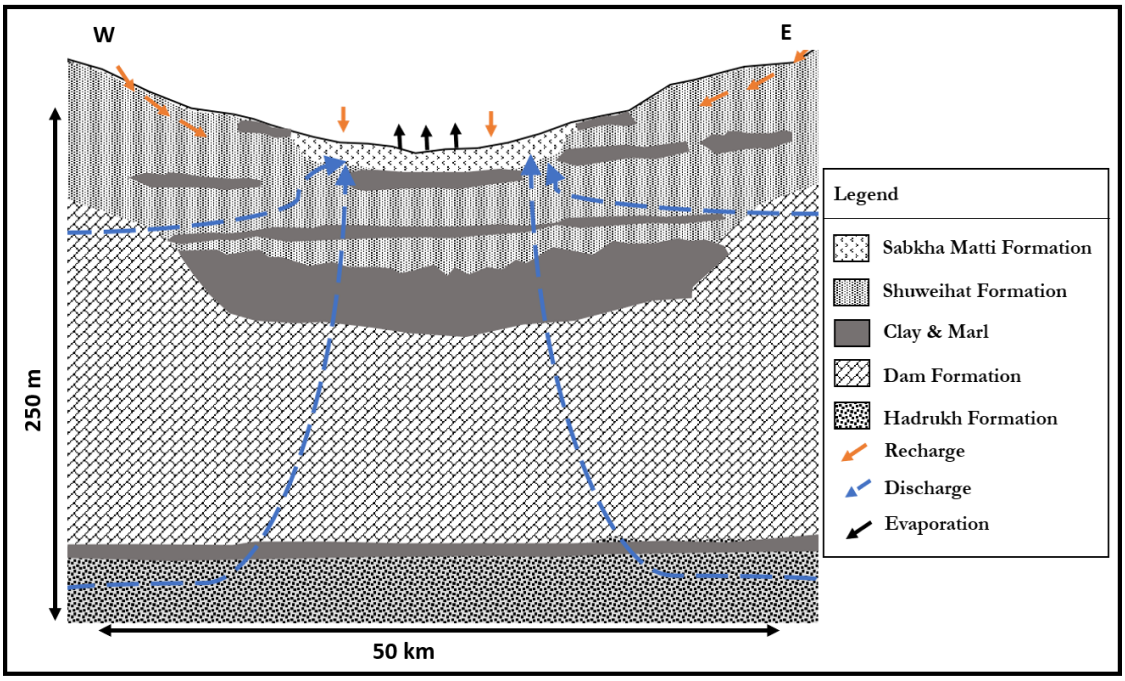

Figure 5-2: Generalized geologic cross-section and conceptual model of potential groundwater flow patterns below Sabkha Matti

In the Late Pleistocene, SM was the site of the confluence of two major paleo-drainage systems, Wadi ad Dawasir from SSW and SW and Wadi as Sahba from WSW and W (Goodall, 1995). Incision by these drainage systems together with wind deflations combined to convert the area into a paleo deltaic and lacustrine environment. In this setting, fluvial sands and gravel plains accumulated. Dating of two samples from the fluvial sand yielded dates of 40,000 and 147,000 BP (Goodall, 1995). These data reveal that the geomorphology of the region has been influenced by at least two separate instances of large-scale fluvial activities in the past 150,000 years. In the Late Pleistocene-Holocene, the area was tectonically active, and rapid subsidence and uplift events occurred (Wood et al., 2012). This phase is evidenced by the sporadic presence of older erosional cliffs within SM. In the Mid-Holocene, the groundwater table in the SM area began to rise in response to a ~140 m rise in the Arabian Gulf (Sanford and Wood, 2001). In this setting, reworking and dissection of the alluvial sediments occurred as deflation removed sands down to the level of

the rising water table and caused the formation of both the coastal and inland Sabkha Matti (Alsharhan and Kendall 2002). Currently, the Sabkha Matti Formation (SMF) has an average thickness of about 5 m, and extends inland within the border of Saudi Arabia to the south for nearly 100 km. Within the fluvial sands in the SMF, evaporite facies have developed either as surface precipitates or shallow subsurface diagenetic constituents.

5.3 Sampling and Methodology

Figure 5.1 shows the location of the sampling holes drilled in the study area. Holes for 111 shallow piezometers (<10 m) were drilled between 1 and 2m below the water table by using a direct push machine (Geoprobe Geoprobe model 6620DT). Nine piezometers of intermediate depth (>10 m and <25 m) were drilled by a rotary drill rig mounted on a 4x4 truck. All shallow and intermediate piezometers were constructed from 50mm-diameter schedule 40 PVC pipe, slotted by a hacksaw on the bottom 1.5 m, covered with filter sock, with threaded joints containing couplings. The holes were backfilled, with the loose sand collapsed around the piezometers. Water samples were collected using a plastic bailer. Six deep wells (> 100 m) were drilled with rotary drills into the underlying Dam and Hadrukh Formations. These wells were finished with 18 5/8" of surface casing and were left without casings (i.e., open hole) for the remainder of the depth, with typical open interval lengths ranging from 15 to 30 meters. Each of the six deep wells were provided with a cap, shut-off valve, and pressure gauge. All the deep wells were under flowing artesian conditions, which allowed the easy collection of water samples. Eight pre-existing open pits were available at the site, and one water sample was collected from each of the eight open pits. These samples were used for indications of evaporation greater than precipitation from a free-water surface. Analyses of all water samples for electrical conductivity (EC), pH, temperature, and dissolved oxygen content were carried out in the field using a portable HQ40d meter (Hach Ltd.).

Field measurements of alkalinity were made using a Hach field titration kit and expressed as mg/L of equivalent HCO_3. All the water samples were filtered through 0.45μm filters, and then one set was acidified with double-distilled nitric acid for cation analysis and the other set was preserved unacidified for anion analysis. Analyses of the major and minor ions were performed by the Isobrine Solutions Laboratory (Edmonton, Canada) and the ALS laboratory group (Waterloo, Canada). Analyses of the stable and radioisotopes were performed at the Isotope Tracer Technologies Inc. (IT^2) laboratory in Waterloo, Canada. Sulfate (gypsum and anhydrite) samples were collected from outcrops in the western SM and from a series of shallow boreholes drilled into the Dam, Shuweihat, and Sabkha Matti Formations. The sulfate samples were measured for strontium isotopes at the IT^2 laboratory (Waterloo, Canada).

5.4 Results and Discussion

5.4.1 Hydrogeological approach:

The deep and shallow structure at Sabkha Matti has been delineated by using seismic and well data. Based on these data, the structure of Sabkha Matti is interpreted as a nearshore deep depression that dips gently from the coast toward the centre of the regional Rub' al Khali topographic basin. The western edge of the Sabkha Matti basin coincides with the eastern edge of the Qatar Arch, a large arch that developed from the Lower Palaeozoic to the Oligocene (Perotti et al. 2011). To the east, the Matti basin is bounded by a strike-slip fault in a basement known as the Amad ridge. All the geological strata within the Matti basin contain a remarkably high presence of marl and clay deposits. These fine sediments are known to settle out of stagnant waters with occasional shallow water conditions in a coastal lagoon environment, consistent with the depositional environment of the Sabkha Matti. Based on these data, it is proposed here that major cycles of transgression and regression of paleo-seawater formed a lagoonal environment in the

area. In this setting, it is likely that autochthonous brine aquifers were formed by the entrapment of paleo-seawater during the depositional time of these geological formations.

Hydrostatic head data were investigated to evaluate the relative contributions of different sources of water and solutes to SM. The depth to groundwater in SMF varies over the area, but is generally within 1 or 2m of the land surface. The measured water level data were utilized to estimate the lateral fluxes of groundwater into and out of the sabkha by using Darcy's law:

$q = -K (dh/dl)$

where q is the flux in dimensions of length per time (L/T), K is the hydraulic conductivity of the porous medium in dimensions of length per time (L/T), and dh/dl is the gradient in the hydraulic head in the direction of flow in dimensions of length per length (dimensionless). The gradient in SMF is toward the coastline and has a typical value of approximately 2m per 10 km. Slug tests performed on a series of wells indicate that the hydraulic conductivity of SMF has a mean value of about 1.4 m/d. From these two values, the lateral groundwater flux using Darcy's law is 0.2 mm/d, or about 9 cm/year. A flux value can be converted to a seepage velocity by dividing the flux by the effective porosity. Several laboratory analyses of the sand from the SMF yield a consistence porosity of approximately 0.38. Given this value of porosity, the lateral seepage velocity through SMF is estimated to be about 20 cm/year. Based on these data, the required time for the lateral groundwater flux to transit from the recharge to the discharge zone in SM is calculated by dividing the length of the sabkha flow path (150 km) by the seepage velocity. Accordingly, this would require an average water residence time of 325,000 years, and given that the age of the SMF averages about 5000 years old, it is concluded that lateral influx of groundwater has not caused a significant discharge of solutes from SM. The regional hydrostatic head data

suggest that upward leakage from the underlying regional aquifers to SM might have a substantial solute flux, which is based on the fact that groundwater flow in the regional aquifers is toward the discharge area at SM and that all the deep aquifers have piezometric surfaces significantly higher than the water table in the SMF (Fig. 5.2). This observation is consistent with the ascending brine hypothesis for the origin of solutes (Sanford and Wood, 2001; Wood et al., 2002; Wood and Sanford, 2002; Yechieli and Wood, 2002; Kraemer et al., 2014). The result of these two input sources and a lack of significant discharge indicate that the dissolved solids will continue to accumulate, controlled only by the thermodynamics of mineral precipitation.

5.4.2 Hydrochemical and isotopic approach:

Origin of solutes

Concentrations of major ionic constituents are plotted as a Schoeller diagram in Figure 5.3. A Schoeller diagram is a semi-logarithmic diagram that has the advantage of representing major ions constituents in water and demonstrates different hydrogeochemical water types on the same diagram. What the data on the Schoeller diagram show (Fig. 5.3) are regardless of the aquifer; all the water samples are of Na-Cl water types and have similar ionic compositions. This similarity in water type and ionic compositions among all groundwater samples suggests that the waters may have the same or similar origins. The average total dissolved solid (TDS) content of the collected water samples from the Hadrukh, Dam, Shuweihat, and Sabkha Matti Formations were 35 g/L, 43 g/L, 85 g/L, and 285 g/L, respectively (Table 5.1). The boron isotope ratios ($\delta^{11}B$) were used to separate marine from non-marine sources. Owing to the long residence time of boron in seawater (about 10 Ma), the seawater has a fairly constant $\delta^{11}B$ value of around +40‰ (Spivack and Edmond, 1987). Accordingly, brines which originated solely from seawater should hypothetically resemble the $\delta^{11}B$ value of seawater (Vengosh et al., 1992). In contrast, a low $\delta^{11}B$ value of the

brines is regularly attributed to a non-marine source. Brine samples from the four studied aquifers gave $\delta^{11}B$ values in a range between +23 and +45‰ (Fig. 5.4). These enriched $\delta^{11}B$ values are typical of saline waters derived from a marine origin dominated by cyclic salts (Vengosh et al., 1991a; Vengosh et al. 1991b). Based on detailed sedimentological and geochemical analyses, Saeed et al. (in press) interpreted the source of saltwater in the Paleocene-Eocene-Oligocene aquifers in the vicinity of SM to be associated with discrete events of evaporated paleo-seawater entrapment in a lagoonal environment. Some of the $\delta^{11}B$ values overlap with those of seawaters and brackish/fresh surface waters, which may be attributed to the mixing of brine of marine origin with waters of terrestrial origin with low $\delta^{11}B$ values. On the other hand, some other samples showed slightly heavier $\delta^{11}B$ values than seawater, which may indicate further interaction of brine with detrital sediments (Vengosh et al., 1991a). During such an interaction, the lighter isotope of boron (^{10}B) is preferentially adsorbed onto the sediment surfaces, while the dissolved marine boron becomes enriched in the heavier isotope (^{11}B) (Keren et al., 1981). This raises the final brine to $\delta^{11}B$ values higher than seawater.

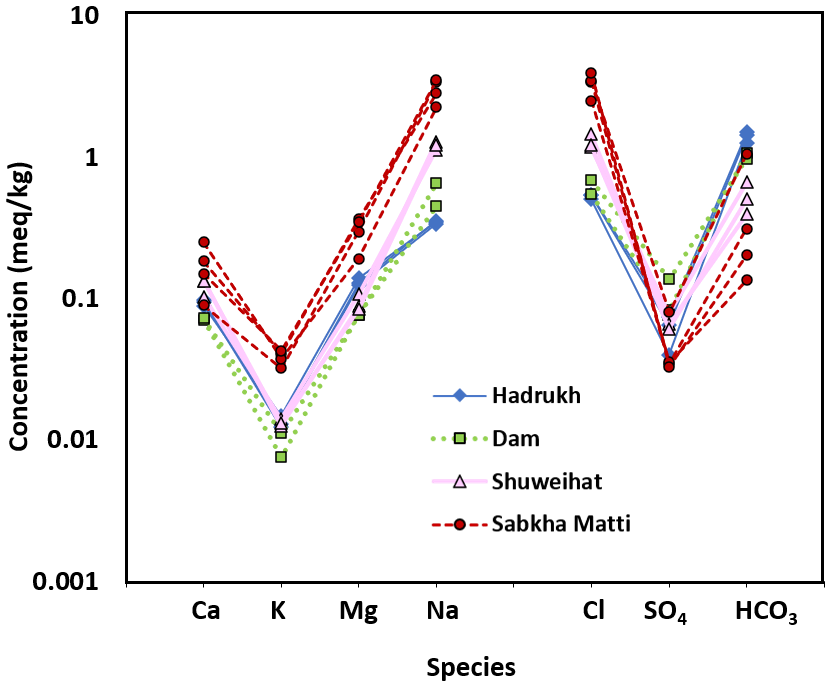

Figure 5-3: Schoeller diagram showing the chemical compositions of water samples collected from different aquifers in the Sabkha Matti area showing that the water type is Na-Cl rich. HCO_3 refers to total alkalinity expressed as HCO_3.

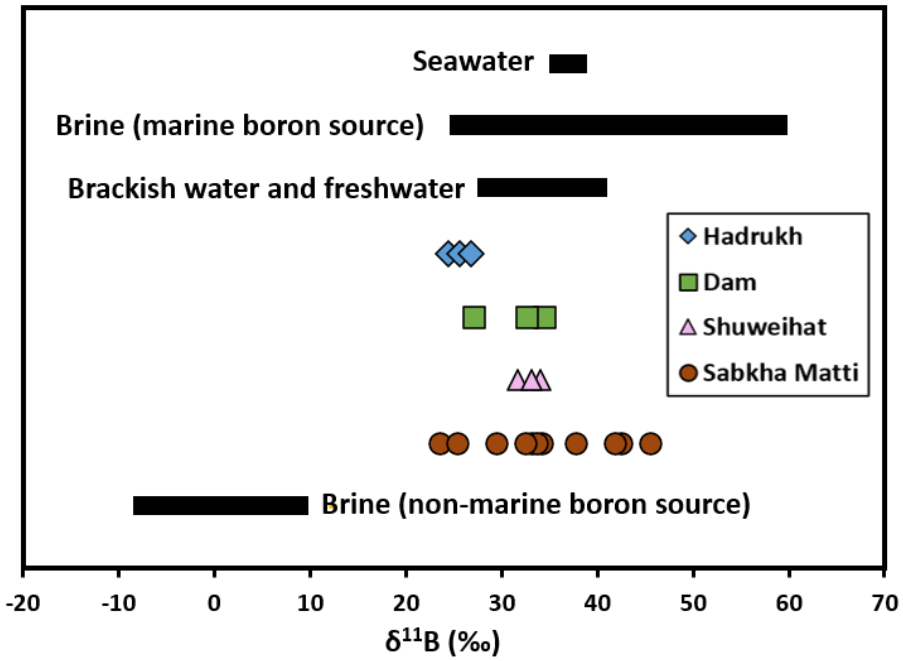

Figure 5-4: Comparison of boron isotope values from water samples from the studied aquifers in sabkha Matti area with those reported in the literature for seawater and different water types present in sabkha environments (Vengosh et al., 1991a; Vengosh et al., 199 b).

Although the boron isotope data suggest a seawater origin for the elevated salinity in all the studied aquifers at SM, it is unlikely under the current hydraulic conditions that modern seawater has contributed significantly to the observed salinization trend. This is supported by the current hydraulic gradient in all the aquifers, which is toward the coastline. Moreover, field visits to the proximal coastal edge of SM confirmed that the extent of the supratidal zone of the current Arabian Gulf is less than 5km wide, landwards of the storm beach. Thus, the results from the boron isotope ratios, which suggest a marine origin for the elevated salinity, and the hydrogeological data that rejects modern seawater intrusion, might seem contradictory. To resolve this apparent contradiction, strontium isotope data were evaluated to ascertain whether the source of salinization in the studied aquifers was associated with an entrapment of paleo-seawater in the geological formations during their depositional time. Strontium isotope ratio $^{87}Sr/^{86}Sr$ is a conservative tracer that does not change during chemical reactions or physiochemical processes such as evaporation (Faure, 1986; Müller et al., 1990). This makes the $^{87}Sr/^{86}Sr$ ratio an ideal tracer for determining the primary source of strontium in water. Moreover, the $^{87}Sr/^{86}Sr$ ratio of marine water has changed in the geological past, and its general trend allows definition of the time of crystallization (Burke et al., 1982). None of the analyzed samples had $^{87}Sr/^{86}Sr$ ratios similar to the ratio in the current Arabian Gulf ($^{87}Sr/^{86}Sr$ ratio = 0.70910). These data provide unequivocal evidence of the limited role that modern seawater may have played on the evolution of SM. The collected water samples from the Dam and Hadrukh Formations produced $^{87}Sr/^{86}Sr$ ratios between 0.70819 and 0.70865 (Fig. 5.5). These ratios are characteristic of the Late Oligocene-Miocene deposits, when the Dam and Hadrukh Formations are proposed to have been deposited (Nairn and Alsharhan, 1997; Bristow, 1999). This suggests that the dissolved strontium in the water samples from the Dam and Hadrukh Formations is representative of values of the depositional conditions that created them.

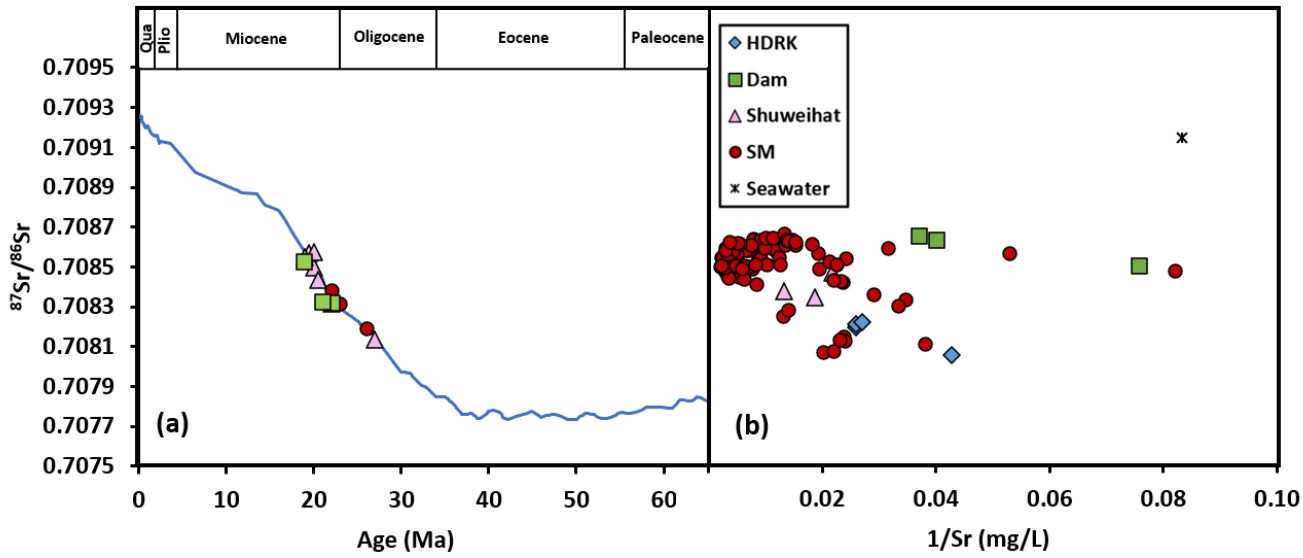

Figure 5-5: (a) Strontium isotope data for sulfate samples (gypsum and anhydrite) from the Dam, Shuweihat, and Sabkha Matti Formations plotted on the marine Sr stratigraphy of the Cenozoic (Depaolo and Ingram, 1985; Capo, 1991; Hess et al., 1991; Sugarman et al., 1993; Hodell et al., 2007); (b) $^{87}Sr/^{86}Sr$ ratios versus 1/Sr concentrations (mg/L) for water samples collected from different aquifers at Sabkha Matti.

5.4.3 Impact of climatic changes on the evolution of Sabkha Matti

The effect that paleoclimatic changes have had on the evolution of SM is assessed by evaluating field observations, stable water isotopes ($\delta^{18}O$, $\delta^{2}H$), and radio isotopes (^{14}C and ^{3}H). It has been documented that the current hyper-arid climate across the region has been punctuated by episodes of increased rainfall (~25 to 30 ka and ~5 to 9 ka) during the Late Pleistocene-Holocene (Clark and Fonte, 1990; Burns et al., 1998; Neff et al., 2001; Stokes et al., 2003; Wood and Imes, 2003). In these wetter phases, stream and tributaries were better developed and carried sediments from upland areas to eventually deposit them into the SM embayment. Field observations support this interpretation, as vast plains of alluvial gravel are observed throughout the flat sabkha. Dating of these fluvial sediments confirms that they were deposited at around 5.3 ka (Glennie et al., 2011). Moreover, heavy precipitation during these wet phases may have diluted the upward leakage brine associated with the Late Pleistocene/Holocene uplift. As a result, the SM embayment was likely

converted into sporadic but perennial saline ponds. The largest components of the groundwaters in all the aquifers are probably related to these wet phases. This is confirmed by the stable ($\delta^{18}O$, $\delta^{2}H$) and radiocarbon (^{14}C) data for the groundwater samples. For instance, the two meteoric water lines in Figure 5.6 reflect the two principle vapor sources for precipitation in the SM area. The Northern Meteoric Moisture Line (NMWL) represents the major source of vapor for current precipitation from the Arabian Gulf (Wood, 2011), whereas the source of moisture during the Pleistocene and Holocene was associated with Southern Indian Ocean vapor (Southern Meteoric Moisture Line; i.e., SMWL) (McClure, 1976; Wehenmeyer et al., 2000; Fleitmann et al., 2003; Wood, 2011). Groundwater samples collected at the foothills of the Miocene outcrops in the western SM are plotted between the two meteoric water lines, which reflects the mixing nature for these samples (Fig. 5.6), further supported by the significantly low water salinity as compared to the brine samples collected from within the sabkha. This may have resulted from dilution of the ancient brine by recent precipitation. Moreover, the high tritium content in some of these samples provides additional evidence of mixing with modern recharges. In contrast, all other water samples from the studied aquifers show high water salinity and are plotted along or close to the SMWL. These data indicate that the major source of groundwater in the four studied aquifers is probably linked to the ancient Indian-Ocean vapor source. This interpretation is also supported by ^{14}C dating, which suggests that the majority of waters in these aquifers were recharged between 3,200 and 14,000 years BP (Fig. 5.7). Similar results were reported for groundwater samples collected from the Gachsaran Formation, equivalent in age to the Dam Formation, near the coast of Abu Dhabi, United Arab Emirates (Wood, 2011).

On the $\delta^{18}O/\delta^{2}H$ diagram (Fig. 5.6), a best-fit line was drawn through the brine samples from the SMF. The slope of this line can provide insight on the influence of climatic conditions on the

isotopic composition of water samples (Craig, 1961; Gonfiantini, 1986). It is known that water becomes progressively enriched in both ^{18}O and ^{2}H during evaporation (Craig, 1961), which will ultimately result in a deviation from the meteoric water line along a line with a lower slope (Gonfiantini, 1986). In Figure 5.6, the regression line through the water samples from SMF gave a slope of 3.4. As expected, this slope is much lower than the slope in the vapor source (i.e., SMWL slope=6.3), which confirms the evaporative nature of these samples. Moreover, the slopes from the SMF samples is similar to the slope derived from the open pit samples (slope = 3.3). This result suggests that the resident water in SMF was evaporated from a free-water surface, such as a lake, before infiltrating into the formation.

The late-stage evolution of the brine in the SMF may have started during the hyper-arid phase, which has prevailed across the region for at least the last 5,000 years (Parker and Rose, 2008). Due to extensive evaporation in this stage, the water surface in the Holocene saline lake descended into the sediment column, where it became the water table. This may have had two effects on the evolution of SM. First, the perennial water body was converted into a regional discharge zone for the subsurface water, and second, evaporite minerals moved from a subaqueous-dissolved setting into precipitates in the capillary and vadose zones. Highly soluble minerals among these precipitates have been repeatedly re-dissolved by annual rainfalls and added to the input of solutes from the ascending regional brine. This ultimately results in an increase in solutes with time.

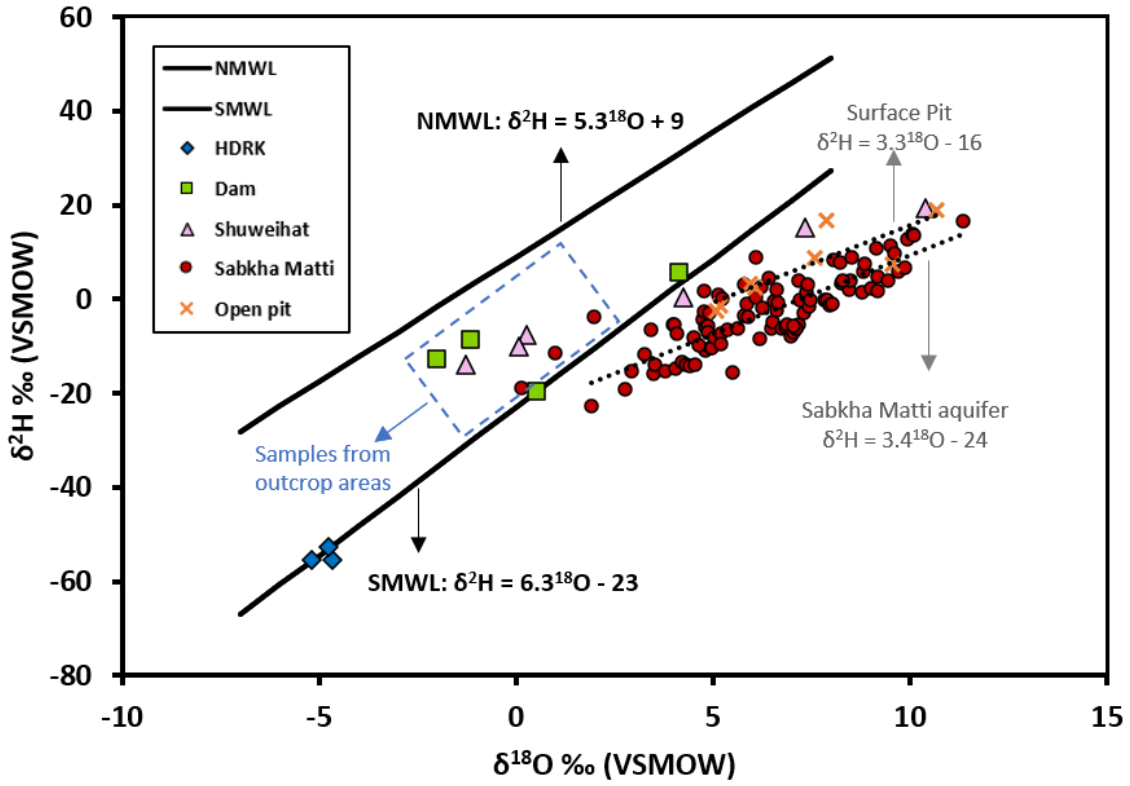

Figure 5-6: Graph showing the relationship of $\delta^{18}O$ versus $\delta^{2}H$ in the surface pits and groundwater samples collected from the Sabkha Matti area. Source of moisture for paleogroundwater in the area uses the Southern Meteoric Water Line (SMWL) as a reference for ancient precipitations. The Northern Meteoric Water Line (NMWL) is determined from measurements of local precipitation (IAEA 2009).

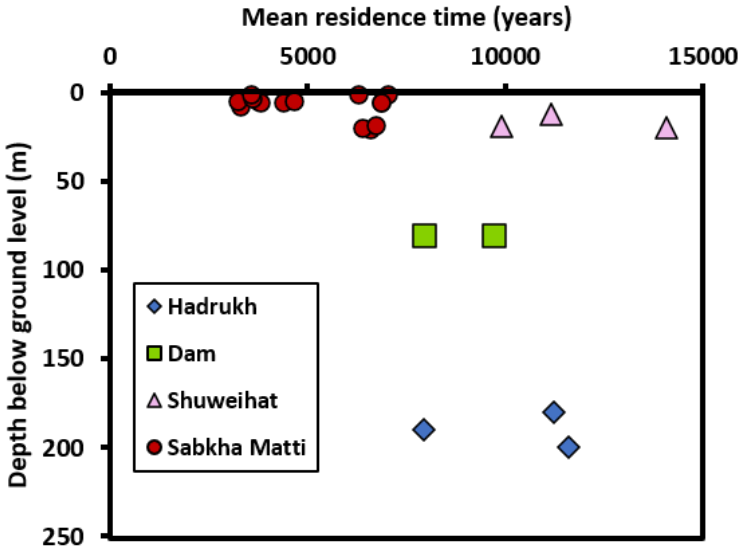

Figure 5-7: Mean residence times for groundwater samples using calibrated ^{14}C data versus depth of samples below ground level

5.4.4 *Hydrochemical processes affecting solutes in Sabkha Matti*

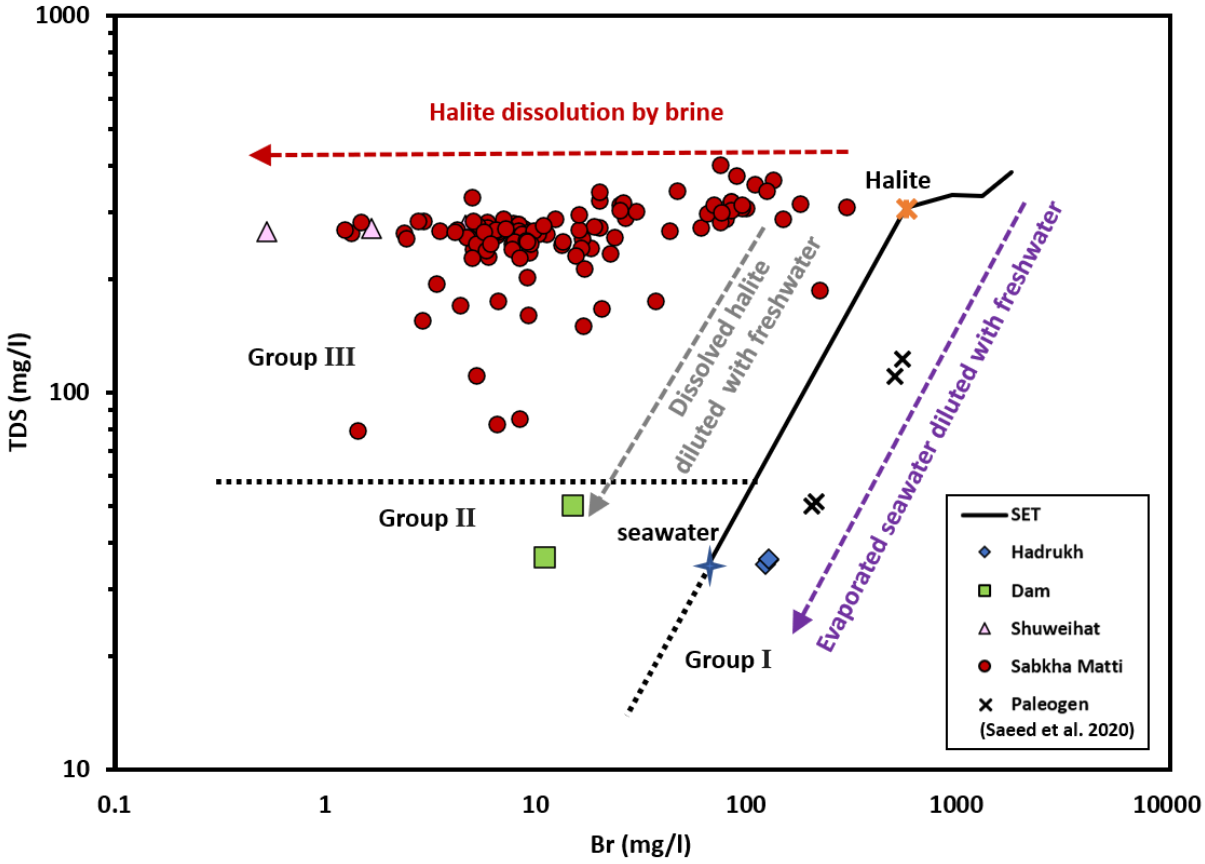

Figure 5-8: Logarithmic plot of the total dissolved solids (TDS) versus bromide for groundwater samples from the Sabkha Matti aquifers. Also shown are the Seawater Evaporation Trend (SET) (Carpenter, 1978) and some possible mixing scenarios after Rittenhouse (1967) with different halite dissolution products and different end-member waters.

Groundwater quality data for the collected samples from the studied aquifers are presented in Table 5.1. The average TDS of the water samples collected from the Hadrukh, Dam, Shuweihat, and Sabkha Matti Formations were 35 g/L, 43 g/L, 85 g/L, and 285 g/L, respectively. As the hydrogeological, hydrochemical, and isotope data confirmed similar origins of salinity (i.e., a marine source), the observed large variations in TDS concentrations among the aquifers may be attributed to the addition or removal of solutes in response to different chemical or physical processes. One way of identifying these processes that influence the chemical composition of the waters is to examine the change in a conservative ion concentration with an increasing

concentration factor. In evaporative environments such as SM, bromide concentrations are often used to represent the concentration factor of water. This is because bromide is not involved in most mineral-solution reactions and also tends to be excluded from evaporite minerals (Rittenhouse, 1967). To interpret the evolutionary processes of bromide in the water samples, the seawater evaporation trend (SET) method is typically used (Carpenter, 1978). Carpenter (1978) experimentally evaporated seawater and computed the trends of different ions during evaporation (Fig. 5.8). According to the SET method, formation waters that plot directly on the SET are interpreted as evaporated seawaters, but evaporite-dissolution-waters are plotted above the SET. Figure 5.8 also shows some mixing scenarios between several end members (e.g., evaporated seawater and freshwater) and shows the affect of dissolving halite by water with high TDS content (Rittenhouse, 1967). In Figure 5.8, the formation waters from the SM area can be subdivided into at least three groups based on their bromine content as well as their location in relation to the SET.

Group I include water samples from the Hadrukh aquifer, which are plotted below the SET. The Br and TDS content of the water samples from this group approximate those to be expected from simple concentrations of seawater. The downward displacement of the saline samples relative to the SET might have been due to a dilution of the evaporated seawater with water of low TDS content, with the latter being a product of fresh meteoric water. A similar conclusion has been drawn for the origin and dilution of saltwater in the deep Paleogene aquifer in the vicinity of SM (Saeed et al., in press). The origin of saltwater was interpreted to be associated with the entrapment of evaporated paleo-seawater during the time of deposition which was later diluted by fresh meteoric water during the Late Pleistocene-Holocene period.

Water samples from the Dam Formation represent **Group II**, in which the TDS content is greater than that of seawater but the Br content is lower than would be expected from simple mixing of

seawater with water of low TDS and Br content. In addition to the primary source of solutes, which has been proven by the isotopic data in the previous section (i.e., trapped paleo-seawater), the position of these samples above the SET indicates that they may have some dissolved halite diluted with water of low TDS and Br content. Due to the absence of halite deposits within the Dam Formation and to the lack of tritium (^{3}H) in water samples from this group, these conditions suggest no recent recharge has reached the aquifer. Hence, it is proposed that the resident saline water in the Dam Formation may have originated from near-surface halite dissolution by heavy rain during one of the ancient wet phases and consequent recharge through the formation outcrops and subcrops.

Group III is represented by high-saline and brine samples from the Shuweihat and Sabkha Matti Formations. Samples from this group have somewhat more, to about twice as much, TDS content than the seawater, but the Br content is less than would be expected from simple concentrations of seawater. In relation to the SET, the Group III samples are plotted in the zone of halite dissolution by brine. The chemical compositions of the water samples from this group may have been influenced by repeated evapo-concentration and precipitation/dissolution reactions during the dry episodes. A mechanism for increasing the solute concentrations in these waters can be explained by the density-driven convection model (Van Dam et al., 2009, 2014). In this model, annual rainfalls dissolve near-surface evaporite minerals and return them to shallow, unconfined aquifers. This recharge solution is denser than the pre-existant waters in the aquifer, which allows it to sink to the bottom of the formation (Wood et al., 2002). Eventually, the returned solutes are added to the solute inputs from underlying regional aquifers, which results in an increase of solutes with time. Consequent evaporation will cause the re-precipitation of retrograde minerals like anhydrite, calcite, and gypsum in the unsaturated zone, and soluble salts at the sabkha surface. The

observation that tritium exists in some of the SMA water samples is consistent with the density-driven free-convection model.

5.4.5 Hydrogeochemical Evolution Model for Sabkha Matti

The schematic model presented in Figure 5.9 shows the hydrogeochemical evolution of Sabkha Matti. In the marine stage (Phase I), major cycles of transgression and regression of Neogene seawater formed lagoon and sabkha environments in the study area. In this setting, autochthonous brines were formed in the Hadrukh and Dam Formations during their time of deposition. The structural evolution stage (Phase II) is characterized by rapid Late-Pleistocene/Holocene tectonic events and subsequent erosion of the Miocene rock plateau. This causes a hydraulic balance alteration in the shallow aquifer system. As a result, brine from the artesian Hadrukh and Dam Formations migrates upward into the overlain Shuweihat Formation. Consequent evaporation concentrates cyclic evaporite minerals in the unsaturated zone. During a wet episode, the Sabkha Matti depression may impound rainwater after heavy precipitation and due to a rise in the groundwater table in response to the ~140 m rise in the Arabian Gulf. In this setting, the pre-existing evaporite minerals in the unsaturated zone are dissolved in sporadic lacustrine areas (Phase III). Finally, the evaporative stage (Phase IV) has prevailed across the study area for the last 5,000 years. Extensive evaporation during this hyper-arid climate has lowered the water surface in the Holocene saline lake into the sediment column. As a result, SM was converted again into a regional discharge zone for the underlying aquifers, and evaporite minerals were moved from a sub-aqueous setting into the unsaturated zone. Annual rainwater dissolves this evaporite layer, increases the brine salinity in the SMF, and then evaporates slowly to precipitate a new evaporite layer.

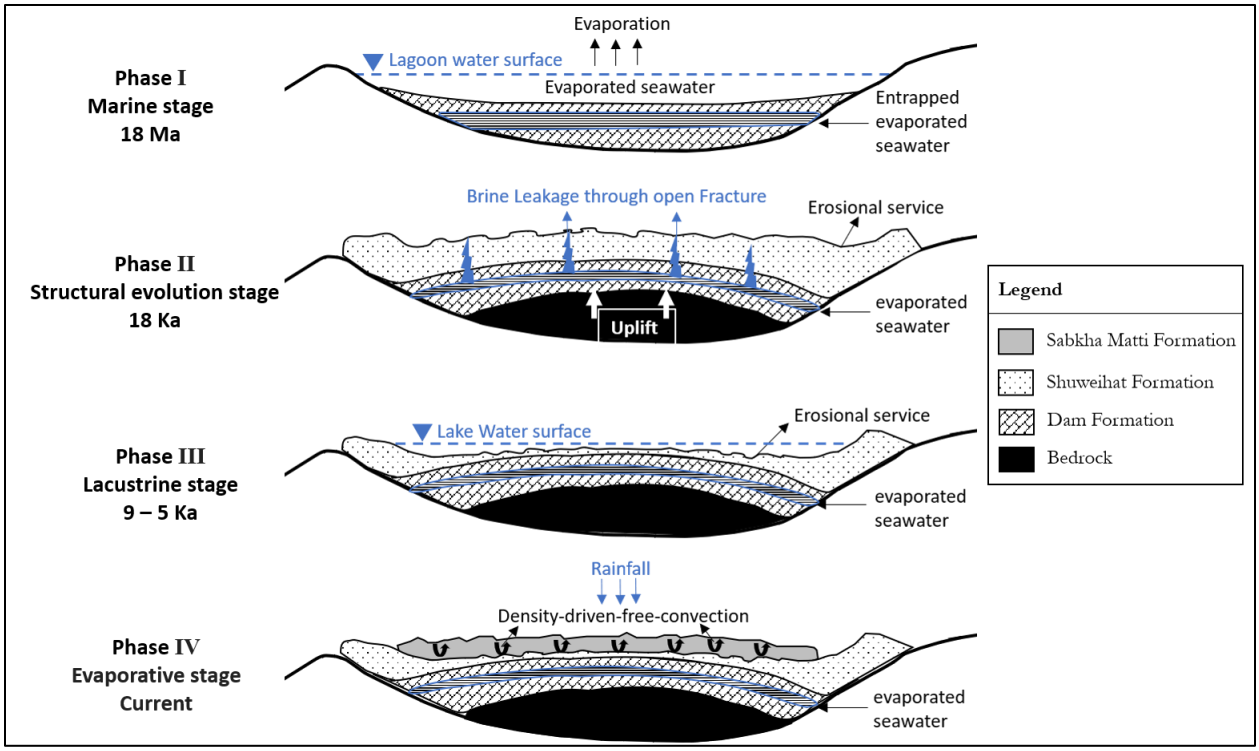

Figure 5-9: Schematic evolution model of Sabkha Matti

5.5 Conclusion

A combination of geological, hydraulic, hydrochemical, and isotopic methods were utilized as an approach to understand the hydrogeochemical evolution of Sabkha Matti and the underlying regional aquifers in the Rub' al Khali topographic basin. The geological structure of the Sabkha Matti basin is interpreted as a nearshore deep depression which dips gently from the coast toward the centre of the regional Rub' al-Khali basin. Inside this coastal basin, major cycles of transgression and regression formed a lagoonal environment, within which autochthonous brine aquifers were formed by the entrapment of paleo-seawater during the time of deposition of the Hadrukh and Dam Formations. The observed enrichments in the boron isotope data >+23‰ for all the analyzed water samples is consistent with this proposal, and suggests that most of the solutes in the underlying formations initially had a marine origin. Furthermore, it is proposed that a hydraulic balance alteration in the shallow aquifer system may have occurred in conjunction with

the rapid Late-Pleistocene/Holocene tectonic events and subsequent erosion of the Miocene rock plateau. Consequently, the brine trapped in the deep confined aquifers seeped up to the surficial sediments. The hydrostatic head data are in agreement with this model and confirm the potential for upward leakage from the underlying regional aquifers to the sabkha. This is also supported by the observed similarity in major ionic constituents and strontium isotope ratios in the water samples collected from the deep and near-surface formations. The stable water isotopes ($\delta^{18}O$, $\delta^{2}H$) and radio isotope (^{14}C and ^{3}H) data, however, suggest that the majority of the resident waters in all the studied formations were recharged during the Late Pleistocene-Holocene wet period. These data clearly show that water and solutes in Sabkha Matti area are from different sources. During the wet phases in the Late Pleistocene-Holocene, the Sabkha Matti depression may have filled with water from intensive precipitation as well as from the rise in the groundwater table in response to the ~140 m rise in the Arabian Gulf. A change in climate has created a more arid depositional setting for the last 5,000 years. In this setting, reduced precipitation has lowered the water surface in the Holocene saline lake and converted SM again into a regional discharge zone for the underlying aquifers. As a result, evaporite minerals were moved from a sub-aqueous setting into the unsaturated zone. Subsequent annual precipitation dissolves these evaporites, increases the brine salinity in the sabkha, and recharges the aquifer. Based on these data, a conceptual model for the origin of solutes in SM is one of brines ascending from underlying formations and concentrations increasing over time by a combination of evaporation, mineral dissolution by recharge, and density-driven convection through preferential pathways provided by fractures and faults that facilitate solute circulation.

Table 5-1: Solute chemistry of groundwater samples collected from different aquifers (from shallow to deep) in the Sabkha Matti area

Well ID	Ca (mg/L)	K (mg/L)	Mg (mg/L)	Na (mg/L)	Cl (mg/L)	SO_4 (mg/L)	HCO_3 (mg/L)	Br (mg/L)	Sr (mg/L)	pH	TDS (mg/L)
Sabkha Matti aquifer Median (N = 117)											
	6320	3140	6080	73500	178000	1137	10	8.9	141	6.6	269,552
Shuweihat aquifer											
Shuw-1	2160	581	1370	27100	43909	3914	35	5	46	7.3	79,000
Shuw-2	2840	522	1150	31200	54927	3350	21	1	75	7.5	94,000
Shuw-3	2800	541	1090	29500	45567	3083	27	2	54	7.2	82,600
Dam aquifer											
Dam-1	1450	300	950	10500	19700	4050	55	11	25	7.4	36,700
Dam-2	1500	450	950	15500	25000	6750	50	15	27	7.4	50,251
Hadrukh aquifer											
HDRK-1	1920	494	1540	7830	18086	1951	64	116	49	7.7	35,800
HDRK-2	1980	519	1600	8330	19426	3177	74	121	37	7.4	36,100
HDRK-3	1820	591	1720	8090	19583	3652	76	124	46	8.5	35,100

Chapter 6 Groundwater and Solute Budget

This chapter is published as follows:

Saeed, W., Shouakar-Stash, O., Wood, W., Parker, B., & Unger, A. (2020). Groundwater and solute budget (A case study from sabkha Matti, Saudi Arabia). Hydrology, 7(4), 94. DOI: 10.3390/hydrology7040094

6.1 Introduction

Sabkha is an Arabic term that is widely used for a salt flat. Evaporation greater than precipitation and a source of solutes are the main requirements for the occurrence of this phenomenon. Sabkhat (plural of Sabkha) are characterized by flat landscapes, shallow groundwater levels (usually less than one meter), and high-water salinities. In the Arabian Peninsula, there are two types of sabkhat: coastal and inland. Coastal sabkhat are marginal marine areas (Wood et al. 2002; Robinson and Gunatilaka 1991). In contrast, inland sabkhat are found in basins, away from the coast, and typically surrounded by sand dunes (Yechieli and Wood 2002). The formation of both coastal and inland sabkhat are explained by evaporation of continental groundwaters through the surface, which produces brines and subsequently causes the precipitation of evaporite minerals (Wood et al. 2002). Thus, the inland sabkha systems are important in water resource assessments owing that they represent discharge points of local and regional groundwater systems. In certain large, closed basins such as the Caspian Sea in Eurasia, Great Salt Lake, in North America, Lake Eyre in Australia, Lake Titicaca in South America, and Lake Chad in Africa surface water rather than groundwater dominates the solute input.

The Rub' al Khali (RAK) structural basin lies below the largest sand desert in the world. The structural basin covered an area of approximately 650,000 km^2 and is bound by the Central Arabian Arch in the north, the Oman Thrust in the east, the Hadhramaut-Dhofar Arch in the south, and the Arabian Shield in the west (Figure 6.1a). Sabkha Matti (SM) is a flat salt covered portion of the sabkha Matti drainage basin (>250,000 km^2) that is located in the Ar Rub al Kali desert and is underlain by the larger Ar Rub al Kali structural basin (Figure 6.1a,b). SM extends about 150 km south from the western Abu Dhabi coastline and across the border between the United Arab Emirates and Saudi Arabia (Saeed et al. In Press). At the coast of Abu Dhabi, SM is characterized

by a narrow strip of supratidal carbonate sands and evaporites that form a coastal sabkha. Southward, it grades into an area of inland siliciclastic sediments. The conceptual model for the origin of solutes in the coastal sabkha is the ascending brine model given by Wood et al. 2002. That is, the origin and evolution of solutes and mineral precipitation involves: 1) upward leakage of brines from the regional aquifers that underlay the sabkha; 2) deflation that removed sand down to the level of the water table; and 3) extensive evaporation that causes the formation of halite crust and accumulation of anhydrite and gypsum in the shallow subsurface. The question addressed in the current study is this ascending brine conceptual model viable for the Sabkha Matti inland sabkha? Thus, the aim of the current study is to quantitively estimate the water and solute fluxes to SM, which would ultimately lead to a better overall understanding of the regional hydrology in the Rub' al Khali structural basin and to investigate the role of SM in the regional hydrogeological system as a potential surface discharge point. It is assumed that the proposed conceptual model of the hydrology for sabkha Matti is applicable to the rest of the inland sabkhas of the Arabia Peninsula and to many ancient environments of deposition observed in the geologic record.

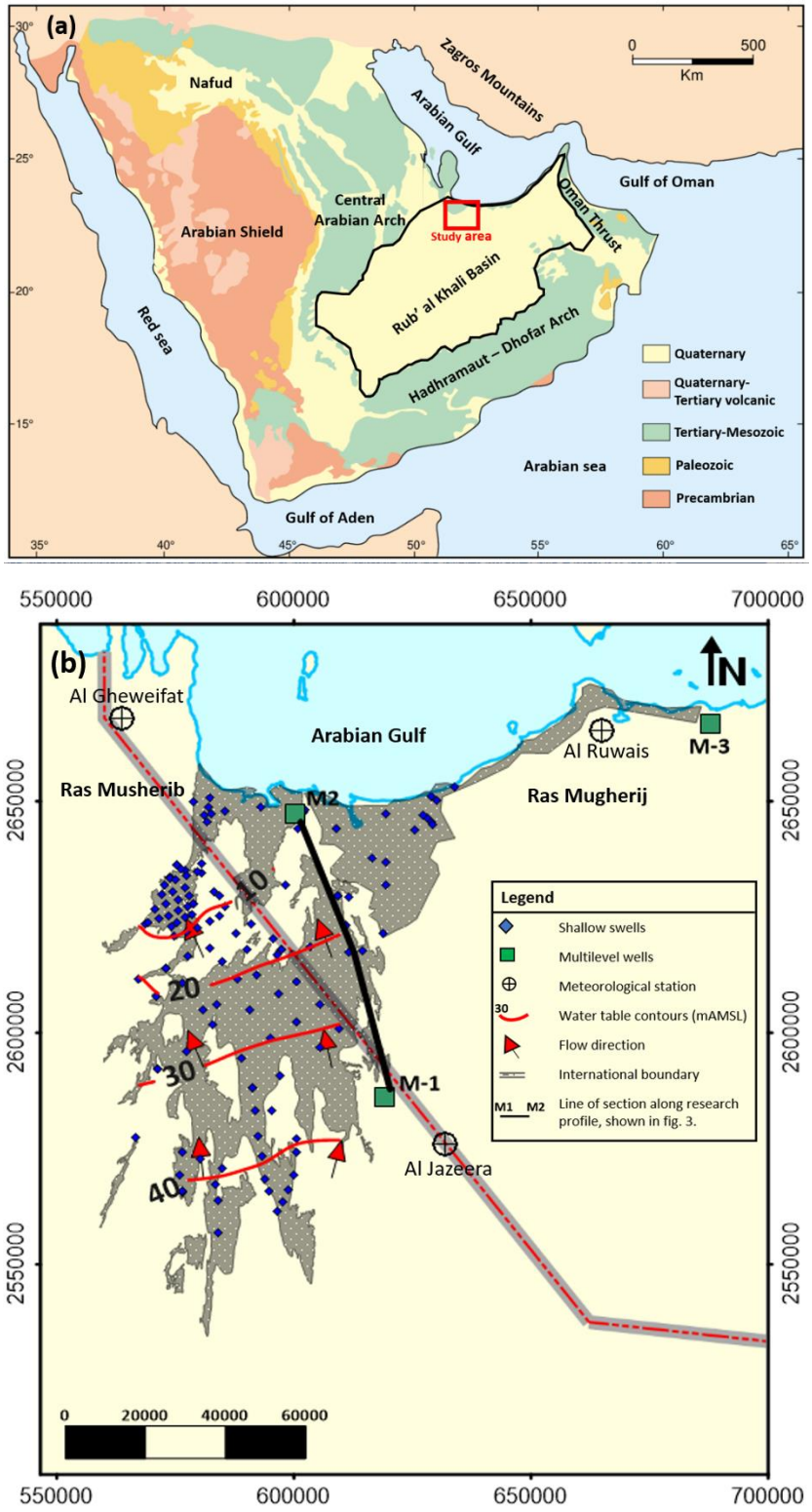

Figure 6-1: (a) Geologic sketch map of the Arabia Peninsula showing the location and boundaries of the Rub' al Khali structural basin ((Modified after (Wender et al., 1998), (b) map showing the location of sabkha Matti, sampling locations, water level contours and flow direction in the sabkha.

6.2 Geological Setting

Matti sabkha is a wide, north-south trending, salt-covered area that extends about 150 km south from the western Abu Dhabi coastline and across the border between the United Arab Emirates and Saudi Arabia (Figure 6.1). It covers a portion of the sabkha Matti (SM) drainage basin (>250,000 km^2) that is located in the Ar Rub al Kali desert and is underlain by the larger Ar Rub al Kali structural basin (Figure 6.1). The sabkha part of the larger drainage system is bound in the south by the sand dune system of the Rub' al Khali desert. The western and eastern boundaries of the sabkha are formed by N-S linear margins of Neogene-age outcrops, known as Ras Musherib and Ras Mugherij, respectively (Goodall 1995). A generalized W-E geologic cross section of the SM is shown in Figure 2. Beneath the sabkha lies a thick (6000-8000 m) Paleozoic-Cenozoic sedimentary sequence of carbonates, clastics, and evaporites that accumulated on the stable Arabian platform (Nairn and Alsharhan 1997). Above this sequence is a clastic deposit of Late Oligocene-Miocene age, known as the Hadrukh Formation. Following the deposition of the Hadrukh, the area now occupied by the Arabian Gulf area was subject to lagoonal-evaporitic deposition (Ziegler 2001). In this setting, marl, clay, dolomite, dolomitic limestone, anhydrite, and nodular gypsum of the Dam Formation were deposited (Powers et al. 1966). In Mid-Miocene, the area was subject to gentle tilting and rapid erosion of the Arabian shield basement as a result of the Miocene-Pliocene uplift (Zagros Orogeny) (Alsharhan et al. 2001). This setting favoured the deposition of continental clastic sediments of the Shuweihat Formation in fluvial, aeolian, and sabkha environments (Bristow 1999). Since Late Miocene-Pliocene, the Arabian Gulf foredeep basin has developed in front of the rising Zagros Mountains in response to a regional compressional event between the Arabian and Eurasian plates (Orang et al. 2018). In Late Quaternary, the region of SM was the site of drainage systems which derived fluvial sediments

from rising mountains in western Saudi Arabia and Oman and deposited them into the Matti drainage basin (Goodall 1995). Limited reworking and desiccation to these fluvial sediments occurred in Mid-Holocene in response to rises in the groundwater table in response to the ~140 m rise in the Arabian Gulf (Wood et al. 2002). Subsequent deflation removed sands down to the level of the rising water table that caused the development of evaporite facies within the fluvial sands (Alsharhan and Kendall 2003; Saeed et al. In Press). It is proposed that this fluvial sequence, within which the evaporite minerals have developed, be given the name Sabkha Matti Formation (SMF), because of its extensive development The SMF has an average thickness of about 5 m, is laterally continues by 50-80 km E-W, and extends inland N-S from the Arabian coast for nearly 150 km.

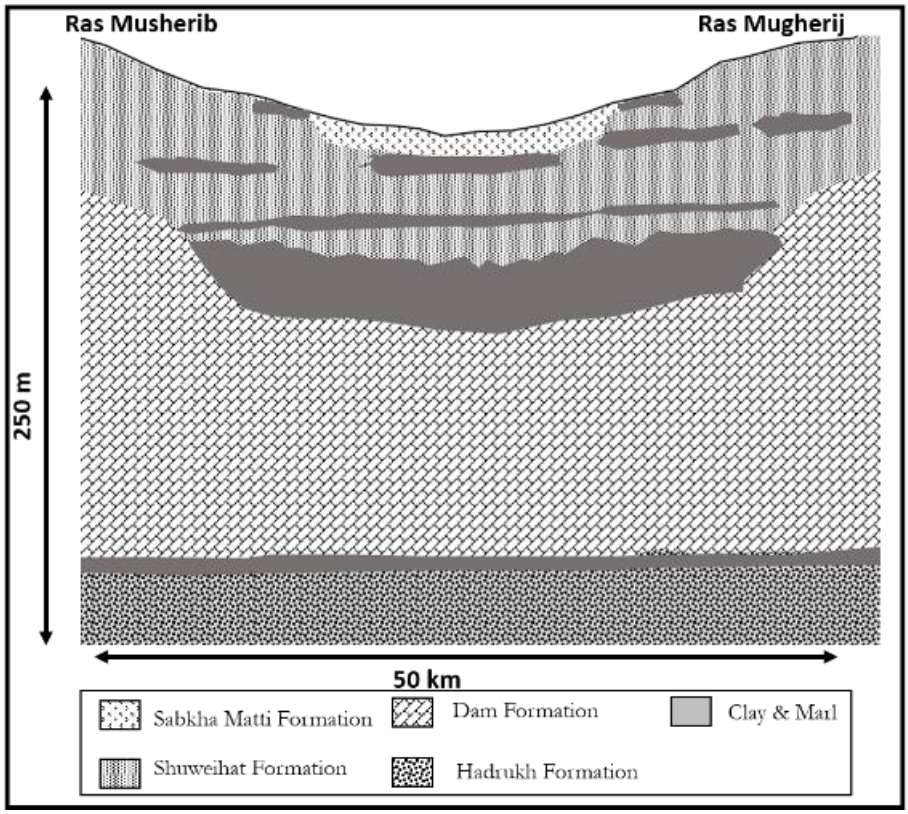

Figure 6-2: Generalized geologic cross section of the sabkha Matti from Ras Musherib in the west to Ras Mugherij in the east, as shown in Fig. 6.1.

6.3 Sampling and Methodology

Figure 6.1 shows the location of the drilled holes in the study area. Within the border of Saudi Arabia, holes for 102 shallow piezometers (<10 m) were drilled between 1 and 2m below the water table by using Geoprobe, Model 6620DT, and direct push machine. Nine piezometers of intermediate depth (>10 m and <25 m) were drilled by a rotary drill rig (B53, manufactured by Mobile Drill Intl) mounted on a 4x4 truck. All shallow and intermediate piezometers were constructed from 50mm-diameter schedule 40 PVC pipe, slotted by a hacksaw on the bottom 1.5 m, covered with filter sock, with threaded joints containing couplings. The holes were backfilled, with the loose sand collapsed around the piezometers. Within the border of Abu Dhabi, water samples were collected from eleven pre-existing monitoring wells. Detail of the well construction data for these wells are reported in Sanford and Wood (2001); Wood et al. (2002) and Wood and Böhlke (2017). Water samples were collected using a dedicated plastic bailer. Three deep wells (> 100 m) were drilled with rotary drills into the Dam and Hadrukh Formations. These wells were finished with 18 5/8-inch diameter steel casings through the overburden sediments to surface and were left as open bedrock borehole completions from the bottom of the casing to the remainder of the depth. Each of the three deep wells were provided with a cap, shut-off valve, and pressure gauge. All three deep wells were under flowing artesian conditions, which allowed collection of water samples at the surface. For this study, five well cluster systems were drilled along a research profile, shown in Fig. 6.3. Each of the cluster wells was completed at different depths, and groundwater samples were collected from each aquifer individually to investigate any chemical variations between the aquifers. Analyses of all water samples for electrical conductivity (EC), pH, temperature, and dissolved oxygen content were carried out in the field using a portable HQ40d meter (Hach Ltd.). Field measurements of alkalinity were made using a Hach field titration

kit and expressed as mg/L of equivalent HCO_3. All water samples were filtered through 0.45-µm filters and then acidified with double-distilled nitric acid for cation analysis and preserved unacidified for anion analysis. Analyses of major and minor ions were performed by Isobrine Solutions laboratory, Edmonton, Canada, and ALS laboratory group, Waterloo, Canada.

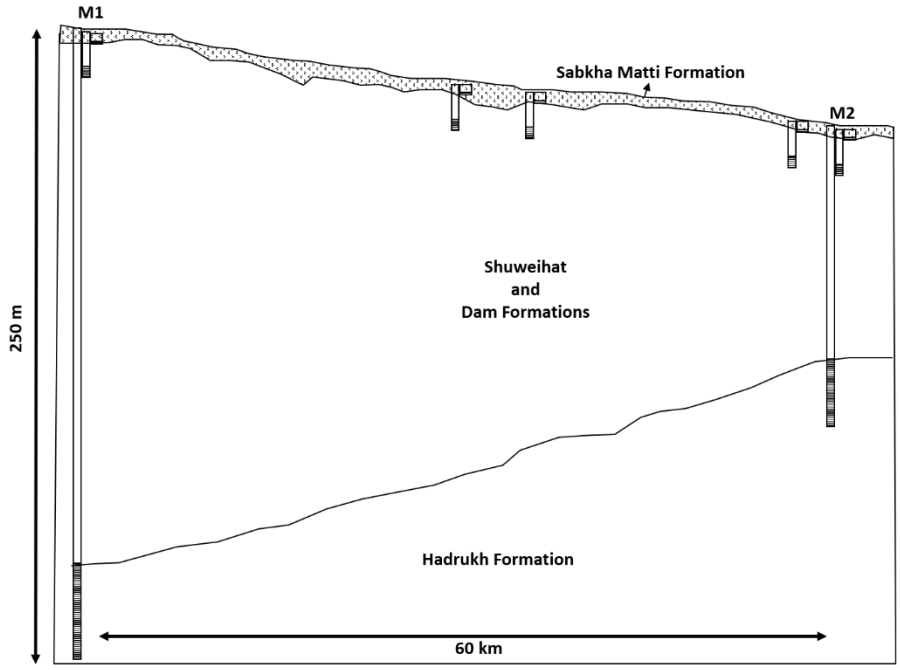

Figure 6-3: Transect M1–M2 showing multi-level observation wells that were installed in the sabkha Matti area. Trace of line of section is shown in Fig. 6.1.

6.4 Hydrologic Budget

A water budget for the SM was developed in order to understand the processes that control the hydrology of the sabkha and to quantify the individual components. The regional-scale system is assumed to operate under a steady-state flow condition, which means that all of the inflows to the sabkha must equal all of the outflows. The steady-state assumption is based on field observations which confirm that hydraulic heads throughout the sabkha area fluctuate very little over long time scales (> 3 years). The budget was developed around a representative control volume parallel to

the groundwater flow direction of the sabkha that is 20 km long, 1 m wide, and 5 m deep (see Fig. 6.4).

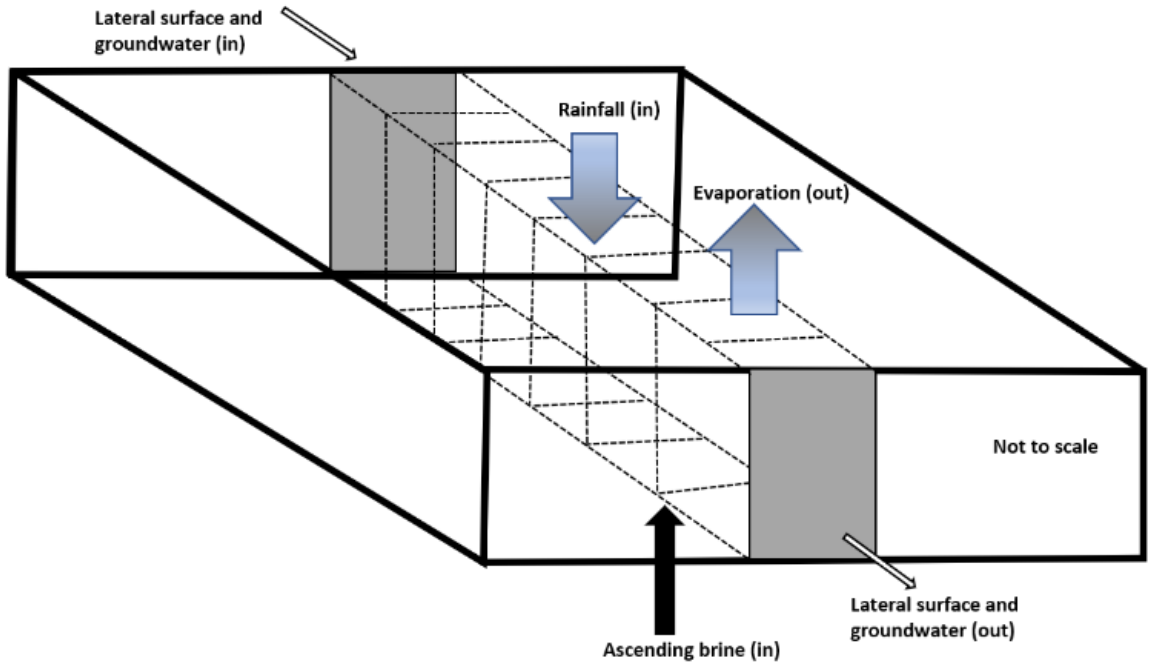

Figure 6-4: Water mass balance in the sabkha Matti

The inflow components to SM include: 1) direct precipitation on the aquifer; 2) shallow groundwater entering SM laterally from the mainland; and 3) upward leakage from the underlying regional aquifers. No substantial surface runoff has occurred to the sabkha through the duration of this study. However, field observations demonstrate that there must have been some recent overland flow in the last 100 years, as many of the surface features have a fluvial not aeolian expression and little of the sabkha is covered with dunes/sand sheets. For simplicity sake and due to the absence of data, surface runoff to and from the control volume is assumed to be negligible. Water may leave the sabkha by discharge laterally to the Arabian Gulf and by direct evaporation.

6.4.1 Lateral Groundwater Fluxes

Darcy's law (Eq. 1) was used to estimate the lateral fluxes of groundwater into and out of the SM.

$$q = -K (dh/dl) \quad (1)$$

where q is the flux in dimensions of length per time (L/T), K is the hydraulic conductivity of the porous medium in dimensions of length per time (L/T), and dh/dl is the gradient in the hydraulic head in the direction of flow in dimensions of length per length (dimensionless). In the SMF, the gradient is toward the coastline and the water table has a typical gradient of approximately 2 m in 10 km (Figure 6.1). To obtain horizontal hydraulic conductivity values (K_h), slug tests were performed on eight short-screened observation wells. The lithology in these wells range from marly sands to clean sand facies, that make them good representative samples of the fluvial and sabkha nature of the SMF. The slug test results give an arithmetic mean K_h value of about 1.4 m/d (Table 6.1). From gradient and K_h values, the lateral groundwater flux in the SMF is 0.2 mm/d, or about 7 cm/year.

Table 6-1 Well information and estimated horizontal hydraulic conductivities for the sabkha Matti Formation, obtained from slug tests.

Well ID	Screen interval (m)	Lithology	Hydraulic conductivity (m/d)
SM-2	4.2-5.7	Sand	2.9
SM-7	4.2-5.7	Sand	0.9
SM-14	4.2-5.7	Sand	0.5
SM-20	4.3-5.8	Sand	1.6
SM-26	4.2-5.7	Sand	1.1
SM-30	4.3-5.8	Marly sand	0.1
SM-49	4.1-5.6	Sand	3.3
SM-82	5.4-6.9	Marly sand	0.5

6.4.2 Upward Leakage

Artesian hydraulic heads in the regional Hadrukh and Dam Formations, and upward hydraulic gradients across the Shuweihat and SM Formations (Table 6.2), are consistent with the fact that regional groundwater is moving slowly upward into the base of the sabkha. From the hydrostatic data, an average upward hydraulic gradient of 0.14 was calculated from three separate pairs of multilevel wells. The hydraulic conductivity in this case is the vertical hydraulic conductivity (K_v) of the least conductive layer underlying the sabkha. Measuring K_v in situ is usually difficult that it must be measured either on cores or as a secondary parameter on a test for horizontal conductivity. However, it has been verified based on field data that a harmonic weighting of the horizontal conductivities can yield a reasonable estimate of the net vertical conductivity (Sanford and Wood 2001). Slug tests were carried out at three observation wells, where the screens were installed within the aquitard underlying the sabkha. The obtained K_h values from the three-slug test are $3x10^{-4}$, $4x10^{-5}$ and $9x10^{-6}$ m/d. Field observation suggests that this variation in the K_h values is mainly due to the high heterogeneity in the aquitard layer, which composes of a mixing of silty sands and well-compacted mudstones. These data reveal that there might be a significant level of uncertainty in the estimated K_v for the aquitard. With this in mind, a harmonic weighting of the K_h value was calculated to be about $2x10^{-5}$ m/d, that is assumed to represent the net K_v value for the confining layer underlying the sabkha. This value corresponds to clayey-sandstones (Domenico and Schwartz 1990), consistent with the geological logs. Using Darcy's law, the mean upward leakage calculated with the above values of head gradient and K_v is approximately 3×10^{-6} m/d or about 1 mm/year. This estimate of the upward flux is a calculation of water flux multiplied by the solute concentration of the upwelling brines provides a mass flux. This estimate of the upward flux is compared with the chemistry of the upwelling brines in the below section, and the results

demonstrates that the estimates are consistent with the solute mass balance. These calculations over the 5000 years given of the age of Sabkha Matti Fm. demonstrates that the estimates are consistent with the origin of solute mass in the aquifer system. A relatively similar vertical water flux of approximately 4 mm/y was reported from the coastal sabkha of Abu Dhabi, United Arab Emirates (Sanford and Wood 2001).

Table 6-2: Water level measurements from the multi-level wells at the sabkha Matti, confirming the potential of upward leakage from the regional Hadrukh and Dam Formations into the sabkha. Water levels are in meters above sea level.

Sampling wells	Formation screened in	Total depth (m)	Water level (mAMSL)
M-1A	Hadrukh	244	64
M-1B	Sabkha	8	39
M-2A	Hadrukh	121	20
M-2B	Sabkha	14	1
M-3A	Dam	89	12
M-3B	Sabkha	15	3

6.4.3 Evaporation and Recharge

Actual evaporation from the surface of the SMF was estimated to be 39 ± 13 mm/y, based on a remote sensing technique (Schultz et al. 2015). The assumption that the SM is operating under a steady-state condition requires that the flux out by evaporation must equal the flux in by rainfall. To evaluate this assumption, the mean annual rainfall was taken over a fourteen-year period from three meteorological stations in the vicinity of the SM (Figure. 6.1). The data range from 44.5 mm at Al Ruwais station in the further northeast to 42.2 mm at Al Gheweifat station in the northwest

to 29 mm at Al Jazeera station southeast of the SM (NCMS 2017). This gives a mean annual rainfall of about 39 mm/year. In order to determine the amount of infiltrated rainwater to the groundwater table, water tables were monitored in three designated wells during the summer, where no rainfall occurred, and one measurement was taken after a 13.3 mm rain event in March of 2017 (Table 6.3). After the rain event, rises in water levels were measured to be 35, 30, and 30 mm. By multiplying these values with the porosity of 0.38, the ratio of infiltrated water to the rain event suggests that between 86% to 100% of the rainfall was accounted for at the water table. The highest recharge ratio to the water table was recorded in a well that is drilled adjacent to a solution collapse feature, which is very common in the area as a result of salt crust dissolution. Similar observations were reported from the coastal sabkha of Abu Dhabi, where more than 80% of the rainfall infiltrates to the water table (Sanford and Wood 2001). The outcome of the evaporation and recharge data provide further evidence of the steady-state nature of the sabkha system, where the water lost by evaporation is balanced by the mean annual recharge.

Table 6-3: Water level measurement data to determine the ratio of infiltrated rainwater to the sabkha Matti Formation.

Well Name	Average water level (m) in dry season	Measured water level (m) after 13.3 mm rain event	Water level rise (mm) after 13.3 mm rain event	infiltrated rainwater (mm)= water level rise * effective Porosity	Infiltrated water vs. rain (%)
SM-15	1.22	1.18	35.00	13.30	100
SM-41	1.26	1.23	30.00	11.40	86
SM-98	1.18	1.15	30.00	11.40	86

6.5 Solute Budget

A solute budget was similarly developed around a volumetric cross section of the sabkha that is 20 km long, 1 m wide, and 5 m deep. Major ionic constituents and strontium isotope ratios in water samples collected from the Hadrukh, Dam and Shuweihat Formations were observed to resemble those ones which were obtained from the near-surface sabkha brine (Saeed et al. In Press). These data along with hydrostatics head measurements suggest a major source for the solutes in the SM to be associated with an ascending brine from the underlying regional aquifers. Yet, solutes may also enter the SM with the surface-water transport, from atmospheric precipitation, form by reaction of the water with the skeleton framework, enter the system by eolian process and may form by reaction with the gasses. Solute may leave the system as transported with the groundwater or surface flow, leave by diffusion, leave by mineral precipitation, leave by eolian process or leave as a gas phase. Solute concentrations are almost certainly transient as will be shown below by their continuous input and relative lack of output.

Table 6-4: Solute chemistry (mg/L) of groundwater samples collected from different aquifers in the sabkha Matti area.

Aquifer	Ca	K	Mg	Na	Cl	SO_4	Sr
Hadrukh	4,800	1,300	2,600	35,000	69,500	2,850	85
Hadrukh	4,500	1,300	2,500	34,000	67,600	2,950	85
Dam	2,160	581	1,370	27,100	43,909	3,914	46
Shuweihat	2,840	522	1,150	31,200	54,927	3,350	75
Shuweihat	2,800	541	1,090	29,500	45,567	3,083	54
Sabkha (n=119)	10,894	3,438	7,854	72,406	170,654	1,739	254

The mean dissolve-solid concentration results from different geological Formation at the SM are shown in Table 6.4. The components of the solute budget can be calculated from multiplying the mean dissolve-solid concentrations, represented by the mean chloride concentrations, by the water budget (Sanford and Wood 2001). By using the lateral water-inflow value of about 445 million L/year and a Cl input concentration value of 160 g/L, the lateral inflow of solutes from upgradient of the sabkha is estimated to be about 70 kg/year. Similarly, a lateral water-outflow value of approximately 1800 L/year multiplied by an outflow concentration of Cl that is 200 g/L, results in an estimated 350 kg/year of solute outflow. Likewise, the upward leakage value of around 22,170 L/year multiplied by a mean Cl concentration of 55 g/L, results in 1,250 kg/year of upward leakage of solutes. It is assumed that concentration increases over time by a combination of evaporation, mineral solution by recharge and density-driven free-convection that is circulating the solutes. It is also assumed that some salt is leaving the system through the land surface by deflation. A compilation of the component values of the water and solute budget is summarized in Table 6.5.

Table 6-5: Components of the water and solute budgets calculated in this study, based on the control volume of the sabkha that is 20 km long, 1 m wide, and 5 m deep.

Budget component flux	Volumetric water flux (m^3/year)	Total solute (kg/year)
Lateral flux in	1	70
Lateral flux out	2	350
Upward leakage	20	1250
Evaporation	780	0
Rainfall	780-670	<1
Increase in storage	0	970

6.6 Discussion

The lateral groundwater flux in the SMF is calculated to be 0.2 mm/d. This flux value can be converted to a seepage velocity by dividing the flux by the effective porosity. Several laboratory analyses of the sand from the SMF yield a consistent porosity of approximately 0.38. Given this value of porosity, the lateral seepage velocity through the SMF is estimated to be about 18 cm/year. The lateral flux out of the SMF was calculated downgradient of the sabkha. In this area, the hydraulic gradient is about 7 m in 10 km (0.0007). Accordingly, the lateral groundwater flux out of SM is calculated to be about 36 cm/year. For the purposes of comparing the magnitude of the different components of the hydrologic budget, the fluxes are multiplied by the width (1 m) and thickness (5 m) of the sabkha to obtain lateral volumetric fluxes. The flux in and out of the sabkha obtains a lateral volumetric flux values of about 0.4 m^3/year and 1.8 m^3/year, respectively (Table 6.5). The average residence time for the lateral groundwater flux to be transmitted from the proximal end to the distal end at the discharge zone is calculated by dividing one half the length of the sabkha (150 km) by the seepage velocity. Accordingly, the average residence time of groundwater is approximately 416,000 years. Given that the age of the SM is approximately 8000 to 5000 years old, it is concluded that lateral influx of groundwater has not contributed significantly to the current volume of water and solutes in the sabkha. The calculated upward flux is multiplied by the width (1 m) and length (20,000 m) of the section to obtain a total upward volumetric flux of about 20 m^3/year. This value is significantly larger than the horizontal flux, of 0.4 m^3/year. These calculations suggest that the upward leakage from the underlying regional aquifers provides an important source of groundwater entering the sabkha. The pore volume of brine that might fill the SMF over its life span was calculated by multiplying the mean upward flux by the porosity and the age of the sabkha. Based on this, an approximately 3 pore volumes should have filled the 5-m-

thick section of the SMF over its saturated life span of 5000 years. Hypothetically, the ratios of the average concentrations of conservative solutes from the underlying regional aquifers to those in the sabkha should be equal to the number of pore volumes that have entered the sabkha. Such ratios are shown in Figure 6.5. Field observations suggest a relatively conservative nature for magnesium and potassium, as no significant precipitations of both minerals were observed throughout the study area. Accordingly, K and Mg were assumed to be the most conservative ions in this geological setting, and their ratios indicate that about 3 pore volumes have entered the sabkha. This result reveals that the solute and water budget estimates of 3 pore volumes are in complete agreement. However, minerals that have significantly precipitated on the sabkha surface show lower ratios. This includes sodium and chloride that precipitate as halite, calcium and sulfate precipitate as anhydrite. Thus, the solute budget is totally in line with the hydrologic budget and the age of SM. Moreover, the actual evaporation from the surface of the SMF of 39 mm/y is multiplied by the section width of 1 m and the section length of 20,000 m to give a volumetric flux out of about 780 m^3/year. As the system is assumed to operate under a steady-state condition, the water lost by evaporation is balanced by the mean annual recharge that is calculated to be between 670-780 m^3/year. These data reveal that evaporation and recharge on the sabkha are the dominant components, whereas lateral and upwelling groundwater components are minor. Note however the solute mass is dominated by upwelling water. The water mass balance in the SM is illustrated in Figure 6.4.

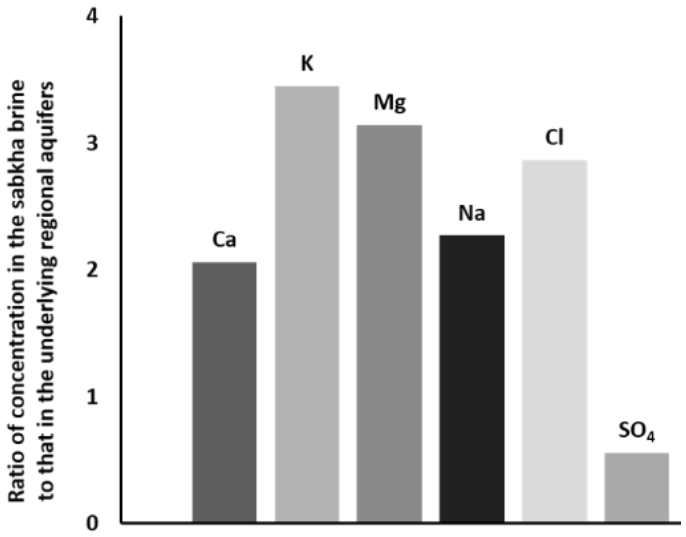

Figure 6-5: Ratios of major-element concentrations for the upwelling regional brine relative to the brine in the sabkha Matti.

6.7 Conclusion

A hydrologic budget of the sabkha Matti was constructed as an approach to better understand the regional groundwater systems of the large drainage area >250,000 km^2 in the Rub' al Khali structural basin. The data reveal that the hydrologic budget for the sabkha Matti system is operating under a steady-state condition where all of the inflows to the sabkha equal all of the outflows. A quantification of the components to the water budget suggests that evaporation and rainfall are the dominant components, whereas lateral and upwelling groundwater components are minor. In contrast, analysis of the solute budget shows that the dominant source of solutes is upward leakage from the underlying regional aquifers, consistent with the ascending brine model proposed by (Sanford and Wood 2001; Wood et al. 2002; Wood and Sanford 2002; Yechieli and Wood 2002; and Saeed et al. In Press). Therefore, this study shows that water and solutes in the sabkha Matti are from different sources. These data also show that about 3 pore volumes of brine may have leaked upward into the control volume of the sabkha since the time it was first formed about 5000 years ago. The proposed conceptual model of the hydrology for sabkha Matti is assumed to apply

to the rest of the inland sabkhas of the Arabia Peninsula and to many ancient environments of deposition observed in the geologic record.

Reference

Abu-Taleb, M., & Egeli, I. (1981). Some geotechnical problems in the eastern province of Saudi Arabia. Proceedings of the Symposium on Geotechnical Problems in Saudi Arabia, , 2 799-811.

Ahmed, M., Abdel Samie, S., & Badawy, H. (2013). Factors controlling mechanisms of groundwater salinization and hydrogeochemical processes in the quaternary aquifer of the eastern Nile delta, Egypt. Environmental Earth Sciences, , 1-26.

Akili, W., & Torrance, J. K. (1981). The development and geotechnical problems of sabkha, with preliminary experiments on the static penetration resistance of cemented sands. Quarterly Journal of Engineering Geology, 14(1), 59-73.

Al-Guwaizani, A. S. (1994). Sedimentology and Geochemistry of Qurayyah Sabkha, Eastern Saudi Arabia,

Allen, P. A. (2007). The Huqf supergroup of Oman: Basin development and context for Neoproterozoic glaciation. Earth-Science Reviews, 84(3), 139-185. Alsaaran, N. A. (2008). Origin and geochemical reaction paths of sabkha brines: Sabkha Jayb Uwayyid, eastern Saudi Arabia. *Arabian Journal of Geosciences, 1*(1), 63.

Alsharhan, A., & Kendall, C. S. C. (2002). Holocene carbonate/evaporites of abu Dhabi, and their Jurassic ancient analogs. Sabkha Ecosystems. Kluwer Academic Publishers, Dordrecht, the Netherlands, , 187-202.

Alsharhan, A., & Kendall, C. S. C. (2003). Holocene coastal carbonates and evaporites of the southern Arabian Gulf and their ancient analogues. *Earth-Science Reviews, 61*(3-4), 191-243.

Alsharhan, A., Rizk, Z., Nairn, A. E. M., Bakhit, D., & Alhajari, S. (2001). *Hydrogeology of an arid region: The Arabian Gulf and adjoining areas.* Elsevier.

Amini, S. V., Faramarzi, N., & Sheikhi, F. (2010). Tectonic activities effects on mineralization in Hormuz island, Persian Gulf, southern Iran. Proc., GSA Conference on Tectonic Crossroads: Evolving Orogens of Eurasia-Africa-Arabia, GSA, Ankara, Turkey, 35-39.

Anton, D. (1984). Aspects of geomorphological evolution; paleosols and dunes in Saudi Arabia. *Quaternary period in Saudi Arabia* (pp. 275-296) Springer.

Appelo, C. A. J., & Postma, D. (2004). *Geochemistry, groundwater and pollution.* CRC press.

Atapour, H. (2012). Geochemical baseline of major anions and heavy metals in groundwaters and drinking waters around the urban areas of Kerman city, southeastern Iran. Environmental Earth Sciences, 67(7), 2063-2076. Bahis, L., & Miller, M. R. (1975). Groundwater seepage and its effect on saline soils.

Bagheri, R., Nadri, A., Raeisi, E., Eggenkamp, H., Kazemi, G., & Montaseri, A. (2014). Hydrochemical and isotopic (δ18O, δ2H, 87Sr/86Sr, δ37Cl and δ81Br) evidence for the origin of saline formation water in a gas reservoir. *Chemical Geology, 384*, 62-75.

Bagheri, R., Nadri, A., Raeisi, E., Kazemi, G., Eggenkamp, H., & Montaseri, A. (2014). Origin of brine in the Kangan gasfield: Isotopic and hydrogeochemical approaches. *Environmental Earth Sciences, 72*(4), 1055-1072.

Bashitialshaaer, R. A., Persson, K. M., & Aljaradin, M. (2011). Estimated future salinity in the Arabian Gulf, the Mediterranean Sea and the red sea consequences of brine discharge from desalination. International Journal of Academic Research, 3(1)

Bear, J., Cheng, A. H., Sorek, S., Ouazar, D., & Herrera, I. (1999). Seawater intrusion in coastal aquifers: Concepts, methods and practices Springer Science & Business Media.

Berner, Z. A., Stüben, D., Leosson, M. A., & Klinge, H. (2002). S-and O-isotopic character of dissolved sulphate in the cover rock aquifers of a Zechstein salt dome. Applied Geochemistry, 17(12), 1515-1528. Birkle, P., Jenden, P., & Al-Dubaisi, J. (2013). Origin of formation water from the Unayzah and Khuff petroleum reservoirs, Saudi Arabia. *Procedia Earth and Planetary Science, 7*, 77-80.

Bishop, M. A. (2010). Nearest neighbor analysis of mega-barchanoid dunes, Ar rub' al Khali, sand sea: The application of geographical indices to the understanding of dune field self-organization, maturity and environmental change doi: https://doi.org/10.1016/j.geomorph.2010.03.029

Brenot, A., Négrel, P., Petelet-Giraud, E., Millot, R., & Malcuit, E. (2015). Insights from the salinity origins and interconnections of aquifers in a regional scale sedimentary aquifer system (Adour-Garonne district, SW France): Contributions of δ34S and δ18O from dissolved sulfates and the 87Sr/86Sr ratio. *Applied Geochemistry, 53*, 27-41.

Bristow, C. (1999). Aeolian and sabkha sediments in the Miocene Shuwaihat Formation, Emirate of abu Dhabi, United Arab Emirates.

Burke, W., Denison, R., Hetherington, E., Koepnick, R., Nelson, H., & Otto, J. (1982). Variation of seawater $^{87}Sr/^{86}Sr$ throughout phanerozoic time. *Geology*, *10*(10), 516-519.

Burns, S. J., Matter, A., Frank, N., & Mangini, A. (1998). Speleothem-based paleoclimate record from northern Oman. *Geology*, *26*(6), 499-502.

Butler, G. P. (1969). Modern evaporite deposition and geochemistry of coexisting brines, the sabkha, trucial coast, Arabian Gulf. *Journal of Sedimentary Research, 39*(1)

Butler, G., Krouse, R., & Mitchell, R. (1973). Sulphur-isotope geochemistry of an arid, supratidal evaporite environment, trucial coast. *The Persian Gulf* (pp. 453-462). Springer.

Carpenter, A.B. (1978) Origin and chemical evolution of brines in sedimentary basins. *Okl Geol Surv Circular* 79:60–77

Capo, R. C. (1991). Application of strontium isotopes to late Cenozoic paleoceanography and stratigraphy.

Chan, L., Starinsky, A., & Katz, A. (2002). The behavior of lithium and its isotopes in oilfield brines: Evidence from the Heletz-Kokhav field, Israel. *Geochimica Et Cosmochimica Acta, 66*(4), 615-623.

Clark, I. (2015). Groundwater geochemistry and isotopes CRC press.

Clark, I. D., & Fritz, P. (2013). *Environmental isotopes in hydrogeology.* CRC press.

Clark, I. D., & Fontes, J. (1990). Paleoclimatic reconstruction in northern Oman based on carbonates from hyperalkaline groundwaters. *Quaternary Research, 33*(3), 320-336.

Craig, H. (1961). Isotopic variations in meteoric waters. *Science (New York, N.Y.), 133*(3465), 1702-1703. doi:133/3465/1702 [pi]

Davis, S. N., Whittemore, D. O., & Fabryka-Martin, J. (1998). Uses of chloride/bromide ratios in studies of potable water. Groundwater, 36(2), 338-350.

Diaw, M., Faye, S., Stichler, W., & Maloszewski, P. (2012). Isotopic and geochemical characteristics of groundwater in the Senegal river delta aquifer: Implication of recharge and flow regime. Environmental Earth Sciences, 66(4), 1011-1020. Dogramaci, S. S., & Herczeg, A. L. (2002). Strontium and carbon isotope constraints on carbonate-solution interactions and inter-aquifer mixing in groundwaters of the semi-arid Murray basin, Australia. *Journal of Hydrology, 262*(1-4), 50-67.

Domenico, P. A., & Schwartz, F. W. (1990). Physical and chemical hydrogeology. Wiley, New York.

Duane, M. J., & Zamel, A. (1999). Modern and ancient sabkha environments-boron isotopes as discriminators of facies and uses in base metal exploration.

Duane, M. J., Al-Zamel, A., & Eastoe, C. J. (2004). Stable isotope (chlorine, hydrogen and oxygen), geochemical and field evidence for continental fluid flow vectors in the al-Khiran sabkha (Kuwait). Journal of African Earth Sciences, 40(1-2), 49-60. doi:10.1016/j.jafrearsci.2004.07.004

Edgell, H. S. (2006). *Arabian deserts: Nature, origin and evolution* Springer Science & Business Media.

Ellis, C. (1973). Arabian Salt-Bearing Soil (Sabkha) as an Engineering Material,

Eastoe, C., Long, A., Land, L. S., & Kyle, J. R. (2001). Stable chlorine isotopes in halite and brine from the gulf coast basin: Brine genesis and evolution. *Chemical Geology, 176*(1-4), 343-360.

Eggenkamp, H. (2014). *The geochemistry of stable chlorine and bromine isotopes.* Springer.

Elasha, B. O. (2010). Mapping of climate change threats and human development impacts in the Arab region. *UNDP Arab Development Report–Research Paper Series, UNDP Regional Bureau for the Arab States.*

Evans, G., Kendall, C. G. S. C., & Skipwith, P. (1964). Origin of the coastal flats, the sabkha, of the trucial coast, Persian Gulf. Nature, 202(4934), 759-761. doi:10.1038/202759a0

Evans, G., Schmidt, V., Bush, P., & Nelson, H. (1969). Stratigraphy and geologic history of the sabkha, abu Dhabi, Persian Gulf. *Sedimentology, 12*(1-2), 145-159.

Faure, G. (1986). Principles of isotope geology, 2nd ed.

Fleitmann, D., Burns, S. J., Neff, U., Mangini, A., & Matter, A. (2003). Changing moisture sources over the last 330,000 years in northern Oman from fluid-inclusion evidence in speleothems. *Quaternary Research, 60*(2), 223-232.

Fontes, J. C., & Matray, J. (1993). Geochemistry and origin of formation brines from the Paris basin, France: 1. brines associated with triassic salts. *Chemical Geology, 109*(1-4), 149-175.

Frape, S., Shouakar-Stash, O., Pačes, T., & Stotler, R. (2007). Geochemical and isotopic characteristics of the waters from crystalline and sedimentary structures of the bohemian massif. *Water Rock Interaction, 12,* 727-733.

Fryberger, S. G., Al-Sari, A. M., & Clisham, T. J. (1983). Eolian dune, interdune, sand sheet, and siliciclastic sabkha sediments of an offshore prograding sand sea, Dhahran area, Saudi Arabia. American Association of Petroleum Geologists Bulletin, 67(2), 280-312.

Gavish, E. (1974). Geochemistry and mineralogy of a recent sabkha along the coast of Sinai, Gulf of Suez. Sedimentology, 21(3), 397-414. doi:10.1111/j.1365-3091.1974.tb02067.x

Genereux, D. P., Webb, M., & Solomon, D. K. (2009). Chemical and isotopic signature of old groundwater and magmatic solutes in a costa Rican rain forest: Evidence from carbon, helium, and chlorine. Water Resources Research, 45(8)

Glennie, K., Fryberger, S., Hern, C., Lancaster, N., Teller, J., Pandey, V., & Singhvi, A. (2011). Geological importance of luminescence dates in Oman and the Emirates: An overview. Geochronometria, 38(3), 259-271.

Gonfiantini, R. (1986). Environmental isotopes in lake studies. *Handbook of Environmental Isotope Geochemistry, 2,* 113-168.

Goodall, T. M. (1995). The Geology and Geomorphology of the Sabkhat Matti Region (United Arab Emirates): A Modern Analogue for Ancient Desert Sediments from North-West Europe. *PhD thesis, University of Aberdeen:* 433 pp.

Guiraud, R., Issawi, B., & Bosworth, W. (2001). Phanerozoic history of Egypt and surrounding areas. *Peri-Tethys Memoir, 6,* 469-509.

Hess, J., Bender, M., & Schilling, J. (1991). Assessing seawater/basalt exchange of strontium isotopes in hydrothermal processes on the flanks of mid-ocean ridges. *Earth and Planetary Science Letters, 103*(1-4), 133-142.

Hodell, D. A., Kamenov, G. D., Hathorne, E. C., Zachos, J. C., Röhl, U., & Westerhold, T. (2007). Variations in the strontium isotope composition of seawater during the Paleocene and early Eocene from ODP leg 208 (Walvis ridge). *Geochemistry, Geophysics, Geosystems, 8*(9).

Holm, D. A. (1960). Desert geomorphology in the Arabian Peninsula. Science, 132(3437), 1369-1379.

Holser WT (1979) Trace elements and isotopes in evaporites. In: Burns RG (ed) Reviews in mineralogy, marine minerals. Mineral Society of America, Washington DC, pp 295–346

Hsü, K., & Schneider, J. (1973). Progress report on dolomitization—hydrology of abu Dhabi sabkhas, Arabian Gulf. *The Persian Gulf* (pp. 409-422) Springer.

Hsü, K. J., & Siegenthaler, C. (1969). Preliminary experiments on hydrodynamic movement induced by evaporation and their bearing on the dolomite problem. Sedimentology, 12(1-2), 11-25. doi:10.1111/j.1365-3091.1969.tb00161.x

Husseini, M. I., & Husseini, S. I. (1990). Origin of the nfracambrian salt basins of the middle east. Geological Society, London, Special Publications, 50(1), 279-292. IAEA (International Atomic Energy Agency). (2010). (Complete daily isotope data 1961-1988).

Johnson, D. H., Kamal, M. R., Pierson, G. O., & Ramsay, J. B. (1978). Sabkhas of eastern Saudi Arabia. Quaternary Period in Saudi Arabia, 1(1), 84-93.

Johnson, K. S. (1997). Evaporite karst in the united states. Carbonates and Evaporites, 12(1), 2-14.

Kalin, R. M. (2000). Radiocarbon dating of groundwater systems. *Environmental tracers in subsurface hydrology* (pp. 111-144) Springer.

Kelly, F. (2005). Seawater intrusion topic paper. WRIA, Island County.

Keren, R., Gast, R., & Bar-Yosef, B. (1981). pH-dependent boron adsorption by Na-montmorillonite 1. *Soil Science Society of America Journal, 45*(1), 45-48.

Kendall, C. S. C., Alsharhan, A., & Whittle, G. (1998). The flood re-charge sabkha model supported by recent inversions of anhydrite to gypsum in the UAE sabkhas. Quaternary Deserts and Climatic Change, 2-17.

Kendall, C., & Caldwell, E. A. (1998). Fundamentals of isotope geochemistry. Isotope Tracers in Catchment Hydrology, , 51-86.

Kendall, Christopher G St C. (1968). Recent algal mats of a Persian Gulf lagoon. Journal of Sedimentary Research, 38(4) Kendall, C., & Doctor, D. H. (2003). In Holland H. D., Turekian

K. K. (Eds.), *5.11 - stable isotope applications in hydrologic studies*. Oxford: Pergamon. doi:https://doi.org/10.1016/B0-08-043751-6/05081-7 "

Kharaka, Y. K., & Hanor, J. (2003). Deep fluids in the continents: I. sedimentary basins. *Treatise on Geochemistry, 5*, 605.

Kharroubi, A., Tlahigue, F., Agoubi, B., Azri, C., & Bouri, S. (2012). Hydrochemical and statistical studies of the groundwater salinization in Mediterranean arid zones: Case of the erba coastal aquifer in southeast Tunisia. Environmental Earth Sciences, 67(7), 2089.

Kinsman, D. J. (1966). Gypsum and anhydrite of recent age, trucial coast, Persian Gulf. Second Symposium on Salt, , 1 302-326.

Kinsman, D. J. (1969). Modes of formation, sedimentary associations, and diagnostic features of shallow-water and supratidal evaporites. *AAPG Bulletin, 53*(4), 830-840.

Kloppmann, W., Girard, J., & Négrel, P. (2002). Exotic stable isotope compositions of saline waters and brines from the crystalline basement. Chemical Geology, 184(1), 49-70.

Knauth, L. P., & Beeunas, M. A. (1986). Isotope geochemistry of fluid inclusions in Permian halite with implications for the isotopic history of ocean water and the origin of saline formation waters. *Geochimica Et Cosmochimica Acta, 50*(3), 419-433.

Kraemer, T. F., Wood, W. W., & Sanford, W. E. (2014). Distinguishing seawater from geologic brine in saline coastal groundwater using radium-226; an example from the sabkha of the UAE. *Chemical Geology, 371*, 1-8.

Lee, C. H. (2010). Impacts of natural salt pollution on water supply capabilities of river/reservoir systems Texas A&M University.

Mace, R., Davidson, S., Angle, E., & Mullican III, W. (2006). Aquifers of the Gulf Coast. Texas Water Development Board Report 365.

Martin, A. Z. (2001). Late Permian to Holocene Paleofacies evolution of the Arabian plate and its hydrocarbon occurrences. *Geoarabia, 6*(3), 445-504.

McClure, H. (1976). Radiocarbon chronology of late quaternary lakes in the Arabian desert. *Nature, 263*(5580), 755-756.

McKenzie, J. A., Hsu, K. J., & Schneider, J. F. (1980). Movement of subsurface waters under the sabkha, abu Dhabi, UAE, and its relation to evaporative dolomite genesis. *Concepts and Models of Dolomitization, ,* 11-30.

Mirnejad, H., Sisakht, V., Mohammadzadeh, H., Amini, A., Rostron, B., & Haghparast, G. (2011). Major, minor element chemistry and oxygen and hydrogen isotopic compositions of arun oil-field brines, SW Iran: Source history and economic potential. Geological Journal, 46(1), 1-9.

Moujabber, M. E., Samra, B. B., Darwish, T., & Atallah, T. (2006). Comparison of different indicators for groundwater contamination by seawater intrusion on the Lebanese coast. Water Resources Management, 20(2), 161-180.

Müller, D. W., McKenzie, J. A., & Mueller, P. A. (1990). Abu Dhabi sabkha, Persian Gulf, revisited: Application of strontium isotopes to test an early dolomitization model. *Geology, 18*(7), 618-621.

Nairn, A., & Alsharhan, A. (1997). *Sedimentary basins and petroleum geology of the middle east* Elsevier.

NCMS (National Center for Meteorology and Seismology (2018). National center for meteorology and seismology, Abu Dhabi, United Arab Emirates. Website. http://www.ncms.ae/en/details.html?id=1525&lid=3300

Neff, U., Burns, S., Mangini, A., Mudelsee, M., Fleitmann, D., & Matter, A. (2001). Strong coherence between solar variability and the monsoon in Oman between 9 and 6 k year ago. *Nature, 411*(6835), 290.

Odhiambo, G. O. (2017). Water scarcity in the Arabian Peninsula and socio-economic implications. *Applied Water Science, 7*(5), 2479-2492.

Orang, K., Motamedi, H., Azadikhah, A., & Royatvand, M. (2018). Structural framework and tectono-stratigraphic evolution of the eastern persian gulf, offshore iran. Marine and Petroleum Geology, 91, 89-107. doi:https://doi-org.proxy.lib.uwaterloo.ca/10.1016/j.marpetgeo.2017.12.014

Parker, A., & Rose, J. (2008). Climate change and human origins in southern Arabia. Paper presented at the *Proceedings of the Seminar for Arabian Studies,* 25-42.

Patterson, R., & Kinsman, D. J. (1977). Marine and continental groundwater sources in a Persian Gulf coastal sabkha: Sediments and diagenesis.

Patterson, R. J., & Kinsman, D. J. J. (1981). Hydrologic framework of a sabkha along Arabian Gulf. American Association of Petroleum Geologists Bulletin, 65(8), 1457-1475.

Patterson, R. J., & Kinsman, D. J. J. (1982). Formation of diagenetic dolomite in coastal sabkha along Arabian (Persian) gulf. *American Association of Petroleum Geologists Bulletin, 66*(1), 28-43.

Peebles, R. (1999). Stable isotope analyses and dating of the Miocene of the emirate of abu Dhabi, United Arab Emirates. *Fossil Vertebrates of Arabia, with Emphasis on the Late Miocene Faunas, Geology, and Palaeoenvironments of the Emirate of Abu Dhabi, United Arab Emirates. Yale University Press, New Haven, Connecticut,* 88-105.

Perotti, C., Carruba, S., Rinaldi, M., Bertozzi, G., Feltre, L., & Rahimi, M. (2011). The Qatar–South Fars arch development (Arabian platform, Persian Gulf): Insights from seismic

interpretation and analogue modelling. *New Frontiers in Tectonic Research-at the Midst of Plate Convergence, ,* 325-352.

Pinti, D. L., Béland-Otis, C., Tremblay, A., Castro, M. C., Hall, C. M., Marcil, J., . . . Lapointe, R. (2011). Fossil brines preserved in the St-Lawrence lowlands, Quebec, Canada as revealed by their chemistry and noble gas isotopes. Geochimica Et Cosmochimica Acta, 75(15), 4228-4243.

Powers, R., Ramirez, L., Redmond, C., & Elberg, E. (1966). Geology of the Arabian Peninsula. *Geological Survey Professional Paper, 560*, 1-147.

Priestley, S. C., Wohling, D. L., Keppel, M. N., Post, V. E., Love, A. J., Shand, P., Kipfer, R. (2017). Detecting inter-aquifer leakage in areas with limited data using hydraulics and multiple environmental tracers, including 4 he, 36 Cl/Cl, 14 C and 87 Sr/86 sr. *Hydrogeology Journal, 25*(7), 2031-2047.

Quinn, O. (1986). *Regional hydrogeological evaluation of the Najd. Open-file Rep*. Public Authority for Water Resources. Sultanate of Oman, Report No. CCEWR 48–86

Richter, B. C., & Kreitler, C. W. (1986). Geochemistry of salt water beneath the rolling plains, North-Central Texas. Groundwater, 24(6), 735-742.

Rittenhouse, G. (1967). Bromine in oil-field waters and its use in determining possibilities of origin of these waters. *AAPG Bulletin, 51*(12), 2430-2440.

Robinson, B. W., & Gunatilaka, A. (1991). Stable isotope studies and the hydrological regime of sabkhas in southern Kuwait, Arabian gulf. *Sedimentary Geology, 73*(1-2), 141-159. doi:10.1016/0037-0738(91)90027-B

Saeed, W., Shouakar-Stash, O., Unger, A., Wood, W. W., & Parker, B., In Press, Chemical evolution of an inland sabkha: A case study from Sabkha Matti, Saudi Arabia

Saeed, W., Shouakar-Stash, O., Unger, A., Wood, W.W., & Parker, B. In Press, Origin of solutes in a regional multi-level sedimentary aquifer system: (a case study from the Rub' al Khali basin, Saudi Arabia)

Sanford, W. E., & Wood, W. W. (2001). Hydrology of the coastal sabkhas of abu Dhabi, United Arab Emirates. *Hydrogeology Journal, 9*(4), 358-366.

Schulz, S., Horovitz, M., Rausch, R., Michelsen, N., Mallast, U., Köhne, M., Merz, R. (2015). Groundwater evaporation from salt pans: Examples from the eastern Arabian Peninsula. *Journal of Hydrology, 531*, 792-801

Shouakar-Stash, O. (2008). Evaluation of stable chlorine and bromine isotopes in sedimentary formation fluids. PhD thesis, University of Waterloo, Canada.

Shouakar-Stash, O., Alexeev, S., Frape, S., Alexeeva, L., & Drimmie, R. (2007). Geochemistry and stable isotopic signatures, including chlorine and bromine isotopes, of the deep groundwaters of the Siberian platform, Russia. *Applied Geochemistry, 22*(3), 589-605.

Shouakar-Stash, O., Frape, S. K., & Wood, W. W. (2006). The role of stable chlorine and bromine stable isotopes in determining the geochemical evolution of the abu Dhabi costal sabkha (UAE). 6th International Conference on the Geology of the Middle East, UAE.

Singleton, M. J., & Moran, J. E. (2010). Dissolved noble gas and isotopic tracers reveal vulnerability of groundwater in a small, high-elevation catchment to predicted climate changes. *Water Resources Research, 46*(10).

Smith, C. L. (1981). Reconnaissance investigation of brine in the eastern rub al Khali, kingdom of Saudi Arabia Ministry of Petroleum and Mineral Resources, Deputy Ministry for Mineral

Smith, A. (2012). A review of the Ediacaran to early Cambrian ('Infra-Cambrian') evaporites and associated sediments of the middle east. Geological Society, London, Special Publications, 366(1), 229-250.

Spivack, A., & Edmond, J. (1987). Boron isotope exchange between seawater and the oceanic crust. *Geochimica Et Cosmochimica Acta, 51*(5), 1033-1043.

Stewart, S. (2016). Structural geology of the Rub' Al-Khali basin, Saudi Arabia. *Tectonics, 35*(10), 2417-2438.

Stokes, S., Bray, H., Goudie, A. S., Wood, W. W., & Alsharhan, A. (2003). Later quaternary Paleo recharge events in the Arabian Peninsula. *Water Resources Perspectives: Evaluation, Management and Policy. Elsevier, Amsterdam, ,* 371-378.

Stokes, S., Bray, H., Goudie, A. S., Wood, W. W., & Alsharhan, A. (2003). Later quaternary Paleo recharge events in the Arabian Peninsula. *Water Resources Perspectives: Evaluation, Management and Policy Elsevier, Amsterdam, ,* 371-378.

Sugarman, P. J., Miller, K. G., Owens, J. P., & Feigenson, M. D. (1993). Strontium-isotope and sequence stratigraphy of the Miocene Kirkwood Formation, southern new jersey. *Geological Society of America Bulletin, 105*(4), 423-436.

Sugarman, P. J., McCartan, L., Miller, K. G., Feigenson, M. D., Pekar, S., Kistler, R. W., & Robinson, A. (1997). Strontium-isotopic correlation of Oligocene to Miocene sequences, New Jersey and Florida. *Proc. Ocean Drill. Prog. Sci. Res.,* 150 (1997), pp. 147-159

Sultan, M., Sturchio, N., Al Sefry, S., Milewski, A., Becker, R., Nasr, I., & Sagintayev, Z. (2008). Geochemical, isotopic, and remote sensing constraints on the origin and evolution of the rub al Khali aquifer system, Arabian Peninsula. Journal of Hydrology, 356(1-2), 70-83.

Sultan, M., Sturchio, N. C., Alsefry, S., Emil, M. K., Ahmed, M., Abdelmohsen, K., Abdullah, M., Eugen, Y., Save, H., Talal, A. Alharbi, T. (2019). Assessment of age, origin, and sustainability

of fossil aquifers: A geochemical and remote sensing–based approach. *Journal of Hydrology, 2019, 576, 325-341, Elsevier*

Thompson, G. R., & Custer, S. G. (1976). Shallow ground-water salinization in dryland farm areas of Montana. Montana University Joint Water Resources Research Center Report, (79)

Thode, H. (1991). Sulphur isotopes in nature and the environment: An overview. *Stable Isotopes: Natural and Anthropogenic Sulphur in the Environment, 43*, 1-26.

United Nations. Economic and Social Commission for Western Asia. (2013). *Inventory of shared water resources in western Asia.* United Nations Publications.

Van Dam, R. L., Eustice, B. P., Hyndman, D. W., Wood, W. W., & Simmons, C. T. (2014). Electrical imaging and fluid modeling of convective fingering in a shallow water-table aquifer. *Water Resources Research, 50*(2), 954-968.

Van Dam, R. L., Simmons, C. T., Hyndman, D. W., & Wood, W. W. (2009). Natural free convection in porous media: First field documentation in groundwater. *Geophysical Research Letters, 36*(11)

Vengosh, A., Chivas, A. R., McCulloch, M. T., Starinsky, A., & Kolodny, Y. (1991 a). Boron isotope geochemistry of Australian salt lakes. *Geochimica Et Cosmochimica Acta, 55*(9), 2591-2606.

Vengosh, A., Starinsky, A., Kolodny, Y., & Chivas, A. R. (1991 b). Boron isotope geochemistry as a tracer for the evolution of brines and associated hot springs from the dead sea, Israel. *Geochimica Et Cosmochimica Acta, 55*(6), 1689-1695.

Vengosh, A., Starinsky, A., Kolodny, Y., Chivas, A. R., & Raab, M. (1992). Boron isotope variations during fractional evaporation of sea water: New constraints on the marine vs. nonmarine debate. *Geology, 20*(9), 799-802.

Wender, L. E., Bryant, J. W., Dickens, M. F., Neville, A. S., & Al-Moqbel, A. M. (1998). Paleozoic (pre-khuff hydrocarbon geology of the Ghawar area, eastern Saudi Arabia. Geoarabia, 3(2), 273-302.

Weyhenmeyer, C. E., Burns, S. J., Waber, H. N., Aeschbach-Hertig, W., Kipfer, R., Loosli, H. H., & Matter, A. (2000). Cool glacial temperatures and changes in moisture source recorded in Oman groundwaters. *Science (New York, N.Y.), 287*(5454), 842-845. doi:8230 [pi]

Whittemore, D. O., & Pollock, L. M. (1979). Determination of salinity sources in water resources of Kansas by minor alkali metal and halide chemistry. Available from the National Technical Information Service, Springfield VA 22161 as PB 80-128911, Price Codes: A 03 in Paper Copy, A 01 in Microfiche. Contribution, (208).

Whybrow, P. J., & Hill, A. P. (1999). *Fossil vertebrates of Arabia: With emphasis on the late Miocene faunas, geology, and palaeoenvironments of the emirate of abu Dhabi, United Arab Emirates* Yale University Press New Haven, CT.

Wood, W. W., & Böhlke, J. K. (2017). Density-Driven Free-Convection model for isotopically fractionated geogenic nitrate in sabkha brine. Groundwater, 55(2), 199-207.

Wood, W. W., Clark, D., Imes, J. L., & Councell, T. B. (2010). Eolian transport of geogenic hexavalent chromium to ground water. Groundwater, 48(1), 19-29.

Wood, W. W., Bailey, R. M., Hampton, B. A., Kraemer, T. F., Lu, Z., Clark, D. W., Al Ramadan, K. (2012). Rapid late Pleistocene/Holocene uplift and coastal evolution of the southern Arabian (Persian) Gulf. *Quaternary Research, 77*(2), 215-220.

Wood, W. W., & Imes, J. L. (2003). Dating of Holocene ground-water recharge in western part of abu Dhabi (United Arab Emirates): Constraints on global climate-change models. *Developments Water Sci, 200350*, 379-385.

Wood, W. W., & Sanford, W. E. (2002). Hydrogeology and solute chemistry of the coastal-sabkha aquifer in the emirate of abu Dhabi. *Sabkha Ecosystems, 1*, 173-185.

Wood, W. W., Sanford, W. E., & Habshi, Abdul Rahman S Al. (2002). Source of solutes to the coastal sabkha of abu Dhabi. *Geological Society of America Bulletin, 114*(3), 259-268.

Wood, W. W., Sanford, W. E., & Habshi, Abdul Rahman S Al. (2002). Source of solutes to the coastal sabkha of abu Dhabi. *Geological Society of America Bulletin, 114*(3), 259-268.

Yechieli, Y., & Wood, W. W. (2002). Hydrogeologic processes in saline systems: Playas, sabkhas, and saline lakes. *Earth-Science Reviews, 58*(3-4), 343-365. doi:10.1016/S0012-8252(02)00067-3

Yurtsever, Y., & Araguas, L. A. (1993). Environmental isotope applications in hydrology: An overview of the IAEA's activities, experiences, and prospects. Iahs Publication, , 3-3.

Zarei, M., Raeisi, E., Merkel, B. J., & Kummer, N. (2013). Identifying sources of salinization using hydrochemical and isotopic techniques, Konarsiah, Iran. Environmental Earth Sciences, 70(2), 587.

Ziegler, M. A. (2001). *Late Permian to Holocene Paleofacies evolution of the Arabian plate and its hydrocarbon occurrences* Gulf Petro Link.

Appendices

Appendix A Major and trace element concentrations for groundwater samples from the Rub' al Khali basin aquifers

Sample ID	Aquifer	Ca (mg/L)	K (mg/L)	Mg (mg/L)	Na (mg/L)	Cl (mg/L)	SO_4 (mg/L)	HCO_3 (mg/L)	Br (mg/L)	Sr (mg/L)	pH	TDS (mg/L)
SM-1	Sabkha Matti	2,090	1,460	4,210	91,000	140,452	4,481	61	20.5	42.0	6.5	243,754
SM-2	Sabkha Matti	1,200	421	883	12,500	148,734	3,951	10	18.3	26.3	6.7	167,699
SM-3	Sabkha Matti	2,210	1,510	3,800	85,800	145,168	4,052		16.6	41.7	5.6	242,539
SM-4	Sabkha Matti	2,150	1,550	5,040	94,200	149,311	4,557	12	23.8	49.6	6.7	256,820
SM-6	Sabkha Matti	1,830	2,290	2,950	95,900	150,404	4,350	5	16.5	34.5	6.5	257,729
SM-7	Sabkha Matti	2,260	2,330	3,240	79,500	150,870	3,545	8	13.2	41.6	6.7	241,753
SM-8	Sabkha Matti	1,940	2,530	3,550	82,600	152,276	4,197	30	20.0	42.5	7.0	247,123
SM-9	Sabkha Matti	2,760	2,870	3,160	86,600	176,381	2,383	7	8.8	51.3	6.8	274,161
SM-13	Sabkha Matti	20,400	5,310	9,420	56,900	180,864	315	32	9.4	463.0	5.8	273,241
SM-14	Sabkha Matti	9,480	3,450	6,510	64,000	150,665	831	11	60.9	220.0	6.4	234,946
SM-15	Sabkha Matti	11,800	4,490	7,790	67,200	181,858	476	10	36.9	283.0	6.3	273,624
SM-16	Sabkha Matti	6,190	2,170	4,070	52,700	108,091	1,673	20	43.4	130.0	6.8	174,914
SM-17	Sabkha Matti	15,600	5,140	8,160	60,200	178,878	413	4	3.5	344.0	6.6	268,394
SM-18	Sabkha Matti	8,730	3,500	6,080	76,400	174,117	714	11	8.2	175.0	6.4	269,552
SM-19	Sabkha Matti	5,500	3,370	4,480	85,000	161,960	1,221	7	6.5	116.0	6.8	261,539
SM-20	Sabkha Matti	6,540	3,190	5,730	74,400	171,027	991	4	13.5	141.0	6.4	261,881
SM-21	Sabkha Matti	5,540	3,600	4,450	84,900	152,428	1,398	14	8.7	114.0	6.7	252,330
SM-22	Sabkha Matti	5,470	2,910	6,230	68,900	176,021	1,017	10	16.7	120.0	6.6	260,557
SM-24	Sabkha Matti	2,270	950	3,070	49,900	89,573	4,834	12	19.0	45.7	7.1	150,609

Appendix A- continued: Major and trace element concentrations for groundwater samples from the Rub' al Khali basin aquifers

Sample ID	Aquifer	Ca (mg/L)	K (mg/L)	Mg (mg/L)	Na (mg/L)	Cl (mg/L)	SO_4 (mg/L)	HCO_3 (mg/L)	Br (mg/L)	Sr (mg/L)	pH	TDS (mg/L)
SM-25	Sabkha Matti	8,960	3,800	6,960	72,800	182,817	583	2	8.0	190.0	6.2	275,922
SM-26	Sabkha Matti	6,320	2,820	5,960	75,300	179,480	888	6	8.0	142.0	6.1	270,774
SM-27	Sabkha Matti	9,350	3,440	7,320	67,300	168,071	699	5	7.8	202.0	6.3	256,185
SM-28	Sabkha Matti	14,400	3,840	9,510	68,400	184,712	404	4	6.4	320.0	6.3	281,270
SM-29	Sabkha Matti	7,090	3,070	7,120	78,400	176,014	862	5	8.3	151.0	6.3	272,561
SM-30	Sabkha Matti	5,860	2,910	6,240	81,900	182,040	993	5	6.6	127.0	6.0	279,948
SM-31	Sabkha Matti	5,000	2,840	5,370	73,200	179,574	1,181	7	8.2	99.0	6.6	267,171
SM-32	Sabkha Matti	5,930	3,050	6,600	79,000	183,307	953	4	7.3	129.0	6.9	278,845
SM-33	Sabkha Matti	5,100	2,700	5,990	78,500	178,341	1,172	8	7.7	109.0	6.4	271,811
SM-34	Sabkha Matti	4,340	2,020	4,370	81,300	153,763	1,749	10	5.9	89.0	6.8	247,553
SM-35	Sabkha Matti	4,260	1,840	5,130	75,500	140,584	1,918	18	11.2	85.9	6.6	229,250
SM-36	Sabkha Matti	9,310	3,300	9,360	67,800	173,787	713	12	15.4	199.0	6.5	264,282
SM-37	Sabkha Matti	10,200	2,300	5,010	72,000	140,619	842	9	5.2	235.0	6.7	230,980
SM-38	Sabkha Matti	3,810	1,230	2,030	39,300	62,048	2,557	25	2.9	81.1	7.3	111,000
SM-39	Sabkha Matti	18,000	5,860	7,130	69,900	183,320	376	2	1.4	405.0	6.5	284,588
SM-41	Sabkha Matti	3,680	2,320	4,720	86,800	178,511	1,758	6	12.4	80.2	6.8	277,795
SM-42	Sabkha Matti	2,110	2,570	2,690	100,000	179,193	2,885	12	2.9	52.1	6.9	289,460
SM-44	Sabkha Matti	1,080	1,040	946	56,700	85,306	10,802	48	5.9	18.9	7.3	155,923
SM-46	Sabkha Matti	20,400	5,960	12,600	60,100	184,354	348	2	7.0	473.0	6.3	283,764
SM-48	Sabkha Matti	12,200	4,360	9,230	77,600	184,870	506	7	5.9	277.0	6.6	288,773

Appendix A- continued: Major and trace element concentrations for groundwater samples from the Rub' al Khali basin aquifers

Sample ID	Aquifer	Ca (mg/L)	K (mg/L)	Mg (mg/L)	Na (mg/L)	Cl (mg/L)	SO_4 (mg/L)	HCO_3 (mg/L)	Br (mg/L)	Sr (mg/L)	pH	TDS (mg/L)
SM-49	Sabkha Matti	4,740	3,430	3,980	82,400	178,875	1,254	4	4.2	109.0	6.7	274,683
SM-52	Sabkha Matti	2,170	2,310	2,170	87,600	173,060	2,929	7	3.6	47.1	7.1	270,246
SM-56	Sabkha Matti	12,200	4,470	10,600	60,300	178,580	523	1	5.3	302.0	6.0	266,674
SM-57	Sabkha Matti	4,330	3,690	3,830	85,600	178,795	1,507	8	2.4	102.0	7.0	277,760
SM-58	Sabkha Matti	14,500	4,700	10,000	57,200	179,036	458	10	8.3	335.0	6.2	265,904
SM-59	Sabkha Matti	8,490	3,200	7,390	65,000	183,245	683	2	7.9	190.0	6.5	268,011
SM-60	Sabkha Matti	1,790	2,810	1,740	75,400	174,246	3,140	4	2.4	44.3	7.0	259,130
SM-61	Sabkha Matti	2,290	1,300	1,430	74,300	176,014	862	14	8.3	43.1	7.2	256,210
SM-62	Sabkha Matti	2,230	1,360	1,240	80,500	166,831	3,073	8	1.3	45.7	7.1	255,242
SM-63	Sabkha Matti	1,590	2,110	1,330	78,000	177,561	3,858	6	2.8	31.7	7.1	264,455
SM-64	Sabkha Matti	7,870	3,010	6,880	83,600	183,974	805	10	9.3	163.0	6.6	286,150
SM-65	Sabkha Matti	12,100	4,630	7,620	66,800	176,074	534	16	6.5	266.0	6.5	267,774
SM-67	Sabkha Matti	13,700	4,080	7,600	66,400	179,772	427	4	5.0	297.0	6.6	271,983
SM-68	Sabkha Matti	16,800	5,140	9,570	73,600	180,370	392	8	4.8	332.0	6.6	285,879
SM-69	Sabkha Matti	15,700	4,420	7,600	60,700	169,861	450	12	8.5	301.0	6.6	258,743
SM-70	Sabkha Matti	9,830	3,340	6,290	64,700	179,252	543	4	6.5	204.0	6.6	263,959
SM-71	Sabkha Matti	12,600	4,140	9,000	61,700	181,660	442	12	9.2	287.0	6.3	269,554
SM-72	Sabkha Matti	1,370	867	1,970	58,100	90,079	8,634	49	8.4	28.9	7.6	161,069
SM-73	Sabkha Matti	1,660	625	1,390	31,400	44,661	5,530	44	6.5	30.0	7.7	85,310
SM-74	Sabkha Matti	14,600	4,320	8,700	58,900	183,723	383	9	6.6	353.0	6.4	270,635

Appendix A- continued: Major and trace element concentrations for groundwater samples from the Rub' al Khali basin aquifers

Sample ID	Aquifer	Ca (mg/L)	K (mg/L)	Mg (mg/L)	Na (mg/L)	Cl (mg/L)	SO_4 (mg/L)	HCO_3 (mg/L)	Br (mg/L)	Sr (mg/L)	pH	TDS (mg/L)
SM-75	Sabkha Matti	4,420	1,520	2,560	58,400	106,172	2,365	26	5.2	97.6	7.1	175,463
SM-76	Sabkha Matti	8,660	2,870	4,840	69,600	158,739	804	30	4.4	188.0	6.6	245,543
SM-77	Sabkha Matti	5,640	1,650	2,610	58,500	100,401	1,916	8	1.5	134.0	7.3	170,724
SM-78	Sabkha Matti	20,400	6,350	9,400	65,400	180,653	349	4	1.2	453.0	6.5	282,556
SM-79	Sabkha Matti	9,990	4,940	5,950	65,800	183,572	566	10	5.1	209.0	6.7	270,828
SM-80	Sabkha Matti	6,840	3,140	4,540	73,400	151,757	1,116	10	4.7	161.0	6.8	240,803
SM-81	Sabkha Matti	3,390	2,120	5,090	76,500	170,082	1,895	6	10.2	68.2	6.2	259,083
SM-82	Sabkha Matti	4,170	2,410	5,090	83,700	166,608	1,631	6	7.9	79.0	6.7	263,615
SM-83	Sabkha Matti	3,560	2,300	4,970	73,700	165,595	1,758	9	9.7	74.6	6.6	251,892
SM-84	Sabkha Matti	4,640	2,630	5,780	72,700	182,598	1,137	6	7.7	100.0	6.5	269,491
SM-85	Sabkha Matti	3,940	1,740	3,840	80,100	149,339	1,712	4	5.2	88.8	6.8	240,675
SM-86	Sabkha Matti	3,760	2,110	4,900	66,000	170,517	1,561		7.1	75.3	6.5	248,848
SM-87	Sabkha Matti	3,560	1,970	4,960	95,400	164,247	1,864	12	9.1	73.1	6.8	272,013
SM-88	Sabkha Matti	3,020	1,460	3,790	69,600	121,811	3,366	12	8.4	55.3	7.1	203,059
SM-89	Sabkha Matti	3,620	1,980	5,000	64,500	151,548	2,038	6	9.0	71.2	6.7	228,692
SM-90	Sabkha Matti	3,300	1,900	4,690	83,600	158,228	2,146	7	10.9	65.9	7.0	253,872
SM-91	Sabkha Matti	8,530	3,010	7,660	77,800	180,144	699	5	5.8	184.0	6.6	277,848
SM-92	Sabkha Matti	3,330	2,040	4,870	71,500	154,945	2,246	18	9.4	65.5	6.6	238,949
SM-93	Sabkha Matti	9,040	3,540	5,470	55,900	174,367	683	7	3.4	195.0	6.3	249,007
SM-94	Sabkha Matti	5,610	1,890	3,740	66,600	114,966	1,721	32	5.7	122.0	6.8	194,560

Appendix A- continued: Major and trace element concentrations for groundwater samples from the Rub' al Khali basin aquifers

Sample ID	Aquifer	Ca (mg/L)	K (mg/L)	Mg (mg/L)	Na (mg/L)	Cl (mg/L)	SO_4 (mg/L)	HCO_3 (mg/L)	Br (mg/L)	Sr (mg/L)	pH	TDS (mg/L)
SM-95	Sabkha Matti	8,240	3,030	5,730	74,600	175,360	700	9	9.1	173.0	6.6	267,669
SM-96	Sabkha Matti	3,140	2,080	5,330	61,400	177,375	1,816	8	17.0	76.5	6.3	251,149
SM-98	Sabkha Matti	2,130	1,320	4,520	66,600	134,869	4,312	25	22.5	43.3	6.8	213,777
SM-99	Sabkha Matti	3,150	1,690	4,580	74,200	147,799	2,635	34	16.1	71.7	6.5	234,088
SM-101	Sabkha Matti	15,000	5,180	8,560	58,400	183,883	392	3	6.1	347.0	5.9	271,419
SM-102	Sabkha Matti	11,400	3,480	6,580	65,400	160,986	657		4.1	273.0	6.3	248,503
SM-AD-001	Sabkha Matti	2,900	2,650	5,800	88,000	166,000	2,500	8	79.7	90.0	6.5	267,858
SM-AD-010	Sabkha Matti	4,700	4,000	6,800	94,000	178,000	1,600	27	85.0	150.0	6.2	289,127
SM-AD-015	Sabkha Matti	24,300	7,700	14,600	73,500	200,000	750	31	100.0	600.0	5.6	320,881
SM-AD-022	Sabkha Matti	11,700	475	10,700	92,000	194,000	600	10	150.0	200.0	6.1	309,485
SM-AD-026	Sabkha Matti	5,600	4,200	7,700	92,000	177,000	1,700	32	85.0	140.0	6.5	288,232
SM-AD-030	Sabkha Matti	26,800	5,200	13,100	75,000	200,000	300	6	20.0	650.0	6.3	320,406
SM-AD-038	Sabkha Matti	26,900	6,250	20,500	64,500	204,000	250	21	20.0	700.0	6.1	322,421
SM-AD-041	Sabkha Matti	43,900	8,200	26,600	43,500	217,000	600	21	26.8	1,025.0	5.9	339,821
SM-AD-043	Sabkha Matti	10,000	2,000	9,500	84,000	185,000	700	16	30.0	325.0	6.4	291,216
SM-AD-046	Sabkha Matti	15,400	4,500	14,000	78,400	190,000	500	20	75.0	450.0	6.1	302,820
SM-AD-049	Sabkha Matti	78,900	10,100	33,000	16,600	263,000	100	19	95.0	2,150.0	5.3	401,719
SM-AD-051	Sabkha Matti	20,500	4,950	10,400	80,000	193,500	400	18	65.4	600.0	6.3	309,768
SM-AD-052	Sabkha Matti	17,700	3,750	14,400	71,000	192,000	400	8	90.0	450.0	6.4	299,258
SM-AD-053	Sabkha Matti	53,000	7,400	38,000	28,000	244,700	5,800	48	5.0	1,400.0	5.4	376,948

Appendix A- continued: Major and trace element concentrations for groundwater samples from the Rub' al Khali basin aquifers

Sample ID	Aquifer	Ca (mg/L)	K (mg/L)	Mg (mg/L)	Na (mg/L)	Cl (mg/L)	SO_4 (mg/L)	HCO_3 (mg/L)	Br (mg/L)	Sr (mg/L)	pH	TDS (mg/L)
SM-AD-054	Sabkha Matti	2,100	1,350	4,300	78,000	142,000	775	33	25.0	60.0	6.9	228,558
SM-AD-055	Sabkha Matti	25,000	4,000	18,500	68,000	198,000	750	25	26.0	700.0	6.0	314,275
SM-AD-056	Sabkha Matti	35,000	5,700	22,300	52,000	203,000	625	24	25.0	1,000.0	6.0	318,649
SM-AD-057	Sabkha Matti	18,500	4,000	13,500	77,000	191,000	800	11	75.0	450.0	6.4	304,811
SM-AD-059	Sabkha Matti	3,600	3,200	6,800	91,000	177,000	1,600	4	47.0	85.0	6.2	283,204
SM-AD-061	Sabkha Matti	35,500	5,100	22,000	56,000	217,500	5,900	31	5.0	750.0	5.8	342,031
SM-AD-065	Sabkha Matti	35,700	5,400	19,400	62,300	206,800	370	461	70.0	800.0	6.3	330,431
SM-AD-067	Sabkha Matti	28,600	5,000	15,700	68,700	196,800	390	61		550.0	6.4	315,251
SM-AD-068	Sabkha Matti	18,400	6,000	11,800	86,000	195,400	530	403	135.0	400.0	6.5	318,533
SM-AD-074	Sabkha Matti	70,000	11,000	27,000	23,000	236,000	700	38	110.0	1,350.0	5.2	367,738
SM-AD-079	Sabkha Matti	2,500	2,100	2,400	135,000	211,000	3,100	41	85.0	55.0	6.8	356,141
SM-AD-082	Sabkha Matti	4,700	5,000	8,000	101,000	184,000	1,950	35	180.0	110.0	6.4	304,685
SM-AD-088	Sabkha Matti	7,200	5,400	8,600	101,500	192,000	1,400	42	76.0	165.0	6.9	316,142
SM-AD-089	Sabkha Matti	3,000	2,100	3,300	108,000	180,600	2,350	616	300.0	65.0	7.1	299,966
SM-AD-090	Sabkha Matti	6,600	4,800	10,000	96,400	191,300	1,200	265	95.0	150.0	6.9	310,565
SM-AD-091	Sabkha Matti	6,400	4,400	7,700	101,200	192,900	1,250	380	125.0	125.0	6.7	314,230
SM-AD-093	Sabkha Matti	29,000	5,300	22,000	64,000	218,000	5,900	40	16.0	800.0	5.9	344,240
SM-AD-099	Sabkha Matti	6,100	4,400	8,000	90,000	187,000	1,600	36	222.7	115.0	6.7	297,136

Appendix A- continued: Major and trace element concentrations for groundwater samples from the Rub' al Khali basin aquifers

Sample ID	Aquifer	Ca (mg/L)	K (mg/L)	Mg (mg/L)	Na (mg/L)	Cl (mg/L)	SO_4 (mg/L)	HCO_3 (mg/L)	Br (mg/L)	Sr (mg/L)	pH	TDS (mg/L)
Shuw-1	Shuweihat	2,160	581	1,370	27,100	43,909	3,914	35	4.7	45.8	7.3	79,000
Shuw-2	Shuweihat	2,840	522	1,150	31,200	54,927	3,350	21	0.5	75.3	7.5	94,000
Shuw-3	Shuweihat	2,800	541	1,090	29,500	45,567	3,083	27	1.7	53.5	7.2	82,600
Dam-1	Dam	1,450	300	950	10,500	19,700	4,050	55	11.0	25.0	7.4	36,700
Dam-2	Dam	1,500	450	950	15,500	25,000	6,750	50	15.0	27.0	7.4	50,251
HDRK-1	Hadrukh	1,920	494	1,540	7,830	18,086	1,951	64	115.7	48.7	7.7	35,800
HDRK-2	Hadrukh	1,980	519	1,600	8,330	19,426	3,177	74	121.0	36.9	7.4	36,100
HDRK-3	Hadrukh	1,820	591	1,720	8,090	19,583	3,652	76	124.0	46.1	8.5	35,100
DMM-1	Dammam	4,510	680	2,510	10,800	31,251	1,809	104	215.2	97.4	7.4	51,199
DMM-2	Dammam	4,430	665	2,440	10,400	30,484	1,827	183	206.8	97.5	7.4	50,068
D-1	Dammam	402		119	165	238	1,361	122	2.1	n.d	7.3	2,409
D-2	Dammam	439		111	592	256	2,324	49	n.d	n.d	8.3	3,771
UER-1	Umm Er Radhuma	6,460	765	2,120	32,000	67,872	820	215	512.8	318.0	7.2	110,000
UER-2	Umm Er Radhuma	7,080	890	2,640	34,600	76,076	1,601	210	554.7	183.0	7.3	122,945
U-1	Umm Er Radhuma	240	20	124	127	145	1,043	118	1.1	n.d	7.8	1,798
U-2	Umm Er Radhuma	313	53	150	597	772	1,374	235	6.2	15.3	7.3	3,321
U-3	Umm Er Radhuma	264	54	140	726	948	1,279	268	7.7	16.1	7.3	3,457
U-4	Umm Er Radhuma	271	53	120	734	999	1,182	268	7.7	17.7	7.4	3,600
U-5	Umm Er Radhuma	276	69	150	1,400	2,029	1,357	268	15.1	20.8	7.3	5,517

Appendix B Stable and radioactive isotopes and tritium for groundwater samples from the Rub' al Khali basin aquifers

Sample ID	Aquifer	$\delta^{18}O$ (‰)	$\delta^{2}H$ (‰)	$\delta^{37}Cl$ (‰)	$\delta^{81}Br$ (‰)	$^{87}Sr/^{86}Sr$	^{3}H (TU)	^{14}C pmc
SM-1	Sabkha Matti	8.5	8.8	0.02	-0.16	0.708144	< 0.8	65.0
SM-2	Sabkha Matti	7.4	1.6	0.02	0.14	0.708109	1.6	
SM-3	Sabkha Matti	8.1	8.4	0.08	0.36	0.708124	< 0.8	44.7
SM-4	Sabkha Matti	9.5	11.4	0.00	0.26	0.708066	< 0.8	64.6
SM-6	Sabkha Matti	11.3	16.6	0.48	0.13	0.708359	< 0.8	60.1
SM-7	Sabkha Matti	9.6	9.7	-0.05	0.38	0.708540	0.9	
SM-8	Sabkha Matti	9.4	4.1	-0.06	0.15	0.708418	1.0	
SM-9	Sabkha Matti	8.8	5.8	-0.04	0.33	0.708484	2.2	
SM-13	Sabkha Matti	6.5	-4.9	0.11	1.73	0.708545	< 0.8	
SM-14	Sabkha Matti	5.0	-8.1	0.28	1.53	0.708515	1.1	
SM-15	Sabkha Matti	6.2	2.6	0.13	0.51	0.708512	1.6	
SM-16	Sabkha Matti	1.9	-22.7			0.708487	< 0.8	
SM-17	Sabkha Matti	6.6	-2.3	0.19	1.21	0.708590	1.3	
SM-18	Sabkha Matti	9.2	4.9	0.07	0.66	0.708580	< 0.8	
SM-19	Sabkha Matti	10.1	13.8	0.29	0.46	0.708562	< 0.8	
SM-20	Sabkha Matti	9.7	6.0	0.10	0.58	0.708497	< 0.8	
SM-21	Sabkha Matti	10.1	13.6	-0.35	0.16	0.708551	1.6	
SM-22	Sabkha Matti	6.7	-6.2	-0.16	0.24	0.708409	< 0.8	
SM-24	Sabkha Matti	8.3	3.9			0.708073	< 0.8	

Appendix B-continued: Stable and radioactive isotopes and tritium for groundwater samples from the Rub' al Khali basin aquifers

Sample ID	Aquifer	$\delta^{18}O$ (‰)	$\delta^{2}H$ (‰)	$\delta^{37}Cl$ (‰)	$\delta^{81}Br$ (‰)	$^{87}Sr/^{86}Sr$	^{3}H (TU)	^{14}C pmc
SM-25	Sabkha Matti	9.0	2.4	0.01	0.43	0.708590	< 0.8	
SM-26	Sabkha Matti	5.0	-10.2	0.03	-0.08	0.708581	< 0.8	
SM-27	Sabkha Matti	5.4	-6.5	0.09	0.98	0.708539	1.2	
SM-28	Sabkha Matti	8.0	-1.1	0.29	1.43	0.708528	1.5	
SM-29	Sabkha Matti	8.9	7.6	0.19	0.90	0.708578	< 0.8	
SM-30	Sabkha Matti	8.3	3.3	0.27	-0.69	0.708638	1.4	
SM-31	Sabkha Matti	8.5	4.0	0.13	0.74	0.708613	< 0.8	
SM-32	Sabkha Matti	8.8	1.4	0.21	1.11	0.708631	< 0.8	
SM-33	Sabkha Matti	9.9	6.8		0.66	0.708629	< 0.8	
SM-34	Sabkha Matti	9.1	10.8	0.06	0.87	0.708604	2.3	
SM-35	Sabkha Matti	9.9	12.9	0.17	0.00	0.708581	< 0.8	
SM-36	Sabkha Matti	7.0	-7.8	0.05	0.83	0.708560	< 0.8	
SM-37	Sabkha Matti	7.2	-0.1			0.708576	< 0.8	
SM-38	Sabkha Matti	5.8	3.3			0.708542	< 0.8	
SM-39	Sabkha Matti	4.8	-2.7	-0.04	0.35	0.708541	1.0	
SM-41	Sabkha Matti	3.5	-13.8	0.31	0.26	0.708509	0.9	74.0
SM-42	Sabkha Matti	3.4	-6.4	1.09	0.69	0.708564	1.6	
SM-44	Sabkha Matti	1.0	-11.4			0.708562	1.2	
SM-46	Sabkha Matti	5.6	-6.1	-0.03	0.84	0.708496	< 0.8	
SM-48	Sabkha Matti	6.6	1.9	-0.35	-0.31	0.708480	1.7	

Appendix B-continued: Stable and radioactive isotopes and tritium for groundwater samples from the Rub' al Khali basin aquifers

Sample ID	Aquifer	$\delta^{18}O$ (‰)	$\delta^{2}H$ (‰)	$\delta^{37}Cl$ (‰)	$\delta^{81}Br$ (‰)	$^{87}Sr/^{86}Sr$	^{3}H (TU)	^{14}C pmc
SM-49	Sabkha Matti	6.5	-0.5	0.11	0.82	0.708537	1.9	
SM-52	Sabkha Matti	7.4	3.2	0.13	0.93	0.708521	1.9	
SM-56	Sabkha Matti	6.3	-1.8	0.01	0.38	0.708532	< 0.8	
SM-57	Sabkha Matti	2.9	-15.3	0.07	0.03	0.70859	< 0.8	
SM-58	Sabkha Matti	5.8	-3.3	-0.06	-0.25	0.708484	< 0.8	
SM-59	Sabkha Matti	7.2	3.9	0.02	0.85	0.708443	< 0.8	
SM-60	Sabkha Matti	5.1	1.0	0.17	0.59	0.708506	1.2	
SM-61	Sabkha Matti	4.8	1.8	0.17	0.58	0.708426	< 0.8	
SM-62	Sabkha Matti	6.4	4.4	-0.02	0.40	0.708430	2.6	
SM-63	Sabkha Matti	2.0	-3.7	0.85	1.04	0.708588	1.4	
SM-64	Sabkha Matti	3.5	-15.8	0.17	0.60	0.708433	1.3	69.4
SM-65	Sabkha Matti	4.5	-8.0			0.708492	< 0.8	
SM-67	Sabkha Matti	4.8	-6.0	0.05	0.85	0.708496	< 0.8	
SM-68	Sabkha Matti	5.9	-3.6	0.03	0.43	0.708469	2.8	43.3
SM-69	Sabkha Matti	7.8	-0.2	0.07	0.44	0.708450	< 0.8	
SM-70	Sabkha Matti	4.9	-5.6	0.03	1.35	0.708499	< 0.8	
SM-71	Sabkha Matti	4.7	-4.2	-0.13	0.73	0.708438	1.7	
SM-72	Sabkha Matti	4.9	-2.8			0.708334	< 0.8	
SM-73	Sabkha Matti	5.2	0.1			0.708302	< 0.8	
SM-74	Sabkha Matti	2.8	-19.1	0.73	0.69	0.708492	3.9	66.0

Appendix B-continued: Stable and radioactive isotopes and tritium for groundwater samples from the Rub' al Khali basin aquifers

Sample ID	Aquifer	$\delta^{18}O$ (‰)	$\delta^{2}H$ (‰)	$\delta^{37}Cl$ (‰)	$\delta^{81}Br$ (‰)	$^{87}Sr/^{86}Sr$	^{3}H (TU)	^{14}C pmc
SM-77	Sabkha Matti	6.1	9.0		0.68	0.708604	1.9	
SM-75	Sabkha Matti	8.2	7.9			0.708506	< 0.8	
SM-76	Sabkha Matti	8.4	2.1	0.02	0.83	0.708502	< 0.8	
SM-78	Sabkha Matti	4.0	-5.5	-0.48	0.30	0.708501	2.0	
SM-79	Sabkha Matti	6.2	-8.4	-0.46	0.53	0.708501	2.8	
SM-80	Sabkha Matti	5.2	-9.5	-0.06	0.18	0.708500	< 0.8	
SM-81	Sabkha Matti	7.2	-5.4			0.708633	1.1	
SM-82	Sabkha Matti	7.1	-6.1			0.708639	< 0.8	
SM-83	Sabkha Matti	7.1	-5.5	-0.29	-0.63	0.708606	< 0.8	
SM-84	Sabkha Matti	4.9	-10.3	-0.25	0.37	0.708641	< 0.8	
SM-85	Sabkha Matti	7.5	-1.4	0.11	0.03	0.708644	< 0.8	
SM-86	Sabkha Matti	6.9	-5.8	-0.05	-0.10	0.708661	1.5	
SM-87	Sabkha Matti	6.9	-5.3	0.25	-0.14	0.708633	1.4	
SM-88	Sabkha Matti	7.3	-2.8	0.18	0.09	0.708609	< 0.8	
SM-89	Sabkha Matti	7.1	-6.3	0.06	0.01	0.708626	< 0.8	
SM-90	Sabkha Matti	7.0	-7.0	-0.05	-0.15	0.708604	< 0.8	
SM-91	Sabkha Matti	4.2	-13.3	-0.18	-1.90	0.708613	< 0.8	
SM-92	Sabkha Matti	8.0	-1.3	0.02	-2.05	0.708619	< 0.8	
SM-93	Sabkha Matti	4.4	-14.1	0.15	0.74	0.708614	< 0.8	58.2
SM-94	Sabkha Matti	4.6	-9.8			0.708507	< 0.8	

Appendix B-continued: Stable and radioactive isotopes and tritium for groundwater samples from the Rub' al Khali basin aquifers

Sample ID	Aquifer	$\delta^{18}O$ (‰)	$\delta^{2}H$ (‰)	$\delta^{37}Cl$ (‰)	$\delta^{81}Br$ (‰)	$^{87}Sr/^{86}Sr$	^{3}H (TU)	^{14}C pmc
SM-95	Sabkha Matti	4.3	-13.9	0.01	0.47	0.708484	< 0.8	
SM-96	Sabkha Matti	5.2	-7.2	0.20	0.22	0.708247	1.0	
SM-98	Sabkha Matti	7.5	-0.1	0.01	0.00	0.708128	1.2	
SM-99	Sabkha Matti	4.9	-7.0	-0.14	0.10	0.708280	< 0.8	
SM-101	Sabkha Matti	5.5	-15.5	0.05	0.54	0.708582	0.9	
SM-102	Sabkha Matti	4.5	-14.0	0.10	0.94	0.70862	< 0.8	44.7
Shuw-1	Shuweihat	10.4	19.4	-0.02	-0.44	0.708465	< 0.8	25.2
Shuw-2	Shuweihat	7.3	15.4	0.21	0.01	0.708373	< 0.8	30.7
Shuw-3	Shuweihat	4.2	0.3	0.55	-0.91	0.708344	< 0.8	18.6
Dam-1	Dam	0.5	-19.5	0.18	0.73	0.70863	< 0.8	31.6
Dam-2	Dam	4.1	5.9	0.09	0.85	0.70865	< 0.8	38.9
HDRK-1	Hadrukh	-5.2	-55.5	0.34	1.88	0.70819	< 0.8	24.9
HDRK-2	Hadrukh	-4.7	-55.4	0.41	1.96	0.70821	< 0.8	72.0
HDRK-3	Hadrukh	-4.8	-52.6	0.51	2.10	0.70822	< 0.8	38.9
DMM-1	Dammam	-8.1	-69.0	1.18	1.79	0.70770	< 0.8	8.1
DMM-2	Dammam	-8.2	-68.9	0.77	1.69	0.70785	< 0.8	38.2
UER-1	Umm Er Radhuma	-3.2	-40.4	-0.16	-0.12	0.7077	< 0.8	10.1
UER-2	Umm Er Radhuma	-2.4	-34.2	0.54	-1.11	0.7079	< 0.8	

Appendix B-continued: Stable and radioactive isotopes and tritium for groundwater samples from the Rub' al Khali basin aquifers

Sample ID	Aquifer	$\delta^{18}O$ (‰)	$\delta^{2}H$ (‰)	$\delta^{37}Cl$ (‰)	$\delta^{81}Br$ (‰)	$^{87}Sr/^{86}Sr$	^{3}H (TU)	^{14}C pmc
U-2	Umm Er Radhuma	-7.9	-62.6	-2.01	-1.33	0.7078	< 0.8	
U-3	Umm Er Radhuma	-7.6	-58.5	-2.00	-1.54	0.7078	< 0.8	
U-4	Umm Er Radhuma	-7.2	-55.8	-1.79	-1.36	0.7078	< 0.8	
U-5	Umm Er Radhuma	-7.6	-59.6	-1.81	-0.92	0.7078	< 0.8	